SUPPORTING INFORMATION

Visible Light Activated Coumarin Photocages: An Interplay Between Radical and Organobase Generation to Govern Thiol-Ene Polymerizations

Meghan T. Kiker[†], Ain Uddin[†], Lynn M. Stevens, Kun-You Chung, Pengtao Lu, and Zachariah A. Page*

Department of Chemistry, The University of Texas at Austin, 105 East 24th Street, Stop A5300, Austin, Texas 78712, United States.

***Corresponding author:** zpage@utexas.edu

Table of Contents

1. EXPERIMENTAL DETAILS

1.1.Materials

Chemicals. All chemicals were used as received unless otherwise noted. Pentaerythritol tetrakis(3-mercaptopropionate) (PETMP, >95%), 3,6-dioxa-1,8-octane-dithiol (DODT, 95%), (2,2,6,6-tetramethylpiperidine-1-yl)oxidanyl (TEMPO, 98%), 7-(diethylamino)-4-methyl-2H-chromen-2-one (99%), boron trifluoride diethyl etherate, and 4-methoxystyrene were purchased from Sigma-Aldrich. Tetraethylene glycol diacrylate (TEGDA, 95%), 1,6-hexanediol diacrylate (HDDA, 85.0+%), sodium borohydride, *N*,*N*-diisopropylethylamine, 1,1,3,3-tetramethylguanidine (TMG), and *N*,*N*-dicyclohexylmethylamine were purchased from Tokyo Chemical Industry. *N*,*N*-dimethylformamide dimethyl acetal (≥ 98%), sodium periodate (99.8+%), and *N*-bromosuccinimide were purchased from Chem Impex. 4-nitrophenyl-chloroformate (98.0+%) and ammonium acetate (crystalline, certified ACS), (4,5-dimethoxy-2-nitrophenyl)methanol (>98%) were purchased from Fisher Scientific. *N*-iodosuccinimide was purchased from Combi-Blocks. Tris(dibenzylideneacetone)dipalladium$^{(0)}$ (97.0%), and Q-phos were purchased from STREM Chemicals. Lawesson's reagent (99%) and 4-dimethylaminopyridine was purchased from Acros Organics. Note that monomers and cross-linkers were not purified prior to use, and as such any inhibitor present (e.g., phenolics) from the commercial source remained.

Synthesis

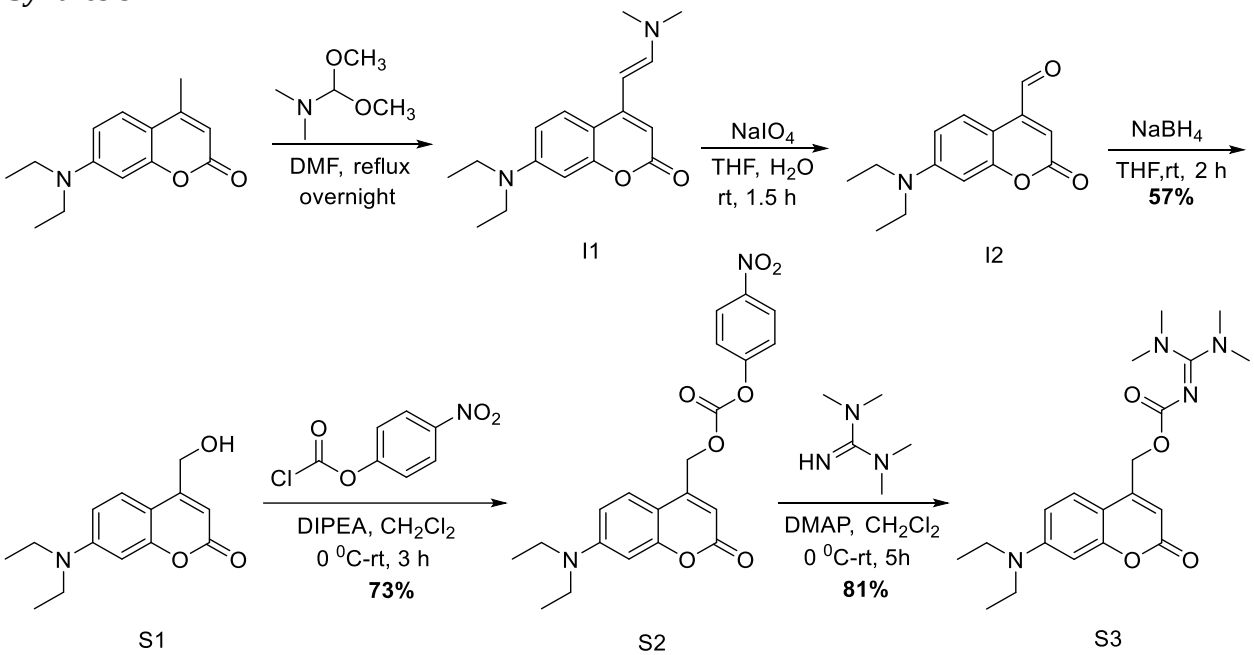

Scheme S1. Synthesis of O-H-CTMG (S3).

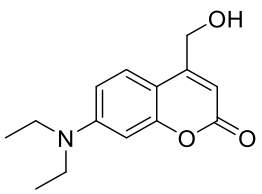

Synthesis of 7-(diethylamino)-4-(hydroxymethyl)-2*H*-chromen-2-one (S1). To a solution of 7-(diethylamino)-4-methyl-2H-chromen-2-one (10.00 g, 43.23 mmol) in 100 mL of *N*,*N*-

dimethylformamide (DMF), *N*,*N*-dimethylformamide dimethyl acetal (11.49 mL, 86.47 mmol) was added. The reaction mixture was heated to reflux at 170 °C for 16 hours under an inert nitrogen atmosphere. The reaction was cooled to room temperature, poured into 200 mL of saturated $NaHCO_{3(aq)}$, and extracted with 3×150 mL of CH_2Cl_2. The combined organic layers were dried over anhydrous $MgSO_4$, filtered, and the solvent was removed under reduced pressure to provide **I1** as a crude product that was used without further purification.

The residue (**I1**) was then redissolved in 50 mL of THF/H_2O (1:1), cooled in an ice bath, and $NaIO_4$ (27.75 g, 129.69 mmol) was then added. After stirring for 3 hours at ambient temperature the precipitate was filtered off and rinsed with THF. To the filtrate was added 300 mL of concentrated $NaHCO_{3(aq)}$ and the mixture was extracted with 3×150 mL of CH_2Cl_2. The combined organic layers were dried over $MgSO_4$, filtered, and the solvent was removed under reduced pressure to provide **I2** as a crude product that was used without further purification.

Subsequently, the residue (**I2**) was dissolved in 100 mL of THF at 0 °C, purged with nitrogen, and $NaBH_4$ (3.29 g, 86.46 mmol) was added in several portions under a positive stream of nitrogen gas. After stirring for 3 hours at ambient temperature, 20 mL of water was added slowly to quench the reaction. Then the reaction mixture was poured into 200 mL of concentrated $NaHCO_{3(aq)}$ and extracted with 3×100 mL of CH_2Cl_2. The combined organic layers were dried over anhydrous $MgSO_4$, filtered, and concentrated under reduce pressure. The crude product was purified by column chromatography with a 0-50% hexanes:ethyl acetate gradient, providing 7-(diethylamino)-4-(hydroxymethyl)-2H-chromen-2-one (**S1)** (6.10 g, 57%) as a yellow solid.^{1}H NMR (400 MHz, $CDCl_3$) δ 7.24 (d, J = 9.1 Hz, 1H), 6.48 (dd, J = 9.0, 2.7 Hz, 1H), 6.38 (d, J = 2.7 Hz, 1H), 6.20 (s, 1H), 4.75 (d, J = 4.8 Hz, 2H), 3.31 (q, J = 7.2 Hz, 4H), 3.06 (t, J = 6.2 Hz, 1H), 1.11 (t, J = 7.1 Hz, 6H). ^{13}C NMR (101 MHz, $CDCl_3$) δ 162.98, 156.08, 155.31, 150.50, 124.43, 108.67, 106.39, 105.27, 97.69, 60.83, 44.72, 12.44. HRMS (ESI): exact mass calculated for $C_{14}H_{17}NO_3$ $[M+Na]^+$ 270.1101, found 270.1106.

General procedure for the synthesis of *para*-nitrophenylcarbonate precurosrs (S2, S5, & S10). To a roundbottom flask under an inert atmosphere was added the hydroxyl precursor (**S1**, **S4**, or **S7**) (1.00 mmol), diisopropylethylamine (5.00 mmol), and 20 mL of dry CH_2Cl_2. The mixture was cooled to 0 °C in an ice bath, followed by dropwise addition of 4-nitrophenyl-chloroformate (3.00 mmol) in 5 mL of dry CH_2Cl_2. Following complete addition, the reaction was allowed to warm to room temperature, stirred for 12 hours, poured into 50 mL of deionized water, and extracted with 3×50 mL of CH_2Cl_2. The combined organic layers were dried over anhydrous $MgSO_4$, filtered, and concentrated under reduce pressure. The crude product was purified by column chromatography with a 0-30% hexanes:ethyl acetate gradient to provide the desired product **S2**, **S5**, or **S10**.

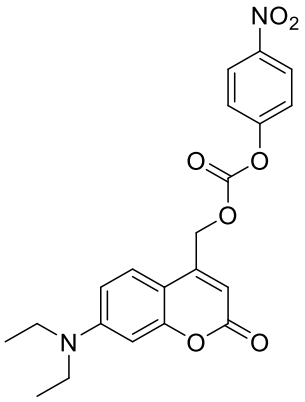

Synthesis of (7-(diethylamino)-2-oxo-2*H*-chromen-4-yl)methyl (4-nitrophenyl) carbonate (S2). Product obtained as a yellow solid (300 mg, 73%). ^{1}H NMR (400 MHz, $CDCl_3$) δ 8.34 – 8.28 (m, 2H), 7.46 – 7.39 (m, 2H), 7.32 (d, *J* = 9.0 Hz, 1H), 6.65 (dd, *J* = 8.8, 2.9 Hz, 1H), 6.57 (d, *J* = 2.5 Hz, 1H), 6.24 (s, 1H), 5.41 (d, *J* = 1.3 Hz, 2H), 3.43 (q, *J* = 7.1 Hz, 4H), 1.22 (t, *J* = 7.1 Hz, 7H). ^{13}C NMR (101 MHz, $CDCl_3$) δ 161.67, 156.32, 155.20, 152.11, 150.83, 147.81, 145.56, 125.38, 124.31, 121.72, 108.85, 106.75, 105.54, 97.85, 65.73, 44.80, 12.38. HRMS (ESI): exact mass calculated for $C_{21}H_{20}N_2O_7$ $[M+Na]^+$ 435.1163, found 435.1164.

General procedure for the synthesis of coumarinylmethyl tetramethyl guanidine photocages (S3, S6, S8, S11, & S13). Under an inert atmosphere, the corresponding *para*-nitrophenylcarbonate precurosr (1.00 mmol) was dissolved in 10 mL of anhydrous CH_2Cl_2, followed by addition of 4-dimethylaminopyridine (1.50 mmol) and then dropwise addition of 1,1,3,3-tetramethylguanidine (2.00 mmol) in 2.0 mL of anhydrous CH_2Cl_2. The reaction mixture was monitored by thin layer chromatography until all of the starting coumarin derivative had been fully consumed, at which point the solution was concentrated under reduced pressure. The crude product was purified directly by column chromatography with a 0-3% CH_2Cl_2:methanol gradient to provide the desired product

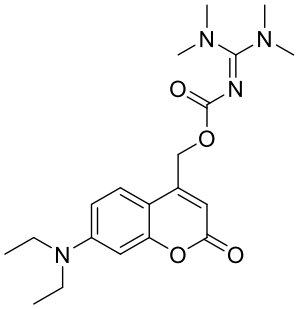

Synthesis of O-H-CTMG (S3). Product obtained as a yellow solid (314 mg, 81%). ^{1}H NMR (400 MHz, $CDCl_3$) δ 7.31 (d, *J* = 8.9 Hz, 1H), 6.49 (dd, *J* = 8.9, 2.6 Hz, 1H), 6.43 (d, *J* = 2.6 Hz, 1H), 6.16 (s, 1H), 5.18 (d, *J* = 1.4 Hz, 2H), 3.33 (q, *J* = 7.1 Hz, 4H), 2.84 (s, 12H), 1.12 (t, *J* = 7.1 Hz, 6H). ^{13}C NMR (101 MHz, $CDCl_3$) δ 166.64, 162.20, 159.28, 156.19, 151.73, 150.46, 124.65, 108.53, 106.48, 106.05, 97.76, 61.96, 44.71, 39.96, 12.44. HRMS (ESI): exact mass calculated for $C_{20}H_{28}N_4O_4$ $[M+H]^+$ 389.2183, found 389.2191.

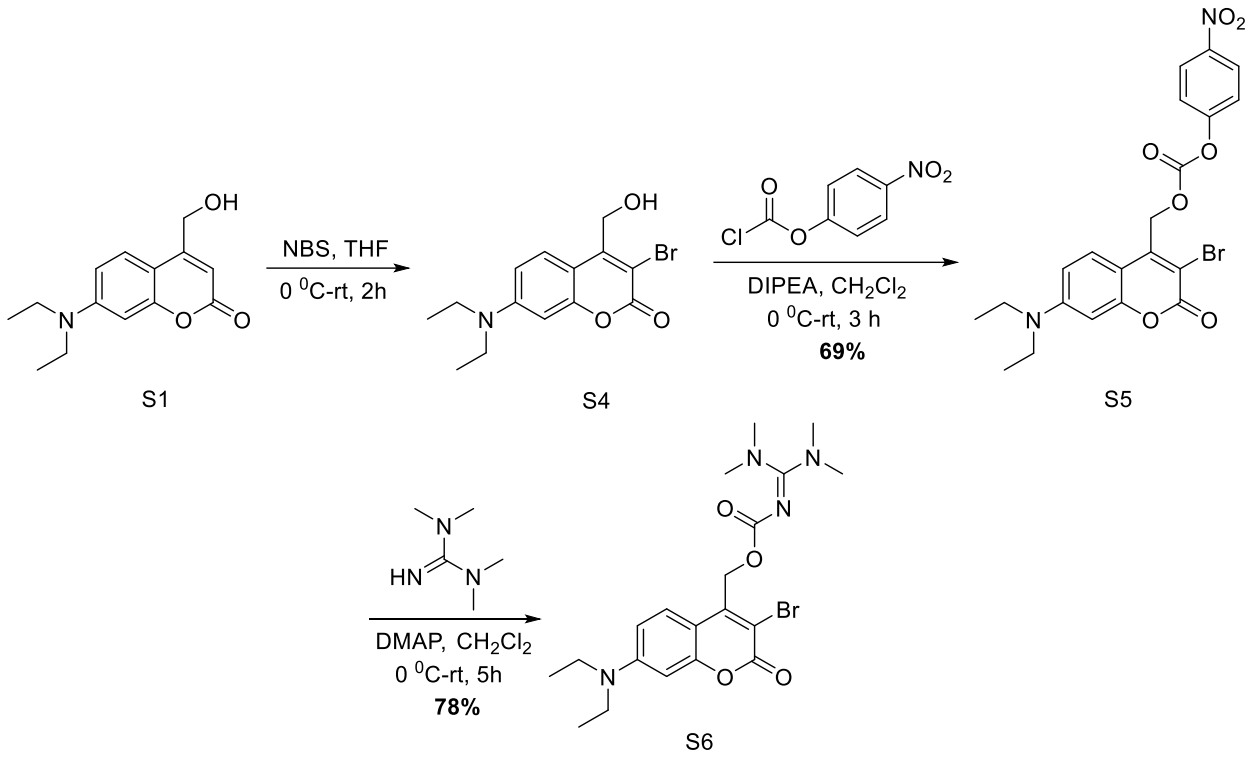

Scheme S2. Synthesis of O-Br-CTMG (S6).

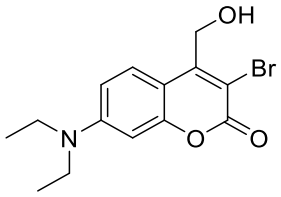

Synthesis of 3-bromo-7-(diethylamino)-4-(hydroxymethyl)-2*H*-chromen-2-one (S4). To a solution of 7-(diethylamino)-4-(hydroxymethyl)-2*H*-chromen-2-one (**S1**) (500 mg, 2.02 mmol) in 10 mL of tetrahydrofuran (THF) cooled in an ice bath under nitrogen was added *N*-bromosuccinimide (433 mg, 2.43 mmol), followed by ammonium acetate (16 mg, 0.21 mmol). The resulting mixture was stirred at room temperature for 2 hours, then poured into 50 mL of deionized water and extracted with 3×100 mL of CH_2Cl_2. The combined organic layers were dried over anhydrous $MgSO_4$, filtered, and concentrated under reduce pressure. The crude product was purified by column chromatography with a 0-50% hexanes:ethyl acetate gradient, providing 3-bromo-7-(diethylamino)-4-(hydroxymethyl)-2*H*-chromen-2-one **(S4)** (550 mg, 84%) as a yellow solid.^{1}H NMR (400 MHz, $CDCl_3$) δ 7.66 (d, J = 9.2 Hz, 1H), 6.62 (dd, J = 9.2, 2.6 Hz, 1H), 6.47 (s, 1H), 4.95 (d, J = 5.5 Hz, 2H), 3.41 (q, J = 7.1 Hz, 4H), 1.20 (t, J = 7.2 Hz, 6H). ^{13}C NMR (101 MHz, $CDCl_3$) δ 158.44, 155.19, 150.98, 150.79, 126.54, 109.40, 107.65, 105.28, 97.39, 61.64, 44.87, 12.44. HRMS (ESI): exact mass calculated for $C_{14}H_{16}BrNO_3$ $[M+Na]^+$ 348.0206, found 348.0209.

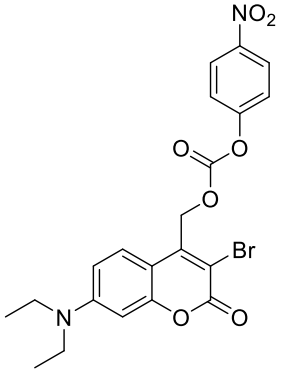

Synthesis of (3-bromo-7-(diethylamino)-2-oxo-2*H*-chromen-4-yl)methyl (4-nitrophenyl) carbonate (S5). See the "General procedure for the synthesis of *para*-nitrophenylcarbonate precursors" section provided earlier for the synthetic protocol. Product obtained as a deep yellow solid (339 mg, 69%). ^{1}H NMR (400 MHz, $CDCl_3$) δ 8.27 (d, *J* = 9.2 Hz, 1H), 7.40 (d, *J* = 9.2 Hz, 1H), 6.66 (dd, *J* = 9.2, 2.6 Hz, 1H), 6.52 (d, *J* = 2.6 Hz, 1H), 5.61 (s, 1H), 3.43 (q, *J* = 7.1 Hz, 2H), 1.22 (t, *J* = 7.1 Hz, 3H). ^{13}C NMR (101 MHz, $CDCl_3$) δ 157.94, 155.28, 155.12, 152.09, 151.02, 145.59, 145.05, 126.15, 125.87, 125.38, 121.70, 115.77, 109.59, 107.94, 107.26, 97.55, 66.30, 44.92, 12.42. HRMS (ESI): exact mass calculated for $C_{21}H_{19}BrN_2O_7$ $[M+Na]^+$ 513.0268, found 513.0268.

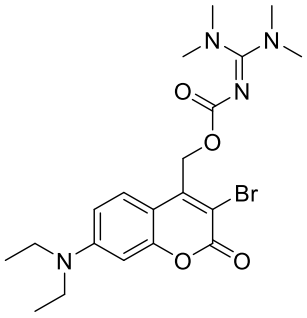

Synthesis of O-Br-CTMG (S6). See the "General procedure for the synthesis of coumarinylmethyl tetramethyl guanidine photocages" section provided earlier for the synthetic protocol. Product obtained as a yellow solid (364 mg, 78%). ^{1}H NMR (400 MHz, $CDCl_3$) δ 7.64 (d, *J* = 9.2 Hz, 1H), 6.51 (dd, *J* = 9.2, 2.6 Hz, 1H), 6.40 (d, *J* = 2.6 Hz, 1H), 5.33 (s, 2H), 3.33 (q, *J* = 7.1 Hz, 4H), 2.79 (s, 12H), 1.12 (t, *J* = 7.1 Hz, 6H). ^{13}C NMR (101 MHz, $CDCl_3$) δ 165.31, 158.21, 157.39, 153.91, 149.56, 147.96, 125.93, 108.21, 107.05, 105.76, 96.17, 62.23, 43.77, 38.89, 11.42. HRMS (ESI): exact mass calculated for $C_{20}H_{27}BrN_4O_4$ $[M+H]^+$ 467.1288, found 467.1292.

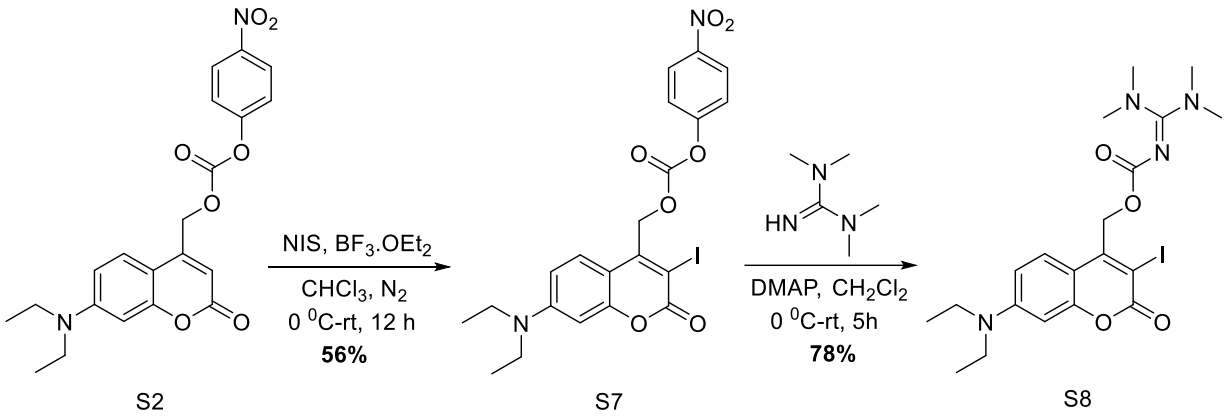

Scheme S3. Synthesis of O-I-CTMG (S8).

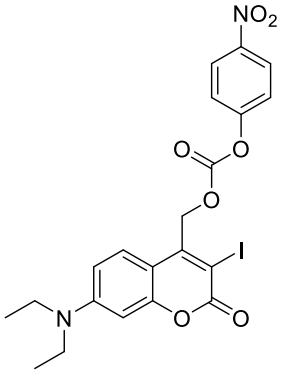

Synthesis of (7-(diethylamino)-3-iodo-2-oxo-2*H*-chromen-4-yl)methyl (4-nitrophenyl) carbonate (S7). To a roundbottom flask under an inert atmosphere was added (7-(diethylamino)-2-oxo-2*H*-chromen-4-yl)methyl (4-nitrophenyl) carbonate (**S2**) (206 mg, 0.50 mmol) in 5 mL of $CHCl_3$, followed by cooling the flask to 0 °C in an ice bath. To the solution was added successively *N*-iodosuccinimide (135 mg, 0.60 mmol) and $BF_3.Et_2O$ (30.8 uL, 0.25 mmol). The resulting mixture was allowed to warm up to room temperature and stirred in the dark for 12 hours. The pink mixture was the quenched with 10 mL of saturated $Na_2S_2O_{3(aq)}$ and extracted with 3×5mL of CH_2Cl_2. The combined organic layers were dried over anhydrous $MgSO_4$, filtered, and concentrated under reduce pressure. The crude product was purified by column chromatography with a 0-30% ethyl acetate:hexanes gradient to provide the desired product (**S7**) (150 mg, 56%) as a red solid. ^{1}H NMR (400 MHz, $CDCl_3$) δ 8.28 (d, *J* = 9.2 Hz, 1H), 7.41 (d, *J* = 9.2 Hz, 1H), 6.63 (dd, *J* = 9.2, 2.6 Hz, 1H), 6.54 (d, *J* = 2.6 Hz, 1H), 5.62 (s, 1H), 3.43 (q, *J* = 7.2 Hz, 2H), 1.22 (t, *J* = 7.2 Hz, 3H). ^{13}C NMR (101 MHz, $CDCl_3$) δ 158.64, 155.83, 155.29, 152.06, 151.14, 149.95, 145.60, 125.84, 125.38, 121.71, 109.41, 107.68, 97.42, 86.16, 71.35, 44.98, 12.43. HRMS (ESI): exact mass calculated for $C_{21}H_{19}IN_2O_7$ $[M+Na]^+$ 561.0129, found 561.0130.

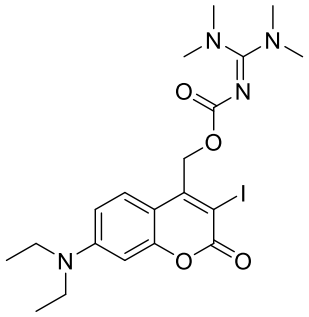

Synthesis of O-I-CTMG (S8). See the "General procedure for the synthesis of coumarinylmethyl tetramethyl guanidine photocages" section provided earlier for the synthetic protocol. Product obtained as a yellow solid (400 mg, 78%). ^{1}H NMR (400 MHz, $CDCl_3$) δ 7.70 (d, *J* = 9.1 Hz, 1H), 6.54 (dd, *J* = 9.2, 2.6 Hz, 1H), 6.46 (d, *J* = 2.6 Hz, 1H), 5.39 (s, 2H), 3.39 (q, *J* = 7.1 Hz, 4H), 2.85 (s, 12H), 1.19 (t, *J* = 7.1 Hz, 6H). ^{13}C NMR (101 MHz, $CDCl_3$) δ 166.44, 159.33, 159.15, 155.63, 153.94, 150.78, 126.89, 108.99, 108.29, 96.95, 84.76, 68.46, 53.44, 44.80, 39.92, 12.45. HRMS (ESI): exact mass calculated for $C_{20}H_{27}IN_4O_4$ $[M+H]^+$ 515.1150 found 515.1159.

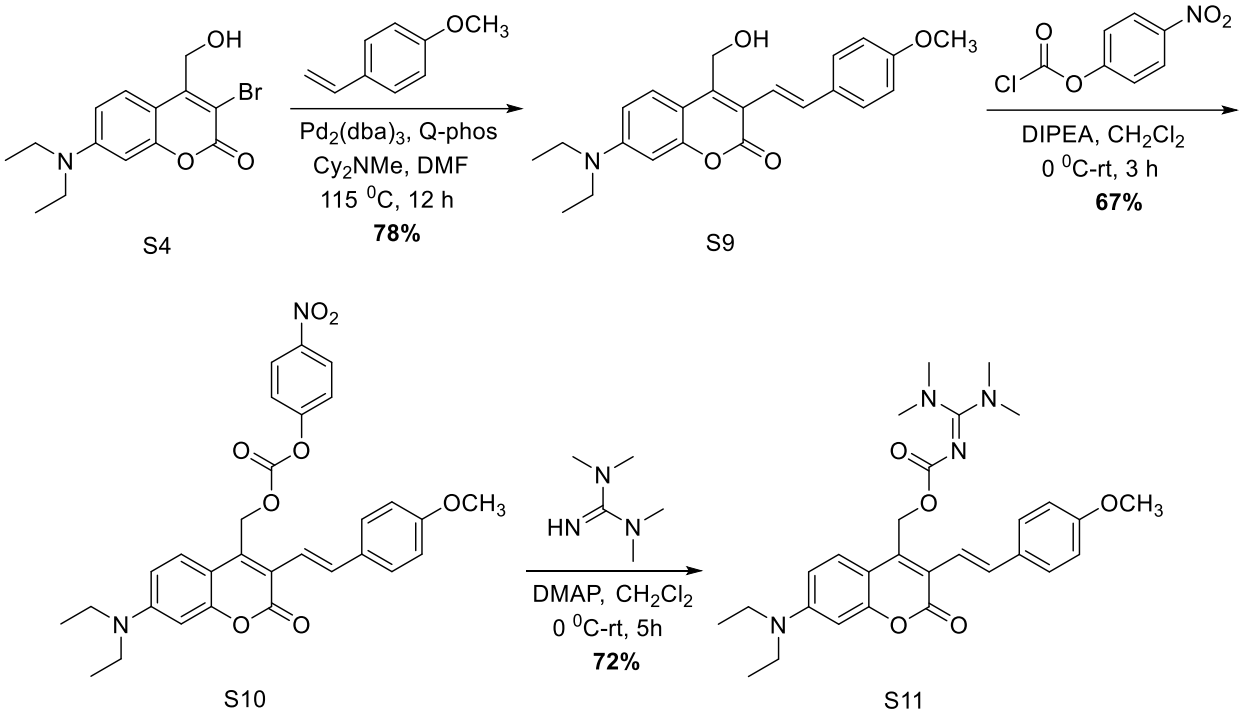

Scheme S4. Synthesis of O-Sty-CTMG (S11).

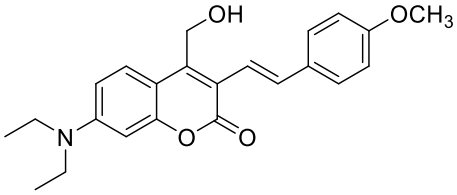

Synthesis of (*E*)-7-(diethylamino)-4-(hydroxymethyl)-3-(4-methoxystyryl)-2*H*-chromen-2-one (S9): In a nitrogen filled glovebox, 3-bromo-7-(diethylamino)-4-(hydroxymethyl)-2*H*-chromen-2-one (**S4**) (326 mg, 1.0 mmol), 4-methoxystyrene (403 mg, 3 mmol), Pd_2dba_3 (45 mg,

0.05 mmol), Q-phos (36 mg, 0.05 mmol), dicyclohexylmethylamine (0.43 mL, 2 mmol), and 5 mL of anhydrous DMF were added to a glass tube, which was sealed and removed from the glovebox. The reaction mixture was then placed in a preheated oil bath set to 115 °C and stirred for 12 hours. After cooling the reaction to room temperature, the mixture was poured into 50 mL of deionized water and extracted with 3×30 mL of CH_2Cl_2. The combined organic layers were dried over anhydrous $MgSO_4$, filtered, and concentrated under reduce pressure. The crude product was purified by column chromatography with a 0-50% hexanes:ethyl acetate gradient, to give the desired product (**S9**) (296 mg, 78%) as a bright yellow solid. ^{1}H NMR (400 MHz, $CDCl_3$) δ 7.65 (d, *J* = 9.2 Hz, 1H), 7.44 (d, *J* = 16.2 Hz, 1H), 7.39 (d, *J* = 8.7 Hz, 2H), 7.03 (d, *J* = 16.2 Hz, 1H), 6.83 (d, *J* = 8.7 Hz, 2H), 6.59 (dd, *J* = 9.1, 2.6 Hz, 1H), 6.40 (d, *J* = 2.6 Hz, 1H), 4.94 (s, 2H), 3.80 (s, 3H), 3.37 (q, *J* = 7.1 Hz, 4H), 1.19 (t, *J* = 7.2 Hz, 6H). ^{13}C NMR (101 MHz, $CDCl_3$) δ 160.81, 158.42, 153.84, 148.97, 144.90, 133.40, 129.51, 126.99, 124.01, 117.29, 116.41, 112.98, 108.10, 107.49, 96.38, 56.72, 54.26, 43.70, 11.51. HRMS (ESI): exact mass calculated for $C_{23}H_{25}NO_4$ $[M+Na]^+$ 402.1676, found 402.1683.

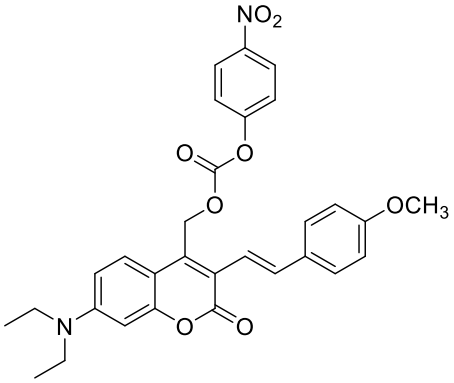

Synthesis of (*E*)-(7-(diethylamino)-3-(4-methoxystyryl)-2-oxo-2*H*-chromen-4-yl)methyl (4-nitrophenyl) carbonate (S10). See the "General procedure for the synthesis of *para*-nitrophenylcarbonate precursors" section provided earlier for the synthetic protocol. Product obtained as a yellow solid (365 mg, 67%). ^{1}H NMR (400 MHz, $CDCl_3$) δ 8.25 (d, *J* = 9.2 Hz, 2H), 7.58 (d, *J* = 10.5 Hz, 1H), 7.55 (d, *J* = 3.7 Hz, 1H), 7.47 (d, *J* = 8.8 Hz, 2H), 7.37 (d, *J* = 9.1 Hz, 2H), 7.11 (d, *J* = 16.1 Hz, 1H), 6.89 (d, *J* = 8.7 Hz, 2H), 6.65 (dd, *J* = 9.1, 2.7 Hz, 1H), 6.53 (d, *J* = 2.6 Hz, 1H), 5.63 (s, 2H), 3.83 (s, 3H), 3.43 (q, *J* = 7.1 Hz, 4H), 1.22 (t, *J* = 7.0 Hz, 6H). ^{13}C NMR (101 MHz, $CDCl_3$) δ 159.91, 158.80, 154.33, 153.79, 151.30, 149.20, 144.52, 138.21, 134.54, 129.28, 127.18, 124.70, 124.32, 120.73, 118.60, 117.03, 113.14, 108.28, 107.06, 96.55, 62.08, 54.32, 43.79, 11.44. HRMS (ESI): exact mass calculated for $C_{30}H_{28}N_2O_8$ $[M+H]^+$ 545.1918, found 545.1928.

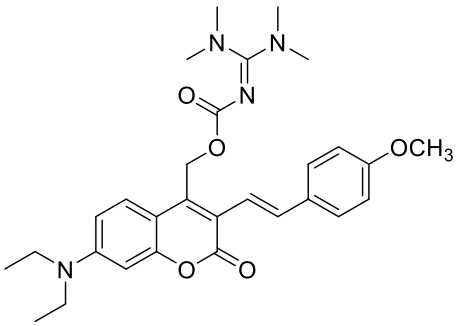

Synthesis of O-Sty-CTMG (S11). See the "General procedure for the synthesis of coumarinylmethyl tetramethyl guanidine photocages" section provided earlier for the synthetic protocol. Product obtained as a yellow solid 374 mg, 72%). ^{1}H NMR (400 MHz, $CDCl_3$) δ 7.68 (d, *J* = 9.1 Hz, 1H), 7.59 (d, *J* = 16.2 Hz, 1H), 7.47 (d, *J* = 8.8 Hz, 2H), 6.85 (d, *J* = 8.7 Hz, 2H), 6.58 (dd, *J* = 9.2, 2.6 Hz, 1H), 6.47 (d, *J* = 2.7 Hz, 1H), 5.39 (s, 2H), 3.81 (s, 3H), 3.39 (q, *J* = 7.1 Hz, 4H), 2.82 (s, 12H), 1.19 (t, *J* = 7.1 Hz, 6H). ^{13}C NMR (101 MHz, $CDCl_3$) δ 165.24, 160.43, 158.70, 158.34, 153.71, 148.87, 142.55, 133.17, 130.00, 127.08, 125.76, 118.20, 117.37, 112.96, 108.03, 96.25, 58.23, 54.29, 43.71, 38.83, 11.52. HRMS (ESI): exact mass calculated for $C_{29}H_{36}N_4O_5$ $[M+H]^+$ 521.2758, found 521.2760.

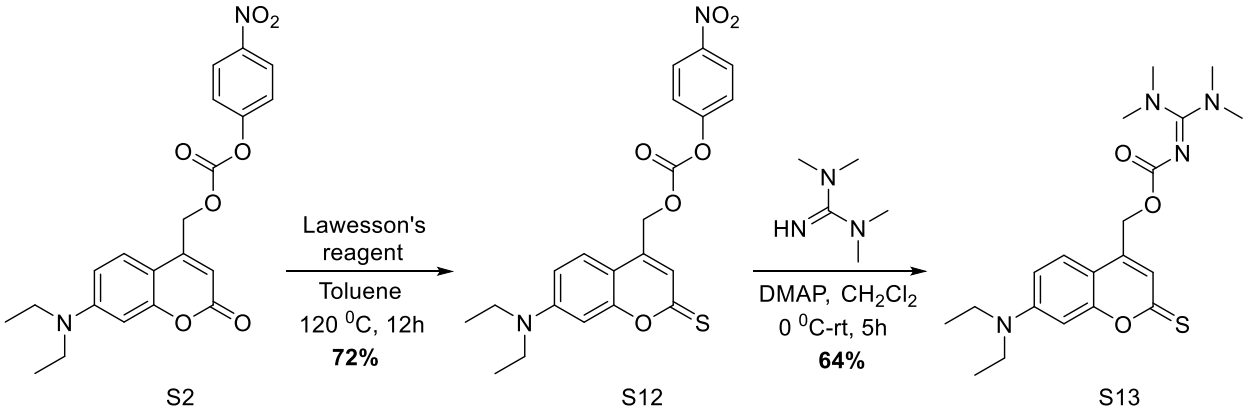

Scheme S5. Synthesis of S-H-CTMG (S13).

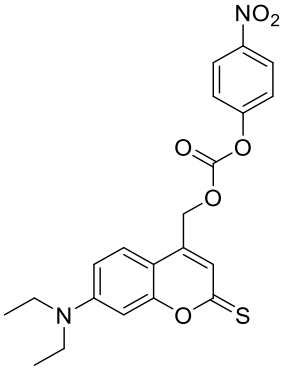

Synthesis of (7-(diethylamino)-2-thioxo-2*H*-chromen-4-yl)methyl (4-nitrophenyl) carbonate (S12): Under a nitrogen atmosphere, Lawesson's reagent (131 mg, 0.33 mmol) was added to a round bottom flask containing a solution of (7-(diethylamino)-2-oxo-2H-chromen-4-yl)methyl (4-nitrophenyl) carbonate (**S2**) (206 mg, 0.50 mmol) in anhydrous toluene (3 mL). The reaction

mixture was refluxed at 120 °C for 5 hours in the dark. After cooling the reaction to room temperature, the solution was purified by flash column chromatography on silica gel with a 0-30% hexanes:ethyl acetate gradient, to give the desired product (**S12**) (155 mg, 72%) as a dark red solid. ^{1}H NMR (400 MHz, $CDCl_3$) δ 8.32 – 8.26 (m, 2H), 7.42 (d, *J* = 9.2 Hz, 2H), 7.37 (d, *J* = 9.7 Hz, 1H), 7.12 (s, 1H), 6.72-6.65 (m, *J* = 2.7 Hz, 2H), 5.36 (s, 2H), 3.44 (q, *J* = 7.2 Hz, 4H), 1.23 (t, *J* = 7.1 Hz, 7H). ^{13}C NMR (101 MHz, $CDCl_3$) δ 195.95, 158.13, 154.21, 151.10, 150.13, 144.61, 138.82, 124.40, 123.40, 120.70, 120.00, 109.44, 106.87, 96.59, 64.47, 44.01, 11.38. HRMS (ESI): exact mass calculated for $C_{21}H_{20}N_2O_6S$ $[M+H]^+$ 429.1115, found 429.1127.

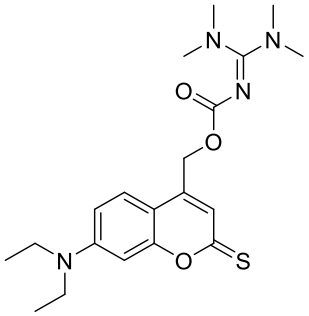

Synthesis of S-H-CTMG (S13). See the "General procedure for the synthesis of coumarinylmethyl tetramethyl guanidine photocages" section provided earlier for the synthetic protocol. Product obtained as a red solid (258 mg, 64%). ^{1}H NMR (400 MHz, $CDCl_3$) δ 7.46 (d, *J* = 8.8 Hz, 1H), 7.16 (s, 1H), 6.67 – 6.61 (m, 2H), 3.41 (q, *J* = 7.1 Hz, 4H), 2.90 (s, 12H), 1.20 (t, *J* = 7.1 Hz, 6H). ^{13}C NMR (101 MHz, $CDCl_3$) δ 197.37, 166.40, 159.05, 150.82, 144.20, 124.89, 120.61, 110.19, 108.69, 97.39, 61.76, 44.90, 40.03, 12.43. HRMS (ESI): exact mass calculated for $C_{20}H_{28}N_4O_3S$ $[M+H]^+$ 405.1955, found 405.1954.

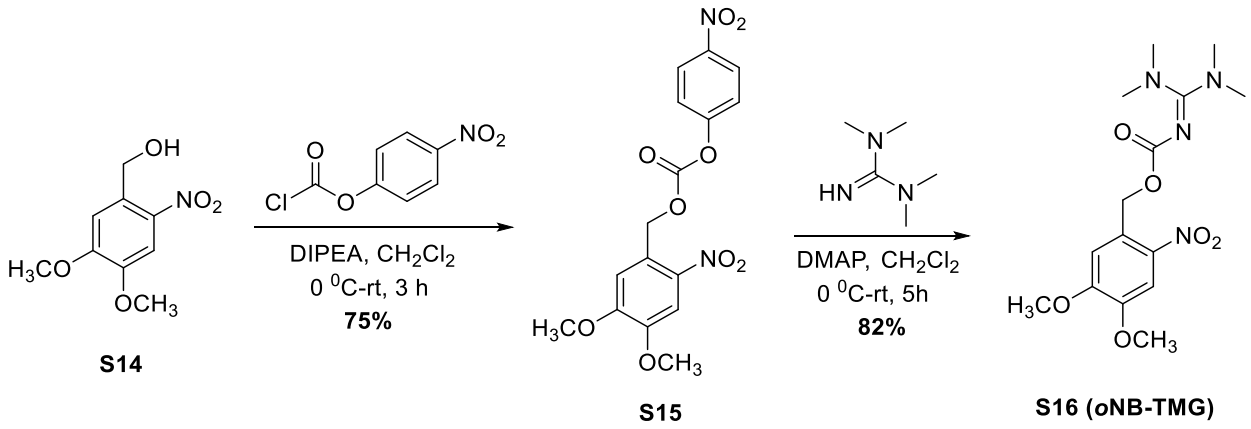

Scheme S6. Synthesis of *o*NB-TMG (S16). A modified protocol was developed for the synthesis of *o*NB-TMG relative to that previously reported by Bowman and coworkers.[S1]

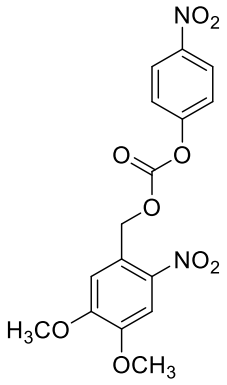

Synthesis of 4,5-dimethoxy-2-nitrobenzyl (4-nitrophenyl) carbonate (S15): Under an inert atmosphere, (4,5-dimethoxy-2-nitrophenyl)methanol (**S14**) (0.50 g, 2.35 mmol) and diisopropylethylamine (2.04 mL, 11.73 mmol) were mixed in 20 mL of anhydrous CH_2Cl_2 at 0 °C. Then 4-nitrophenyl-chloroformate (1.41 g, 7.04 mmol) in 5 mL dry DCM was added dropwise into the solution. The reaction was brought to room temperature after the addition was complete. The reaction was stirred for 12 hours and poured into 50 mL of deionized water and extracted with 3×50 mL of CH_2Cl_2. The combined organic layers were dried over anhydrous $MgSO_4$, filtered, and concentrated under reduce pressure. The crude product was purified by column chromatography with a 0-30% hexanes:ethyl acetate gradient, providing the desired product, 4,5-dimethoxy-2-nitrobenzyl (4-nitrophenyl) carbonate (**S15**) (665 mg, 75%) as a yellow solid. ^{1}H NMR (400 MHz, $CDCl_3$) δ 8.28 (d, J = 9.2 Hz, 2H), 7.76 (s, 1H), 7.41 (d, J = 9.2 Hz, 2H), 7.10 (s, 1H), 5.71 (s, 2H), 4.02 (s, 3H), 3.98 (s, 3H). ^{13}C NMR (101 MHz, $CDCl_3$) δ 155.37, 153.71, 152.10, 148.83, 145.55, 140.03, 125.39, 125.11, 121.74, 110.66, 108.42, 67.71, 56.60, 56.50. HRMS (ESI): exact mass calculated for $C_{16}H_{14}N_2O_9$ $[M+Na]^+$ 401.0592, found 401.0592.

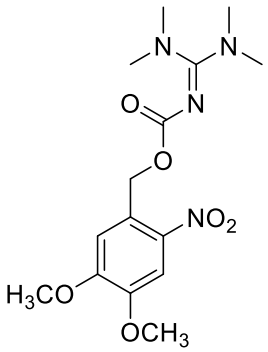

Synthesis of *o*NB-TMG (S16). Under an inert atmosphere, 4,5-dimethoxy-2-nitrobenzyl (4-nitrophenyl) carbonate (**S15**) (0.50 g, 1.32 mmol) was dissolved in 10 mL of anhydrous CH_2Cl_2. Then 4-dimethylaminopyridine (242 mg, 1.98 mmol) was added into the solution, followed by dropwise addition of 1,1,3,3-tetramethylguanidine (TMG) (304 mg, 2.64 mmol) in 2.0 mL of anhydrous CH_2Cl_2. The reaction was monitored by TLC until full conversion of **S15** was achieved. The solution was then concentrated under reduced pressure. The crude product was purified by column chromatography with a 0-3% dichloromethane:methanl gradient, providing the desired product, ***o*NB-TMG** (**S16**) (400 mg, 82%) as a yellow solid. ^{1}H NMR (400 MHz, $CDCl_3$) δ 7.69 (s, 1H), 7.19 (s, 1H), 5.52 (s, 2H), 3.94 (d, J = 9.7 Hz, 6H), 2.88 (s, 12H). ^{13}C NMR (101 MHz, $CDCl_3$) δ 166.74, 159.61, 153.59, 147.62, 139.54, 130.33, 109.73, 107.98, 63.72, 56.36, 39.91. HRMS (ESI): exact mass calculated for $C_{15}H_{22}N_4O_6$ $[M+H]^+$ 355.1612, found 355.1618.

2. INSTRUMENTATION DETAILS

2.1.Light Sources

For FTIR spectroscopy experiments violet and blue LEDs (LCS series, Mightex Systems) were used with an emission centered at ~405 nm and ~470 nm, respectively. These LEDs were used in combination with a current-adjustable driver (SLC-MA02-U, Mightex Systems) for intensity control, such that all intensities between experiments could be matched. Light was delivered via a 3 mm liquid light guide (LLG3-4H, ThorLabs). Irradiation intensities were measured with a ThorLabs PM100D photometer equipped with silicon-based photodiode power sensor (S120VC, ThorLabs).

2.2.Nuclear Magnetic Resonance (NMR) Spectroscopy

NMR spectra were recorded on an Agilent MR 400 MHz spectrometer utilizing chloroform-*d* as the solvent. ^{1}H NMR were carried out coupled and referenced to the chloroform-*d* chemical shift at 7.26 ppm. ^{13}C NMR were carried out decoupled and referenced to the chloroform-*d* chemical shift at 77.16 ppm.

2.3.High Resolution Mass Spectrometry (HRMS)

HRMS was performed on an Agilent Technologies 6530 Accurate-Mass Q-TOF LC/MS using ESI and the data was subsequently analyzed using Agilent MassHunter Qualitative Analysis Software.

2.4.UV-Vis Spectroscopy

UV-vis spectra were obtained using a system from Ocean Insight. The system utilized a balanced deuterium-tungsten halogen light source (DH-2000-BAL) with a typical output of 194 μW (deuterium bulb) and 615 μW (tungsten bulb) through an SMA 905 connector, covering a range from 230 nm – 2.5 μm. Multimode fiber-optic cables with SMA connectors on both ends and a 600 μm core diameter (QP600-025-SR) connected the light source to the sample holder. For dilute solution measurements a qpod cuvette holder (QNW qpod 2e^{TM}) capable of magnetic stirring and peltier-driven temperature control from -30 °C to 105 °C was used. The sample holder was coupled through another multimode fiber to the spectrometer (QEPRO-ABS) having an entrance slit of 5 μm (INTSMA-005 Interchangeable Slit). The spectrometer measured in the range from 200-950 nm, at an optical resolution of 1.7 nm, using a back-thinned, TE cooled, 1024 × 58 element CCD array.

2.5.Fluorimeter

The photoluminescence data was recorded using a Fluorolog3 Fluorimeter, which was equipped with a 450 W ozone-free Xenon arc lamp as the light source and a photomultiplier tube with spectral resolution of 0.1 nm and a detection range from 250 to 1050 nm. Time correlated single photon counting (TCSPC) experiments were also conducted with the Fluorolog3 Fluorimeter. The Xenon lamp was replaced with NanoLEDs (482 nm), providing a time resolution of 300 ps.

2.6.Nanosecond Transient Absorption

The nanosecond transient absorption measurements were conducted using the enVISion® system from MAGNITUDE INSTRUMENTS®. The spectrometer system can measure transient absorption spectra and photoluminescence spectra. The instrument can detect wavelengths from UV to visible to near-IR with a time resolution of ~5 ns.

2.7.Real-Time Fourier Transform Infrared Spectroscopy (RT-FTIR)

Resin formulations were introduced between two 1 mm thick glass microscope slides (cat. no. 12-550-A3, Fisher Scientific) separated by ~100 μm polyester plastic shims (cat. no. 9513K66, McMaster-Carr) to maintain a constant sample thickness over the course of the photopolymerization. Each sample was placed in a horizontal transmission accessory (A043-N/Q, Bruker) equipped on the FTIR spectrometer (INVENIO-R, Bruker), which was controlled using OPUS spectroscopy software. Spectra were collected from 2000 to 7000 cm^{-1} at a rate of 1 scan every 0.36 s. All samples were monitored under ambient conditions (atmospheric and room temperature and pressure). The functional group conversion upon light exposure was determined by monitoring the disappearance of the peak area centered at ~6150 cm^{-1} for the C=C overtone and ~2580 cm^{-1} for the S–H stretch.[S2,S3] Each sample was tested in triplicate.

2.8.High Performance Liquid Chromatography (HPLC)

The LC diagrams were recorded using an Agilent 1260 Infinity II Binary LC System, equipped with a G7165A Multiple Wavelength Detector. The detector recorded UV-Vis spectra ranging from 190 - 950 nm with a repetition rate of 120 Hz. The system was equipped with a C18 reversed phase column (InfinityLab Poroshell 120) as the stationary phase. The mobile phase was a mixture of HPLC grade water and acetonitrile with a typical flow rate of 1 mL/min at room temperature. The injection volume was 1 to 100 μL

3. CHARACTERIZATION

3.1. Emission Quantum Yield Measurements

The emission quantum yields for all derivatives were calculated based on the equation **SE1**:

$$\Phi_{f,x} = \Phi_{f,R} \cdot \frac{A_R}{A_x} \cdot \frac{I_x}{I_R} \cdot \frac{n_x^2}{n_R^2} \qquad \textbf{(SE 1)}$$

where the index *R* denotes the reference dye and *x* denotes the sample, Φ_f is the emission quantum yield, *A* is the absorption, *I* is the integrated emission intensity, and *n* is the refractive index of the solvent being used.[S4] For simplicity, absorption for all samples (in acetonitrile) including the reference dye, Fluorescein (Φ_f = 0.89 in 0.1 M NaOH) were measured under dilute conditions (abs. = 0.1) to prevent aggregation. After recording all the emission spectra for each sample and R6G, the area under the emission curve was integrated to calculate *I*. The refractive indices for acetonitrile and water are 1.34 and 1.33, respectively. Following the equation, Φ_f was calculated for all samples.

Table S1. Summary of photophysical and photochemical properties.

	Abs_{max} (nm)	Em_{max} (nm)	$\varepsilon \times 10^{-3}$ (M^{-1} cm^{-1})
O-H-CTMG	372	463	22 ± 1.8
O-Br-CTMG	399	494	24 ± 2.2
O-I-CTMG	402	-	27 ± 1.5
O-Sty-CTMG	425	516	43 ± 2.8
S-H-CTMG	454	-	22 ± 1.6
o-NB-TMG	349	-	2.8 ± 0.17

Abs_{max}, peak absorption wavelength; Em_{max}, peak fluorescence emission wavelength; ε, molar absorptivity at the peak absorption wavelength

Table S2. Photon counts (photocage absorption and LED emission) relevant to the present study. The calculations were done under the following conditions: [CTMG] = 10^{-5} M in CH_3CN and 405 nm and 470 nm LED set to an impingent intensity of 100 mW/cm^2

	N (405 nm)	N (470 nm)	N' (405 nm)	N' (470 nm)
O-H-CTMG	2.75×10^{17}	5.26×10^{15}	0.17	0.00
O-Br-CTMG	1.08×10^{18}	3.34×10^{16}	0.66	0.02
O-I-CTMG	1.23×10^{18}	6.01×10^{16}	0.75	0.04
O-Sty-CTMG	1.63×10^{18}	6.15×10^{17}	1	0.38
S-H-CTMG	5.42×10^{17}	1.40×10^{18}	0.33	0.86
***o*NB-TMG**	1.07×10^{16}	1.98×10^{15}	0.01	0.00
405 nm LED	2.82×10^{18}	-	-	-
470 nm LED	-	5.47×10^{18}	-	-

N = number of photons absorbed; **N'** = relative number of photons absorbed to **O-Sty-CTMG** with the 405 nm LED.

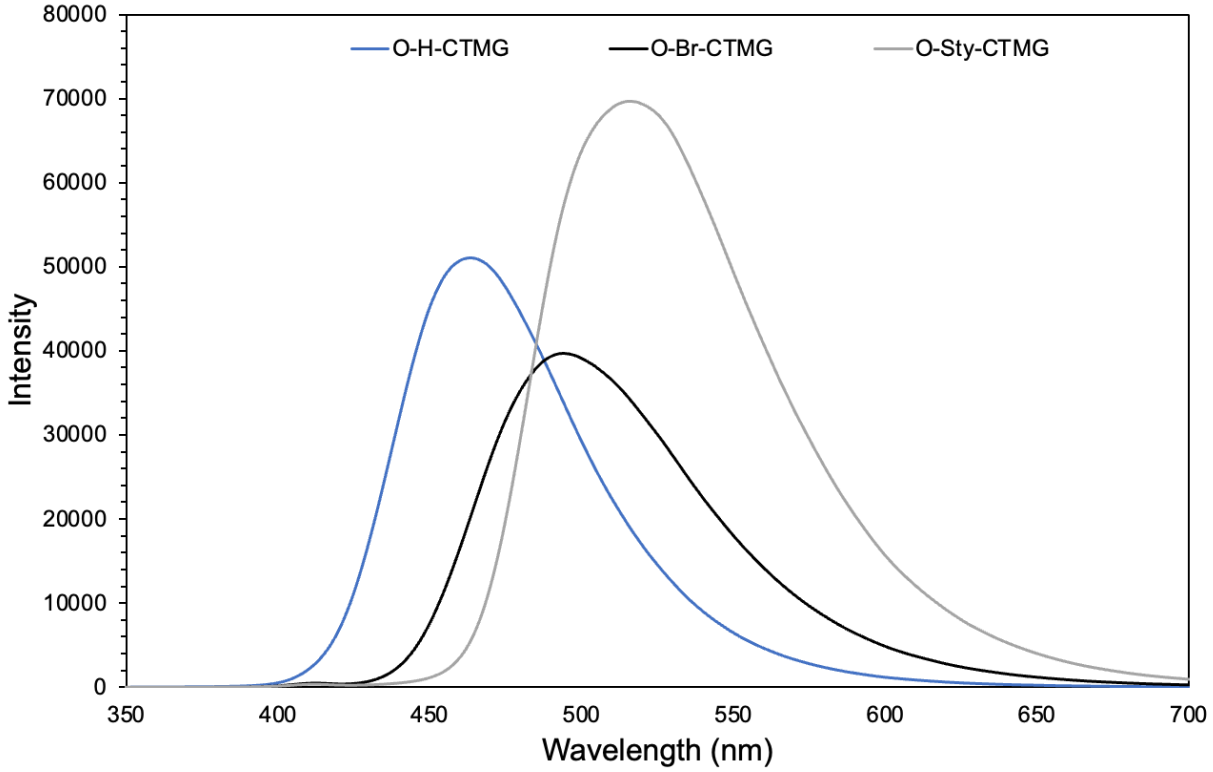

Figure S1. Fluorescence spectra of **O-H-CTMG**, **O-Br-CTMG**, and **O-Sty-CTMG** collected in degassed CH_3CN at a concentration of 10^{-5} M.

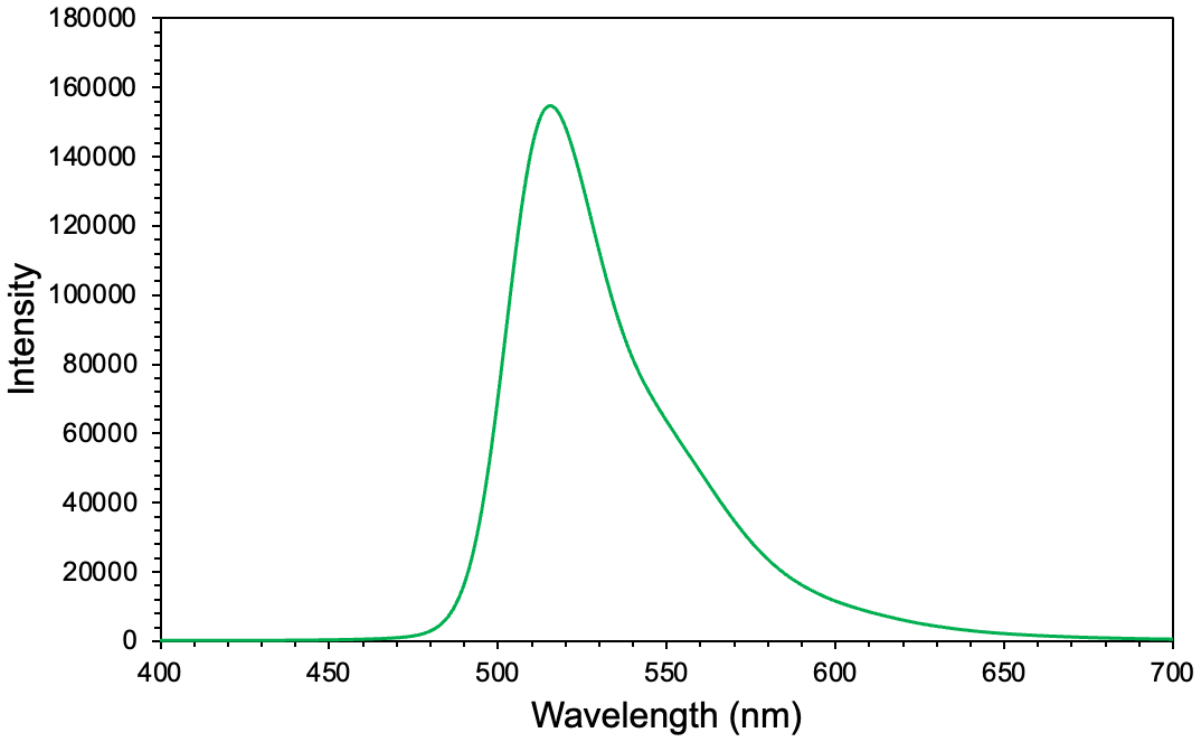

Figure S2. Fluorescence spectrum of Fluorescein collected in degassed CH_3CN at a concentration of 10^{-5} M and used as the emission standard.

3.2. RT-FTIR Data

The difference between "ene" and thiol conversion was calculated using the following equation:

$$\Delta p = (Conversion\ of\ 'ene' - Conversion\ of\ 'thiol') \quad \textbf{(SE 2)}$$

This value was calculated by taking the average maximum conversion for each trial (in triplicate) for C=C and S–H traces, with ±1 standard deviation from the mean provided.

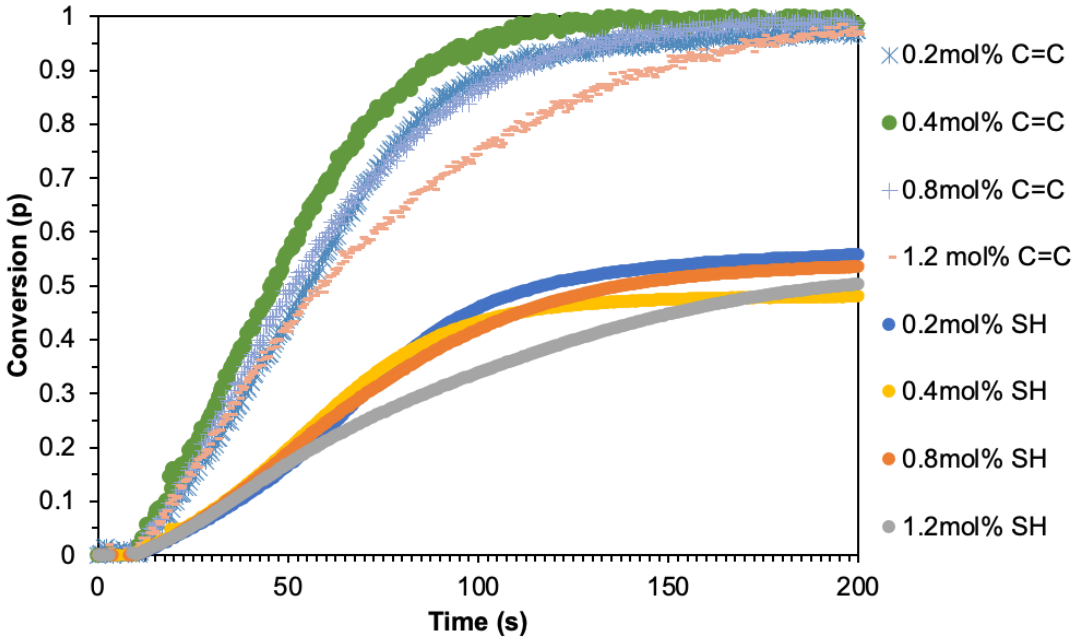

Figure S3. Photopolymerization kinetics gathered using RT-FTIR for different concentrations (mol%) of the **O-H-CTMG** (**S3**) photobase in HDDA (2eq) / PETMP (1eq) resin. The light turned was 'on' at t = 10s (405 nm LED, 20mW/cm^2).

Table S3. Tabulated data from RT-FTIR spectroscopy characterization of O-H-CTMG (S3) (0.4mol%) in different resin mixtures (all 1:1 equal functionality). Samples measured with 405 nm LED (100 mW/cm^2) turned 'on' at t = 10s. Corresponding traces provided Figure S4 below and in Figure 3B of the main manuscript.

Resin Mixture	Rate (mM/s)		Final Conversion (%)		Δp (%)
	C=C	S–H	C=C	S–H	
HDDA/DODT	40.4 ± 3.4	25.4 ± 1.2	100.0 ± 0.0	64.8 ± 0.5	35.2 ± 0.5
HDDA/HDT	32.6 ± 2.1	20.1 ± 1.4	99.7 ± 2.7	62.2 ± 2.5	37.5 ± 3.8
TEGDA/DODT	31.2 ± 5.1	9.7 ± 0.5	99.4 ± 1.0	49.1 ± 1.0	50.3 ± 1.5
TEGDA/HDT	14.3 ± 2.1	4.1 ± 0.3	83.4 ± 0.5	29.4 ± 0.3	54.0 ± 0.2

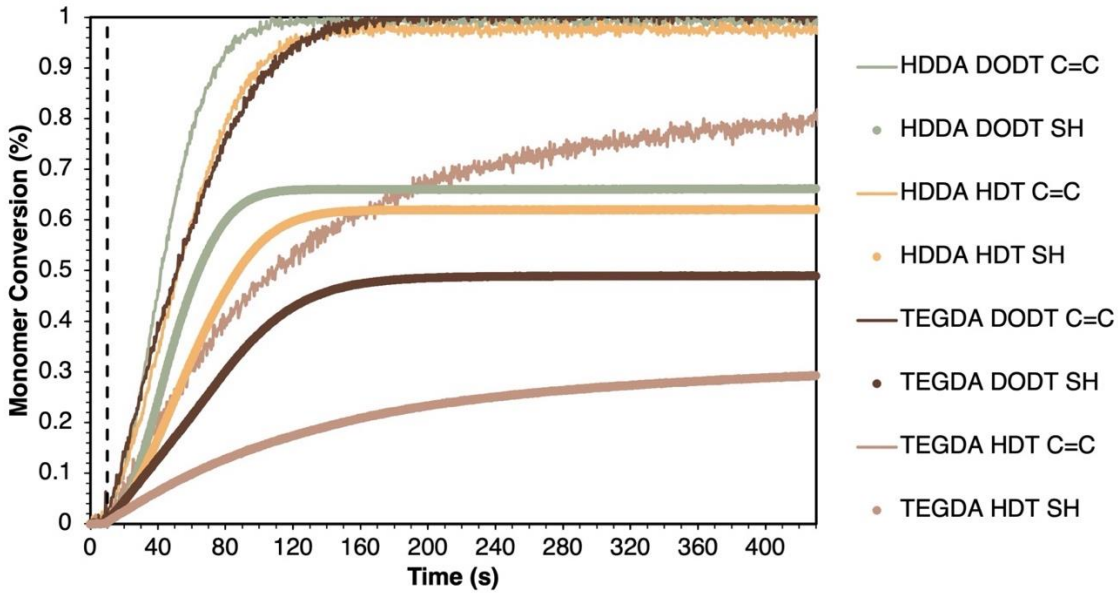

Figure S4. Photopolymerization kinetics gathered using RT-FTIR for 0.4 mol% of the **O-H-CTMG** (**S3**) photobase in in different resin mixtures (all 1:1 equal functionality). The light turned was 'on' at t = 10s (405 nm LED, 100mW/cm^2). Tabulated data provided in **Table S3** above.

Table S4. Tabulated data from RT-FTIR spectroscopy characterization of BAPO (0.4mol%) in HDDA/DODT (1:1 equal functionality). Samples measured with 405 nm LED (0.2 mW/cm^2) turned 'on' at t = 10s. Corresponding traces provided in Figure S5 below.

Resin Mixture	Rate (mM/s)		Final Conversion (%)		$\Delta \rho$ (%)
	C=C	S–H	C=C	S–H	
HDDA/DODT	69.7 ± 12.8	30.3 ± 3.9	100.0 ± 0.4	55.2 ± 1.1	44.8 ± 1.2

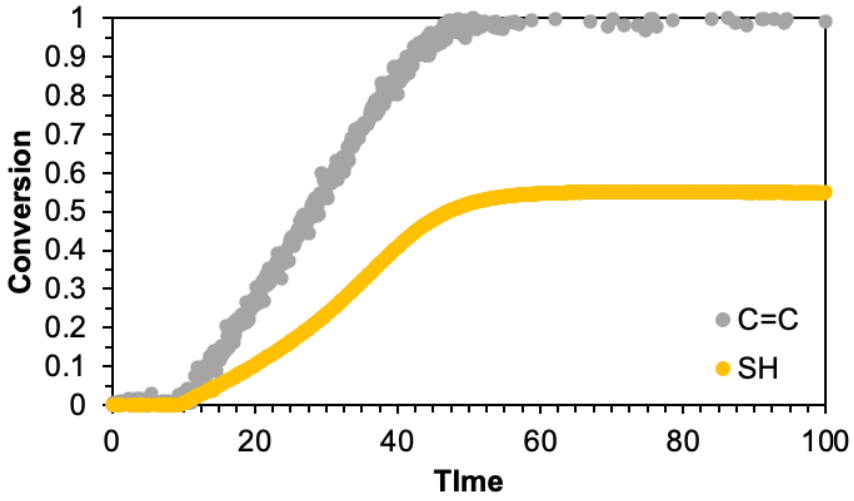

Figure S5. RT-FTIR traces for BAPO (0.4mol%) irradiated with a 405 nm LED at 0.20 mW/cm^2 in HDDA/DODT. Tabulated data provided in **Table S4**.

Table S5. Tabulated data from RT-FTIR spectroscopy characterization of different PBGs in HDDA/DODT (1:1 equal functionality). Samples measured with 405 nm LED (100 mW/cm^2) turned 'on' at *t* = 10s. Corresponding traces provided in Figure 4A in the main manuscript.

Derivative	Rate (mM/s)		Final Conversion (%)		$\Delta\rho$ (%)
	C=C	S–H	C=C	S–H	
O-H-CTMG	40.3 ± 3.4	40.3 ± 3.4	100.0 ± 0.0	64.8 ± 0.5	35.2 ± 0.5
O-Br-CTMG	161.5 ± 15.7	161.5 ± 15.7	99.7 ± 1.3	49.4 ± 0.4	50.3 ± 1.6
O-I-CTMG	77.1 ± 8.3	77.1 ± 8.3	101.1 ± 2.4	56.1 ± 0.9	45.0 ± 2.7
S-H-CTMG	3.9 ± 1.6	3.9 ± 1.6	43.0 ± 19.1	25.5 ± 11.7	17.5 ± 8.3
O-Sty-CTMG	27.5 ± 0.9	27.5 ± 0.9	99.7 ± 0.9	87.3 ± 0.7	12.4 ± 1.4
***o*NB-TMG**	16.8 ± 1.1	16.8 ± 1.1	98.1 ± 1.0	86.0 ± 0.4	12.1 ± 0.7

Table S6. Tabulated data from RT-FTIR spectroscopy characterization of different PBGs in HDDA/DODT (1:1 equal functionality). Samples measured with 470 nm LED (100 mW/cm^2) turned 'on' at *t* = 10s. Corresponding traces provided in Figure 4B in the main manuscript.

Derivative	Rate (mM/s)		Final Conversion (%)		$\Delta\rho$ (%)
	C=C	S–H	C=C	S–H	
O-H-CTMG	1.2 ± 0.3	0.4 ± 0.1	22.1 ± 3.1	5.6 ± 1.6	16.5 ± 3
O-Br-CTMG	27.1 ± 4.5	11.0 ± 2.3	100.5 ± 3.1	52.4 ± 0.9	48.0 ± 4
O-I-CTMG	42.7 ± 2.8	19.4 ± 3.6	100.3 ± 0.2	50.2 ± 0.5	50.1 ± 1
S-H-CTMG	1.2 ± 0.9	0.3 ± 0.2	15.3 ± 8.3	7.0 ± 2.6	8.3 ± 6
O-Sty-CTMG	28.4 ± 1.1	23.7 ± 0.4	100.3 ± 0.7	85.2 ± 0.4	15.1 ± 0.2
***o*NB-TMG**	0.8 ± 0.7	0.1 ± 0.1	6.6 ± 1.3	2.7 ± 1.0	3.9 ± 1

3.3.Uncaging Quantum Yield

The uncaging quantum yield (Φ_u) was determined by the ratio of decay flux (μ_{decay}) and photon flux (μ_{photon}) (**Equations SE3** and **SE4**).[1] The decay flux (μ_{decay}) was measured using RT-FTIR by monitoring the disappearance of stretches from the carbamate bond (~1600 cm^{-1}) during LED irradiation.[S1] The photon flux was calculated from the LED intensity used.

$$\Phi_u = \frac{\mu_{decay}}{\mu_{photon}} \qquad \textbf{(SE3)}$$

$$\mu_{photon}(cm^{-2}s^{-1}) = I\frac{Wcm^{-2}}{E}(J) \qquad \textbf{(SE4)}$$

Table S7. Fluorescence and bond scission quantum yields.

	Φ_f	Φ_s (%)
O-H-CTMG	0.3 ± 0.002	0.06 ± 0.012
O-Br-CTMG	0.23 ± 0.003	0.29 ± 0.033
O-I-CTMG	<0.01	0.35 ± 0.047
O-Sty-CTMG	0.41 ± 0.003	0.043 ± 0.012
S-H-CTMG	<0.01	0.041 ± 0.008
o-NB-TMG	-	5.7 ± 0.32

Φ_f, fluorescence quantum yield; Φ_s, bond scission quantum yield

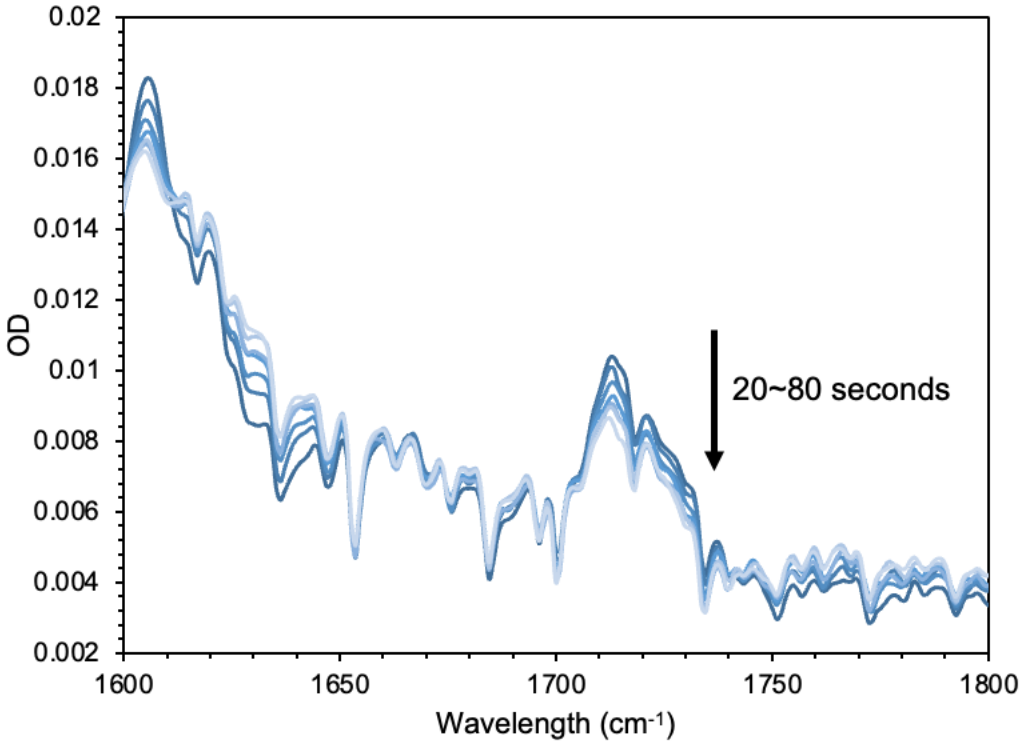

Figure S6. Representative real-time Fourier transform infrared spectra monitoring the carbamate bond decomposition at 1710 cm^{-1} for **O-H-CTMG** using a 405 nm LED at an intensity of 400 mW/cm^2.

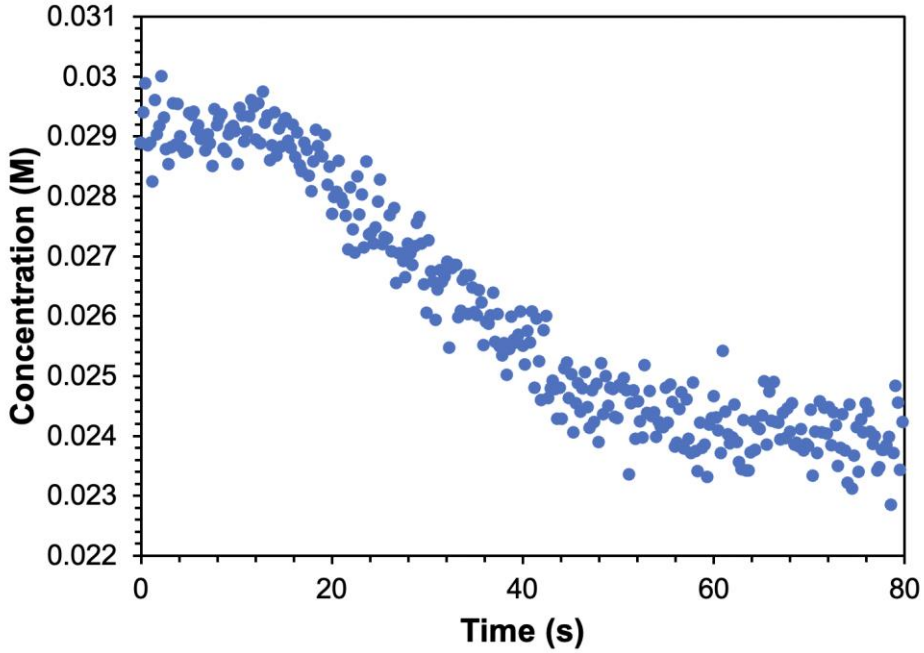

Figure S7. Analysis of the carbamate bond decomposition at 1710 cm^{-1} from real-time Fourier transform infrared spectroscopy for **O-H-CTMG** upon exposure to a 405 nm LED at an intensity of 400 mW/cm^2. **O-H-CTMG** (0.5 mol%) was dissolved in 3,6-dioxa-1,8-octanedithiol (DODT). LED was turned on 15 seconds after the measurement.

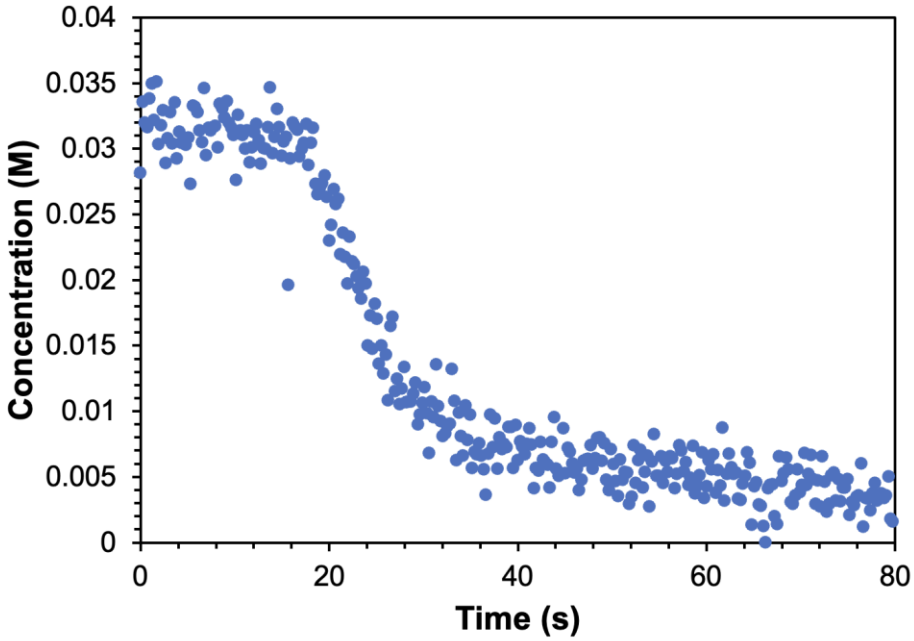

Figure S8. Analysis of the carbamate bond decomposition at 1710 cm^{-1} from real-time Fourier transform infrared spectroscopy for **O-Br-CTMG** upon exposure to a 405 nm LED at an intensity of 400 mW/cm^2. **O-Br-CTMG** (0.5 mol%) was dissolved in 3,6-dioxa-1,8-octanedithiol (DODT). LED was turned on 15 seconds after the measurement.

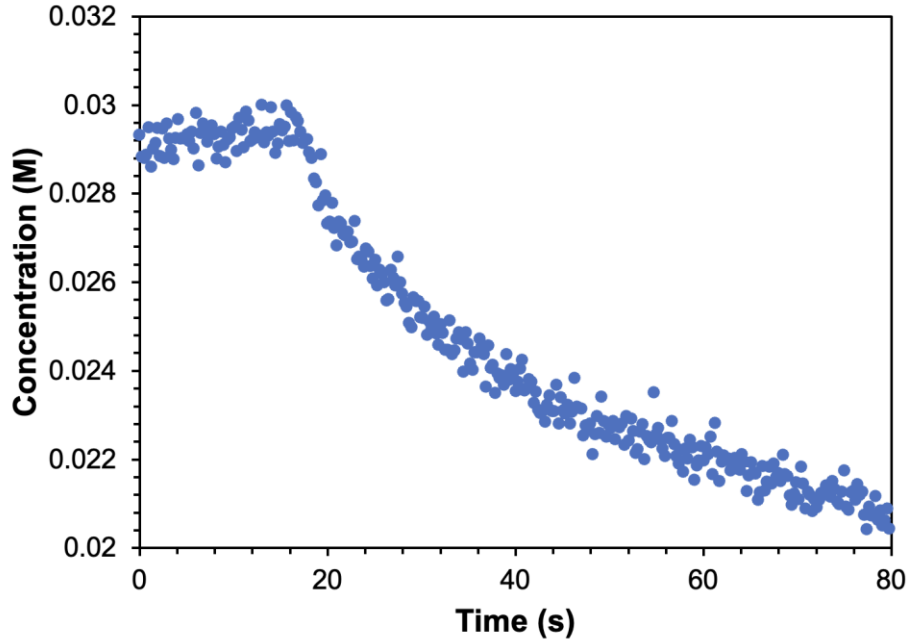

Figure S9. Analysis of the carbamate bond decomposition at 1710 cm^{-1} from real-time Fourier transform infrared spectroscopy for **O-I-CTMG** upon exposure to a 405 nm LED at an intensity of 400 mW/cm^2. **O-I-CTMG** (0.5 mol%) was dissolved in 3,6-dioxa-1,8-octanedithiol (DODT). LED was turned on 15 seconds after the measurement.

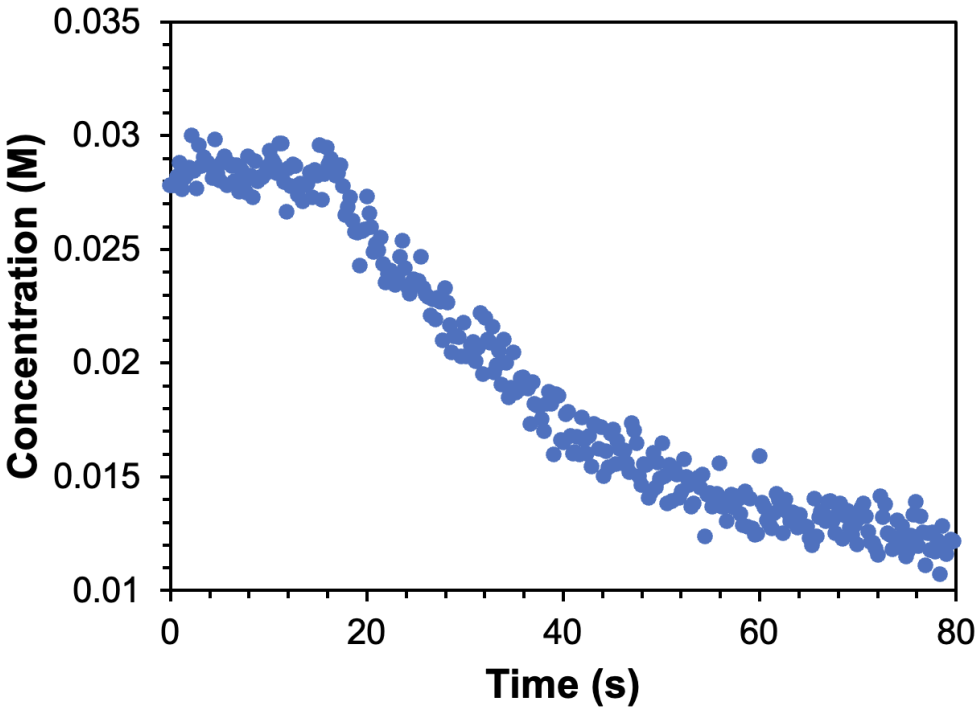

Figure S10. Analysis of the carbamate bond decomposition at 1710 cm^{-1} from real-time Fourier transform infrared spectroscopy for **O-Sty-CTMG** upon exposure to a 405 nm LED at an intensity of 400 mW/cm^2. **O-Sty-CTMG** (0.5 mol%) was dissolved in 3,6-dioxa-1,8-octanedithiol (DODT). LED was turned on 15 seconds after the measurement.

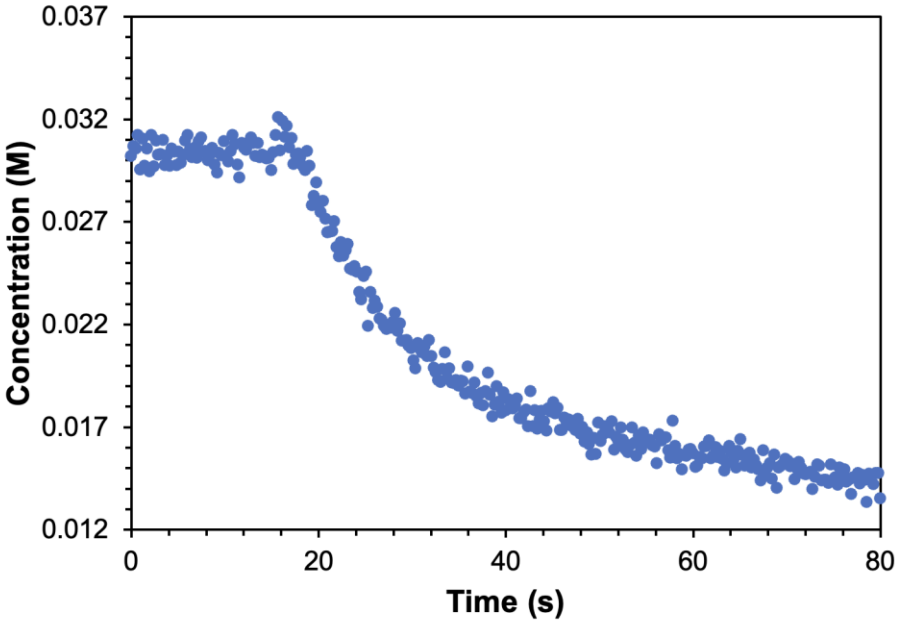

Figure S11. Analysis of the carbamate bond decomposition at 1710 cm^{-1} from real-time Fourier transform infrared spectroscopy for **S-H-CTMG** upon exposure to a 405 nm LED at an intensity of 400 mW/cm^2. **S-H-CTMG** (0.5 mol%) was dissolved in 3,6-dioxa-1,8-octanedithiol (DODT). LED was turned on 15 seconds after the measurement.

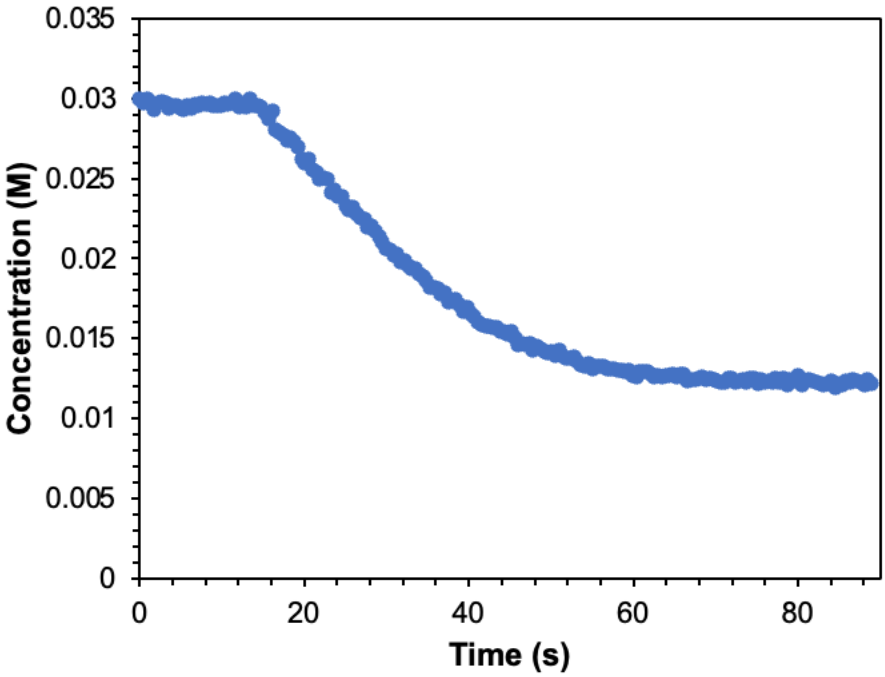

Figure S12. Analysis of the carbamate bond decomposition at 1710 cm^{-1} from real-time Fourier transform infrared spectroscopy for ***o*NB-TMG** upon exposure to a 405 nm LED at an intensity of 400 mW/cm^2. ***o*NB-TMG** (0.5 mol%) was dissolved in 3,6-dioxa-1,8-octanedithiol (DODT). LED was turned on 15 seconds after the measurement.

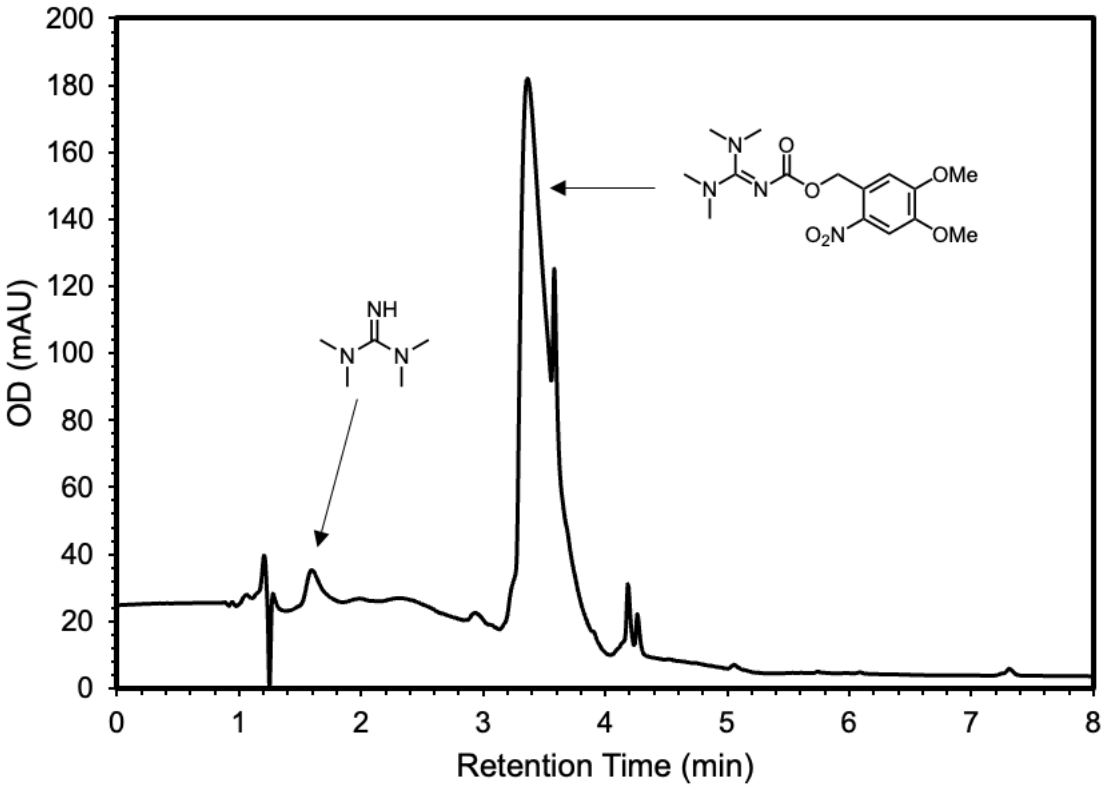

Figure S13. Representative trace from HPLC analysis of ***o*NB-TMG** degradation in CH_3CN/H_2O (*v*:*v* = 4:1) after 60 seconds of LED irradiation (365 nm, 12 mW/cm^2).

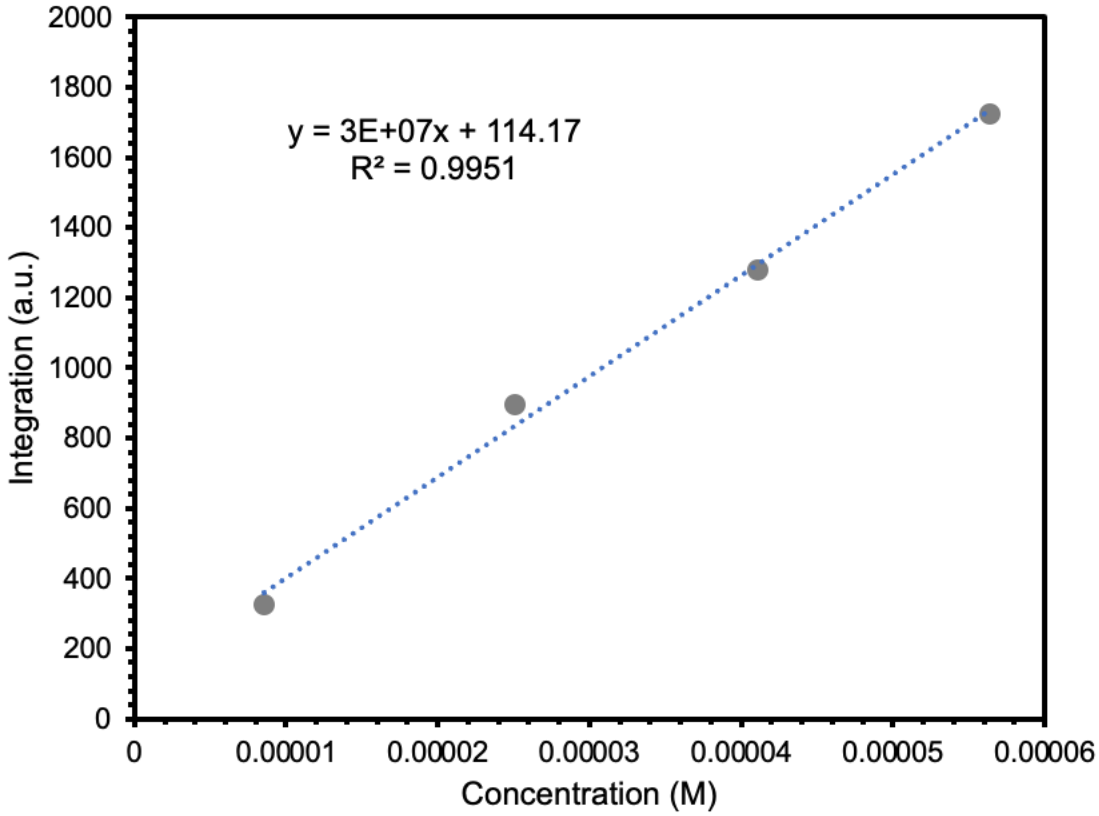

Figure S14. Calibration curve of TMG in CH_3CN from using HPLC to quantify the photouncaging quantum yield for ***o*NB-TMG**.

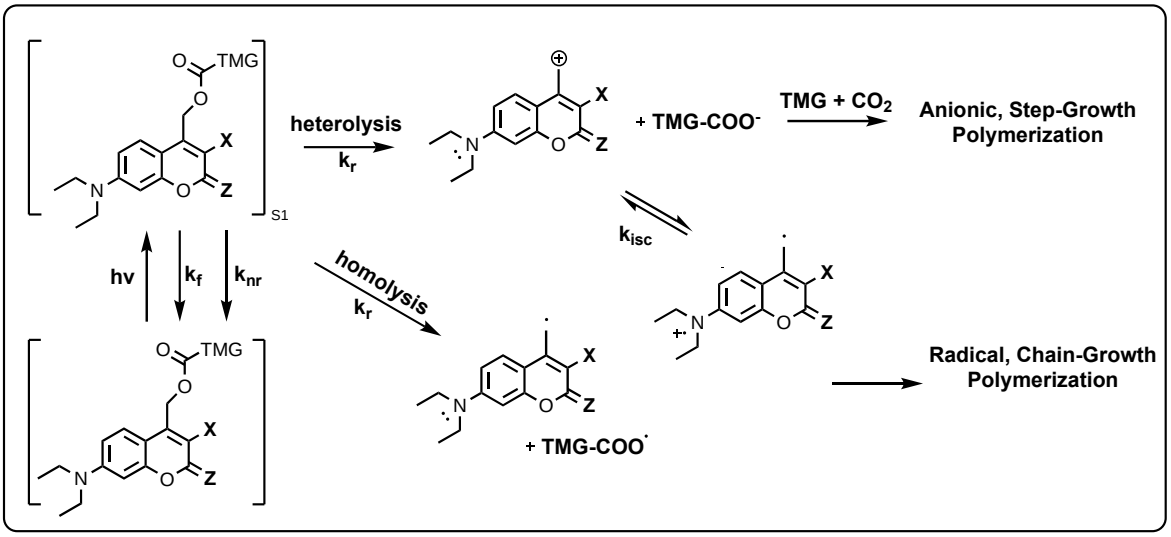

Scheme S7. Proposed uncaging mechanism for **Z-X-CTMG** derivatives.

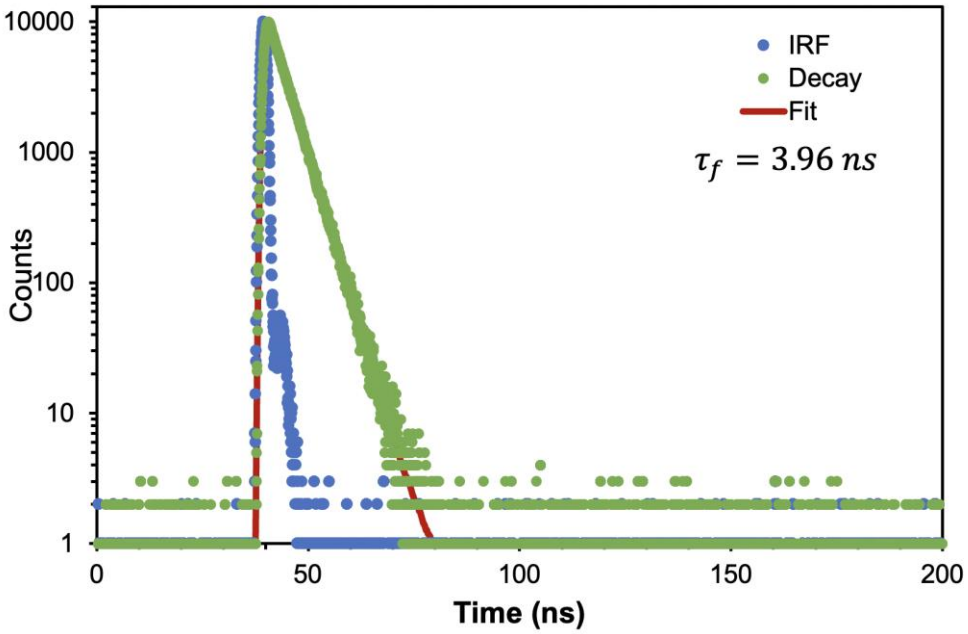

Figure S15. Excited-state relaxation kinetics of **O-H-CTMG** collected in acetonitrile, excited at 402 nm, and monitored at 470 nm.

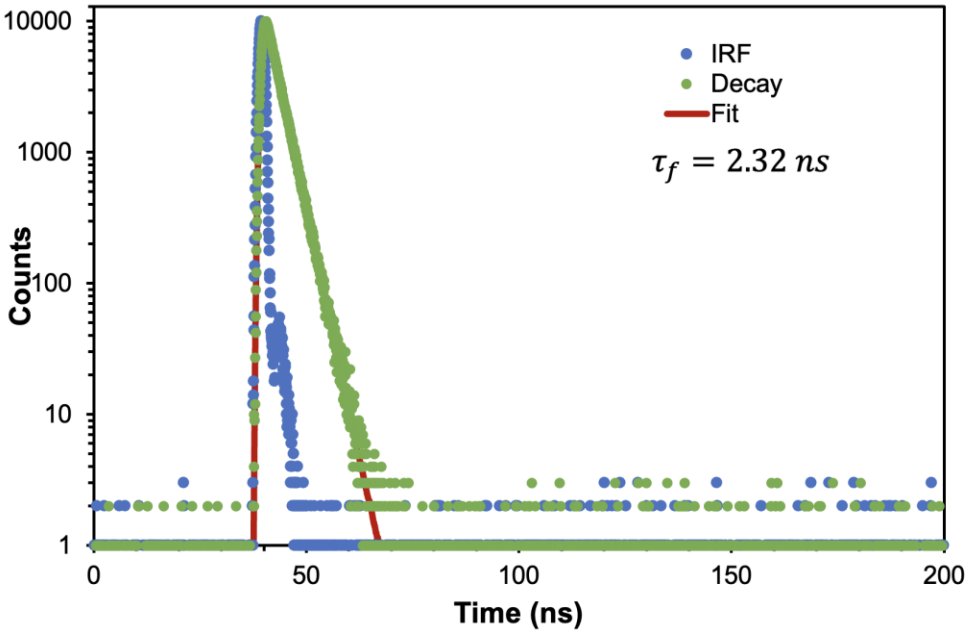

Figure S16. Excited-state relaxation kinetics of **O-Br-CTMG** collected in acetonitrile, excited at 402 nm, and monitored at 500 nm.

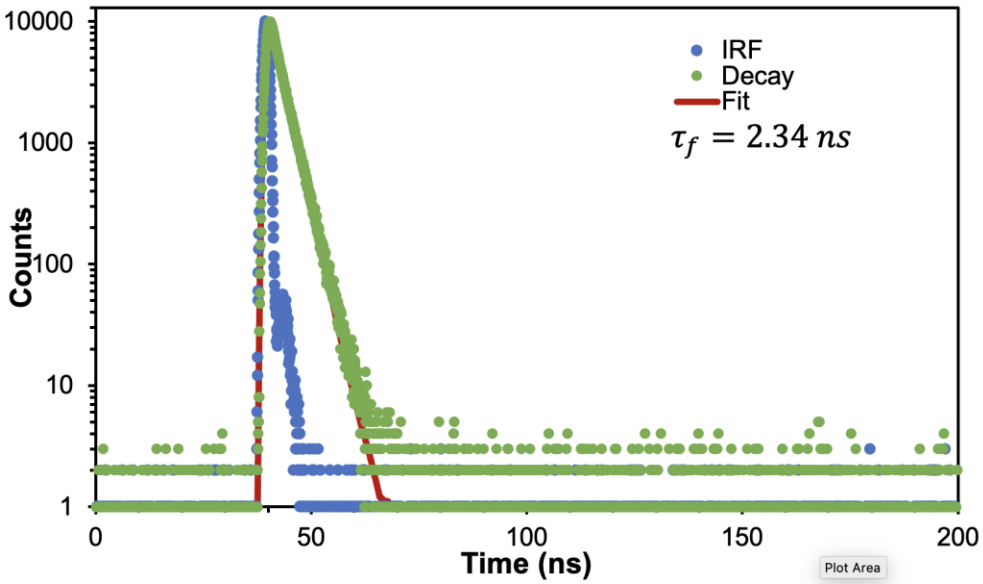

Figure S17. Excited-state relaxation kinetics of **O-Sty-CTMG** collected in acetonitrile, excited at 402 nm, and monitored at 520 nm.

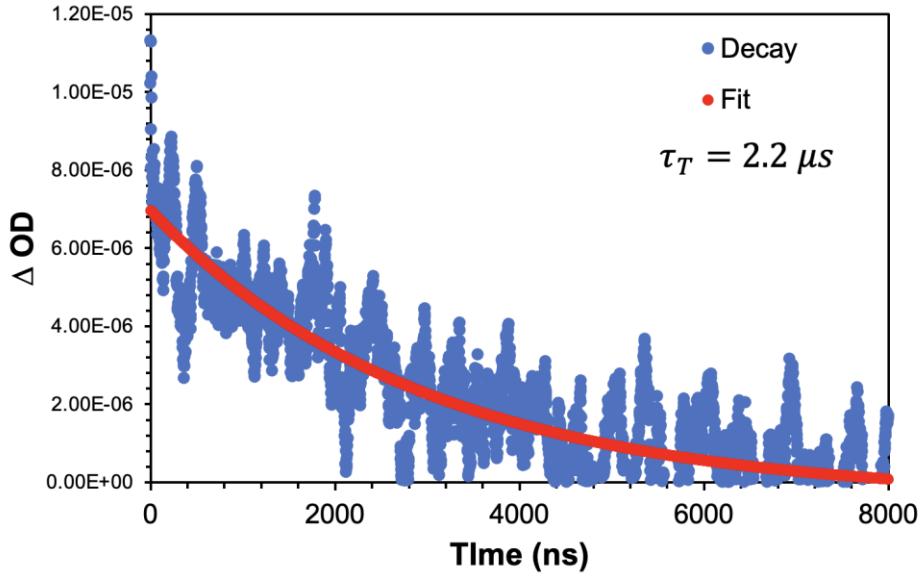

Figure S18. Nanosecond transient absorption data for **O-I-CTMG** collected in acetonitrile, excited at 355 nm, and monitored at 450 nm.

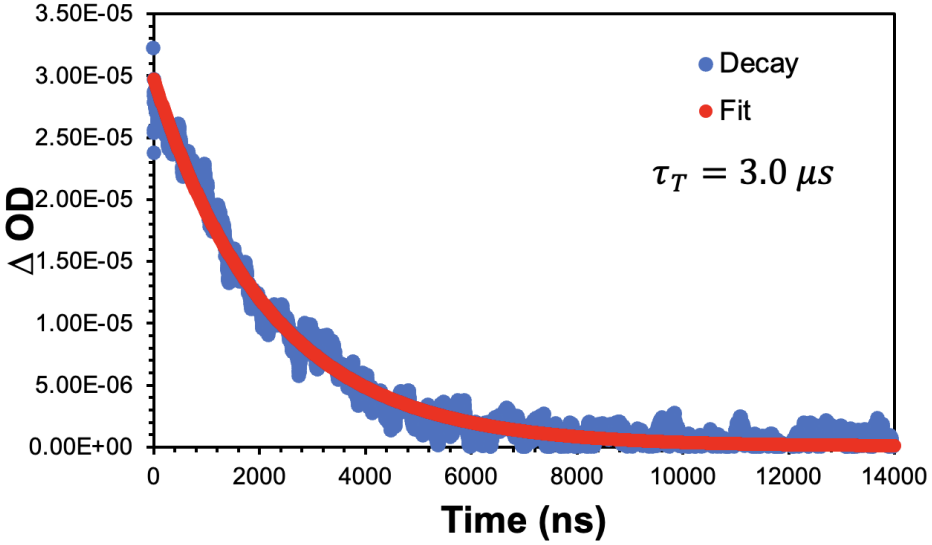

Figure S19. Nanosecond transient absorption data for **S-H-CTMG** collected in acetonitrile, excited at 355 nm, and monitored at 450 nm.

Table S8. Fluorescence and triplet-state lifetimes.

	τ_F (ns)	τ_T (µs)
O-H-CTMG	3.96	-
O-Br-CTMG	2.32	-
O-I-CTMG	-	2.2
O-Sty-CTMG	2.34	-
S-H-CTMG	-	3.0
o-NB-TMG	-	-

τ_F, fluorescence lifetime; τ_T, triplet-state lifetime

3.4.TEMPO Studies

Table S9. Effect of TEMPO concentration on polymerization rate (mM/s) and Δρ (%) for O-H-CTMG derivative (1:1 HDDA/DODT; 405 nm LED, 100mW/cm^2). Corresponding traces provided in Figure 6B in the main manuscript.

Amount of TEMPO (mol%) (equivalents)	Rate (mM/s)		Δρ (%)
	C=C	SH	
0	40.334 ± 3.44	25.37 ± 1.19	35.2 ± 0.5
0.005 (0.0125×)	36.206 ± 0.79	22.188 ± 0.89	29.2 ± 1.0
0.05 (0.125×)	24.94 ± 1.07	22.188 ± 1.37	3.5 ± 1.6
0.1 (0.25×)	25.198 ± 3.62	22.876 ± 1.95	3.3 ± 2.4
0.2 (0.5×)	27.864 ± 0.93	24.854 ± 1.87	3.4 ± 0.8
0.4 (1×)	27.95 ± 1.51	24.338 ± 0.30	6.0 ± 0.9
0.8 (2×)	23.392 ± 0.30	20.554 ± 1.00	6.3 ± 0.8

Table S10. Effect of TEMPO concentration on polymerization rate (mM/s) and Δρ (%) for O-Br-CTMG derivative (1:1 HDDA/DODT; 405 nm LED, 100mW/cm^2). Corresponding traces provided in Figure S20 below.

Amount of TEMPO (mol%) (equivalents)	Rate (mM/s)		Δρ (%)
	C=C	SH	
0	161.51 ± 15.7	78.86 ± 6.1	50.3 ± 1.6
0.05 (0.125×)	95.37 ± 8.1	47.39 ± 2.3	38.5 ± 3.0
0.1 (0.25×)	34.74 ± 4.1	24.25 ± 1.1	41.9 ± 2.0
0.4 (1×)	15.22 ± 2.0	12.13 ± 1.4	9.3 ± 1.2

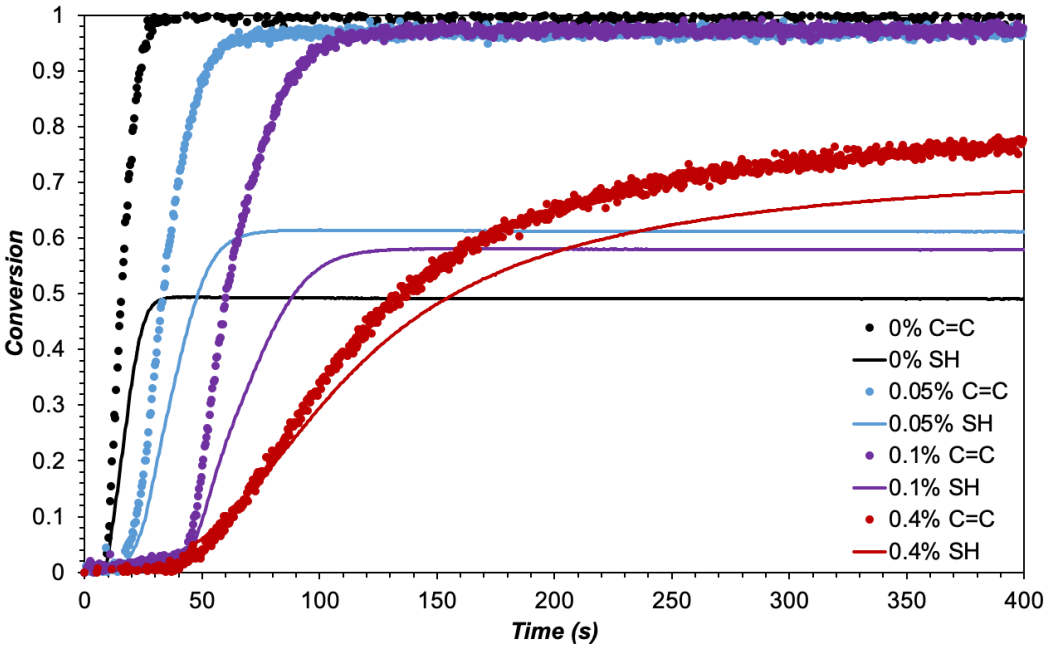

Figure S20. RT-FTIR traces for **O-Br-CTMG** derivative with added TEMPO. Tabulated data in **Table S8**.

Table S11. Effect of TEMPO concentration on polymerization rate (mM/s) and $\Delta\rho$ (%) for O-I-CTMG derivative (1:1 HDDA/DODT; 405 nm LED, 100mW/cm^2). Corresponding traces provided in Figure S21 below.

Amount of TEMPO (mol%)	Rate (mM/s)		$\Delta\rho$ (%)
	C=C	SH	
0	77.1 ± 8.3	39.6 ± 2.0	45.0 ± 2.7
0.4 (1×)	1.52 ± 0.1	16.8 ± 0.8	43.2 ± 0.6
1.0 (2.5×)	0 ± 0	1.2 ± 0.1	3.4 ± 1.0

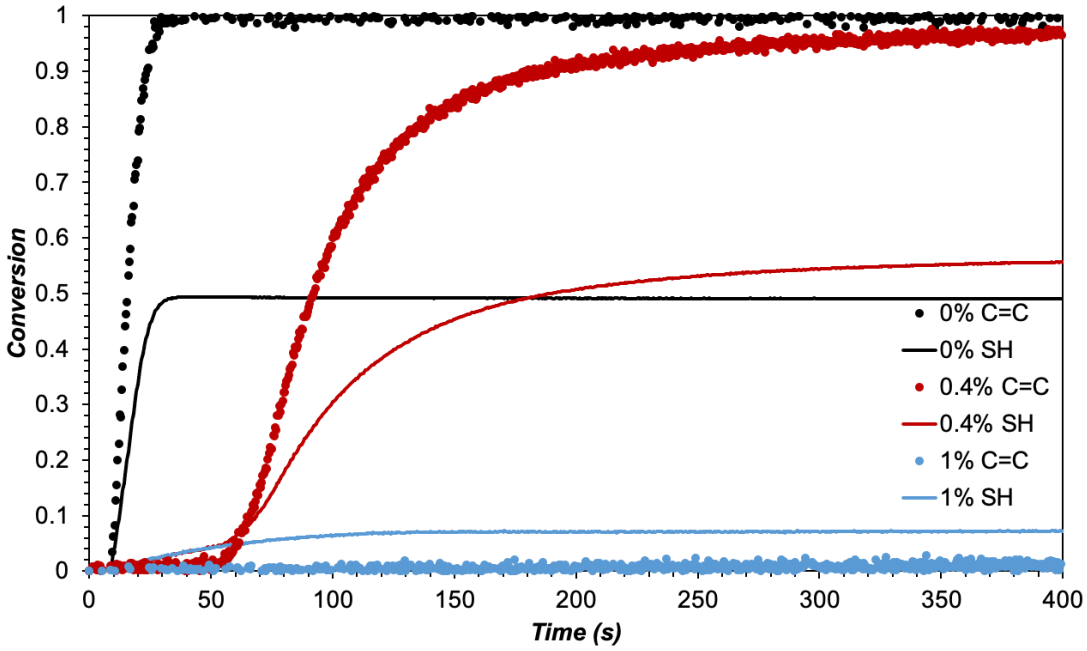

Figure S21. RT-FTIR traces for **O-I-CTMG** derivative with added TEMPO. Tabulated data in **Table S9**.

3.5. ^{1}H- and ^{13}C-NMR Spectra

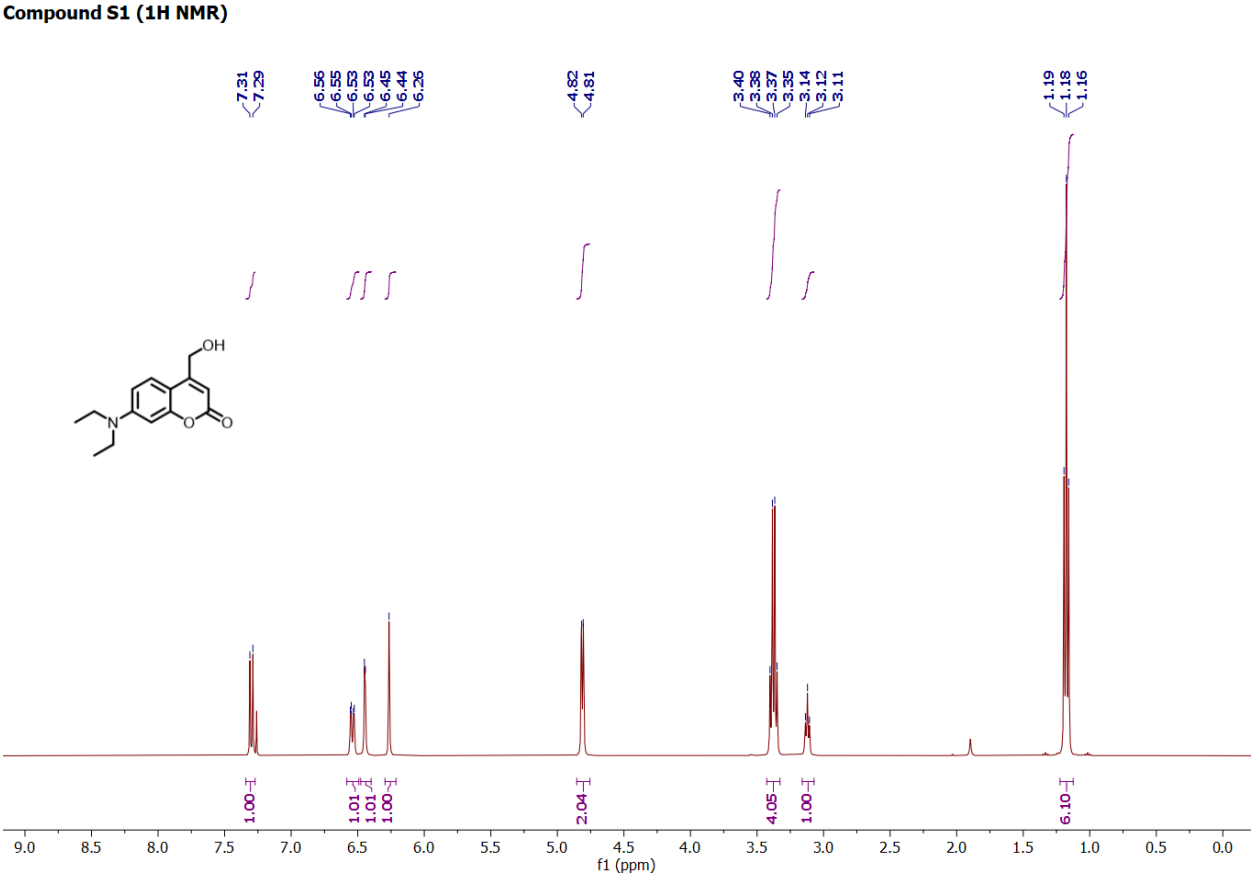

Figure S22. ^{1}H-NMR of compound **S1** in chloroform-*d*.

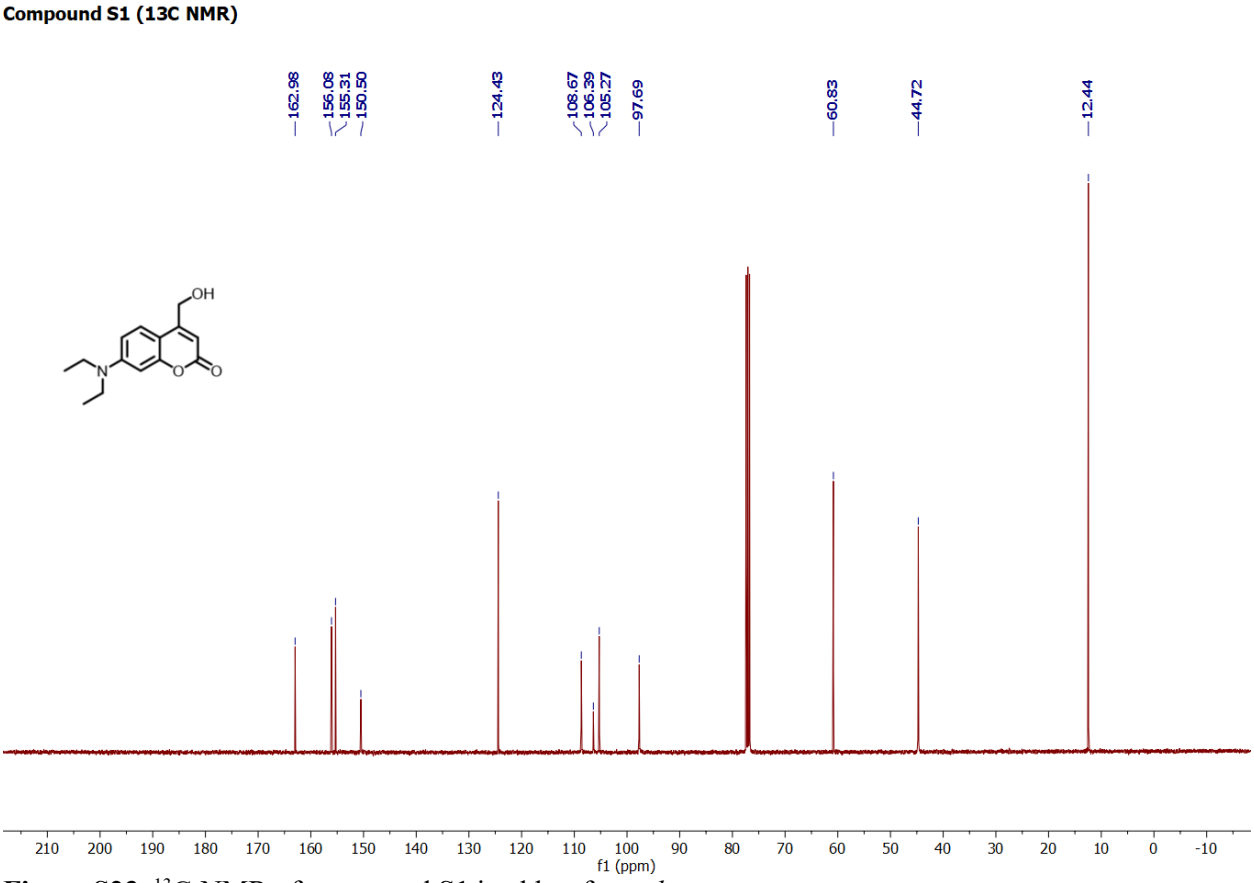

Figure S23. ^{13}C-NMR of compound **S1** in chloroform-*d*.

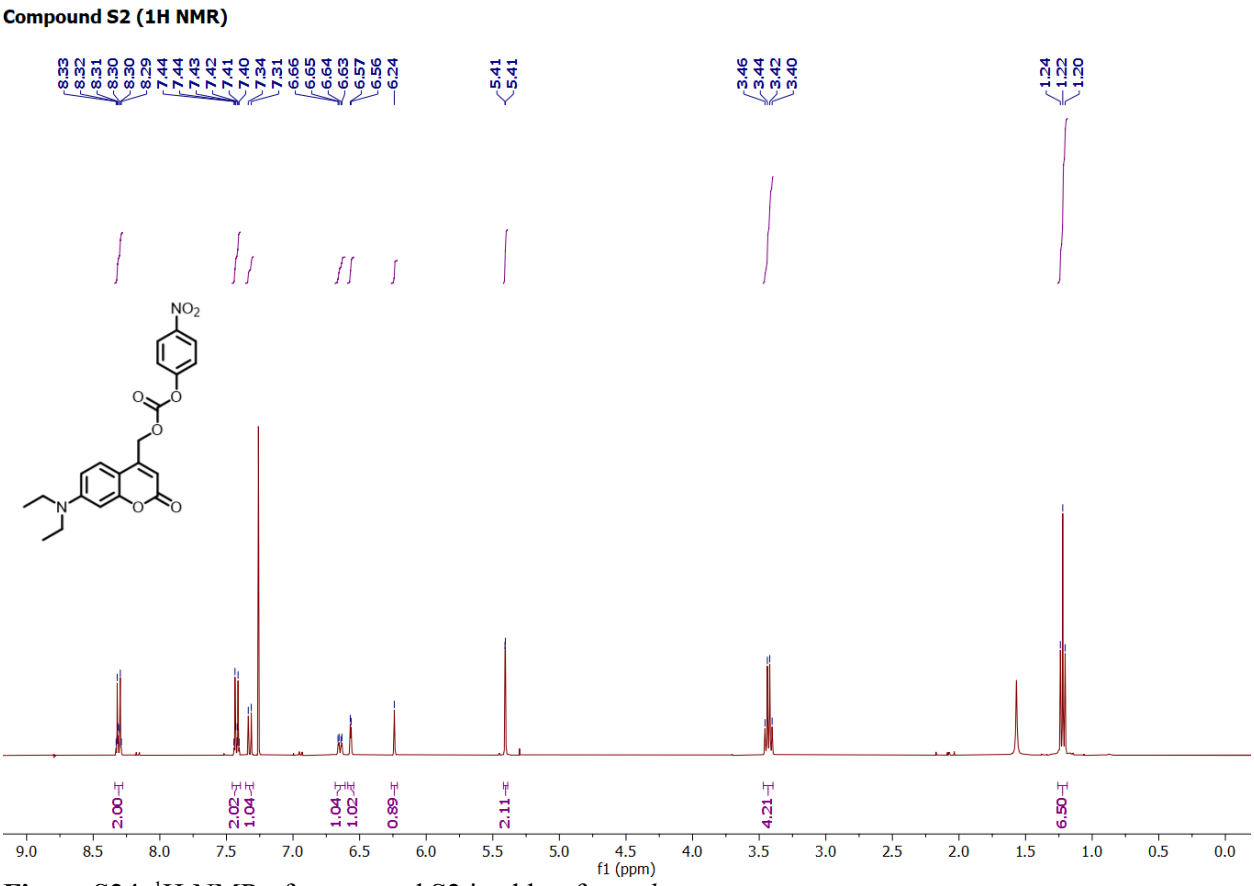

Figure S24. ^{1}H-NMR of compound **S2** in chloroform-*d*.

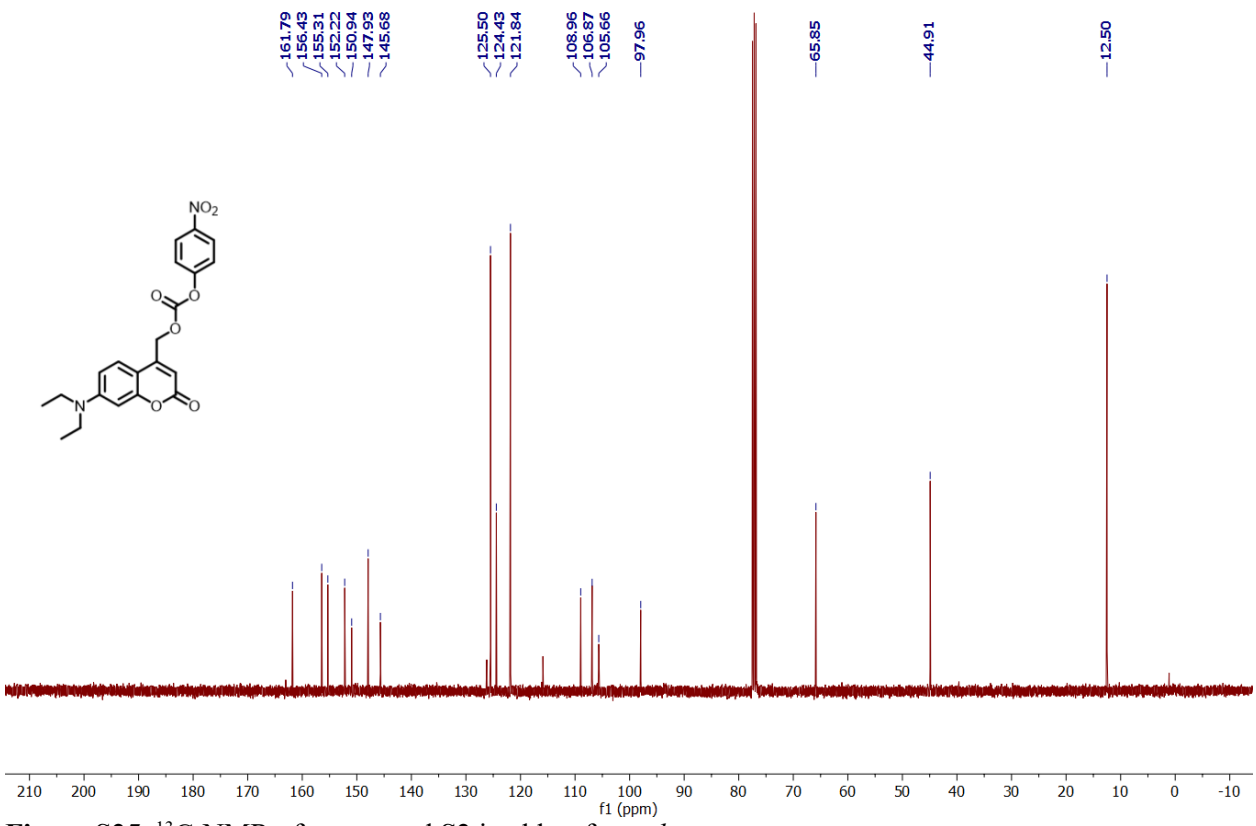

Figure S25. ^{13}C-NMR of compound **S2** in chloroform-*d*.

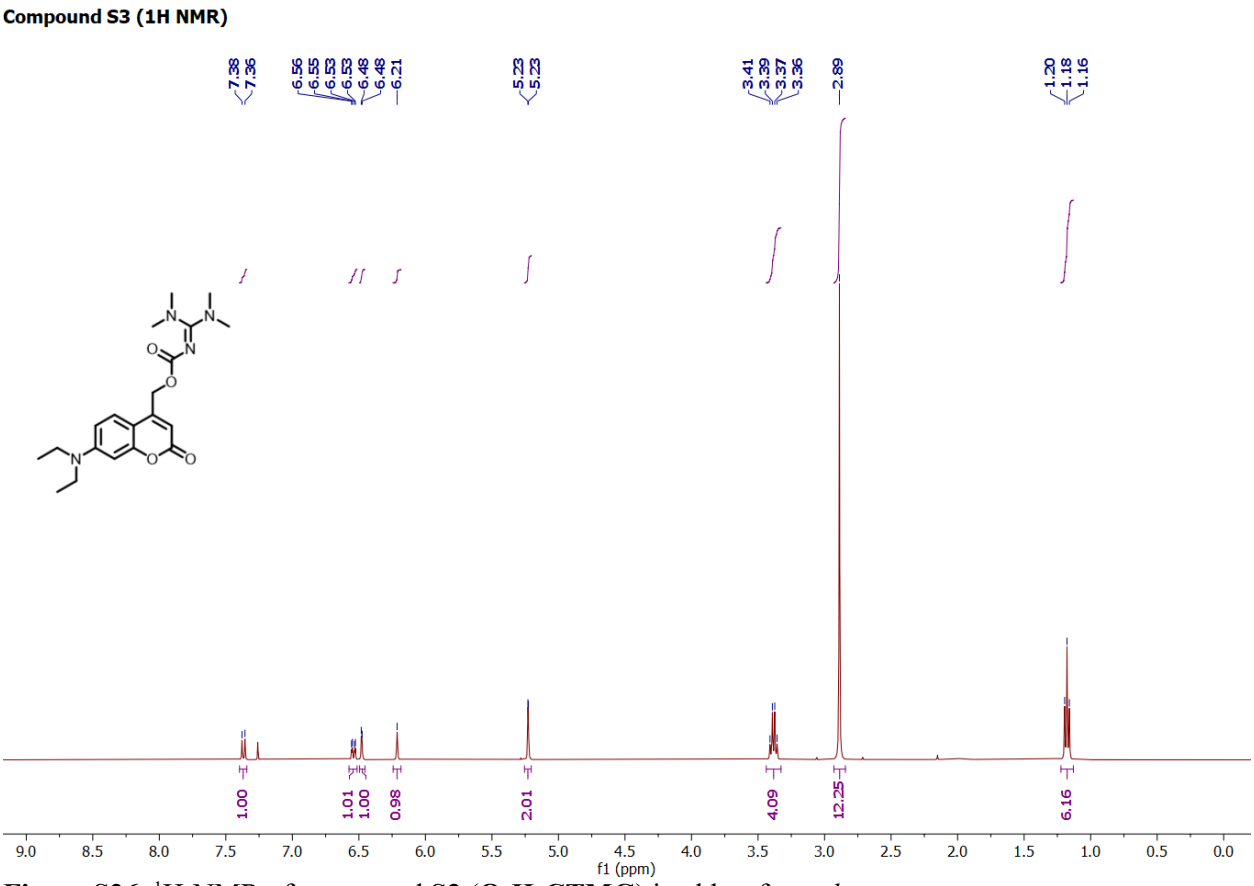

Figure S26. ^{1}H-NMR of compound **S3** (**O-H-CTMG**) in chloroform-*d*.

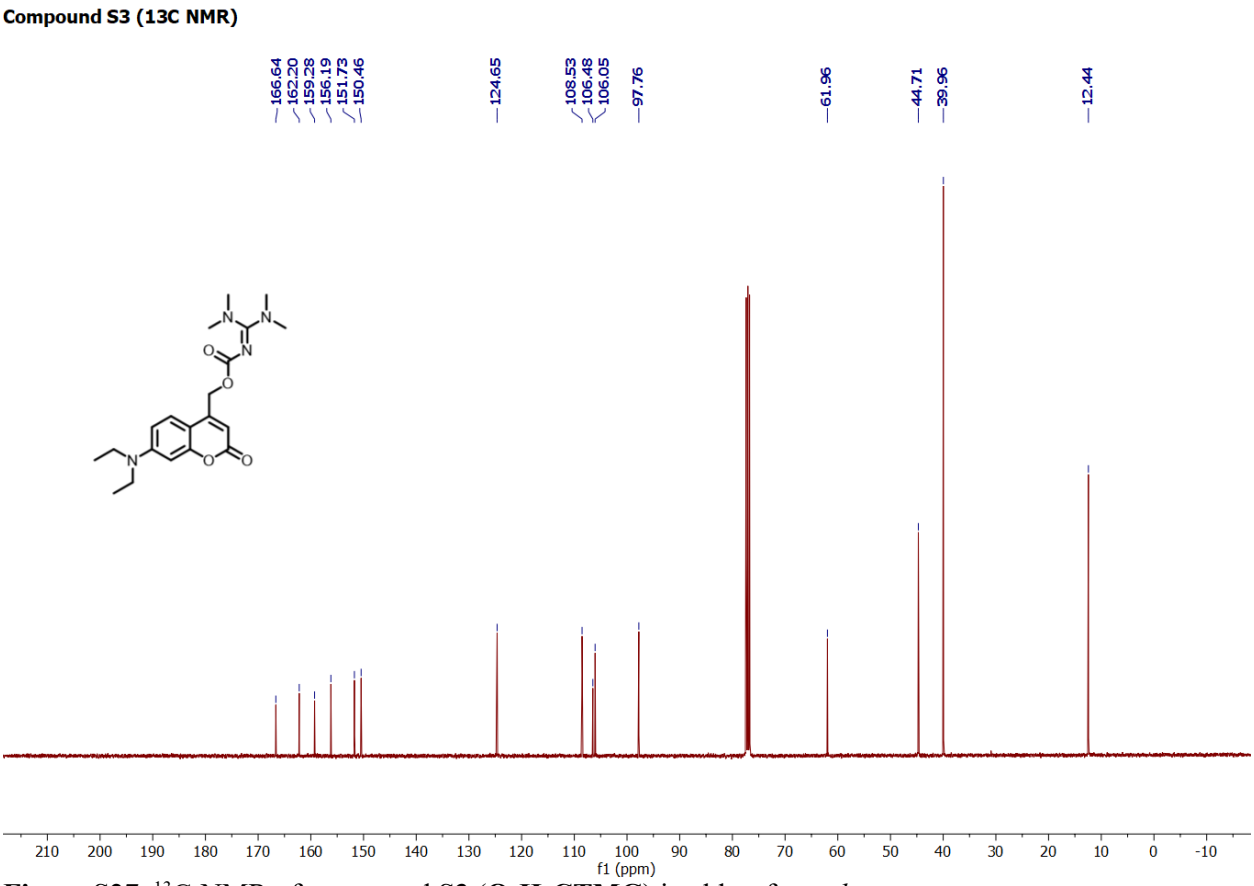

Figure S27. ^{13}C-NMR of compound **S3** (**O-H-CTMG**) in chloroform-*d*.

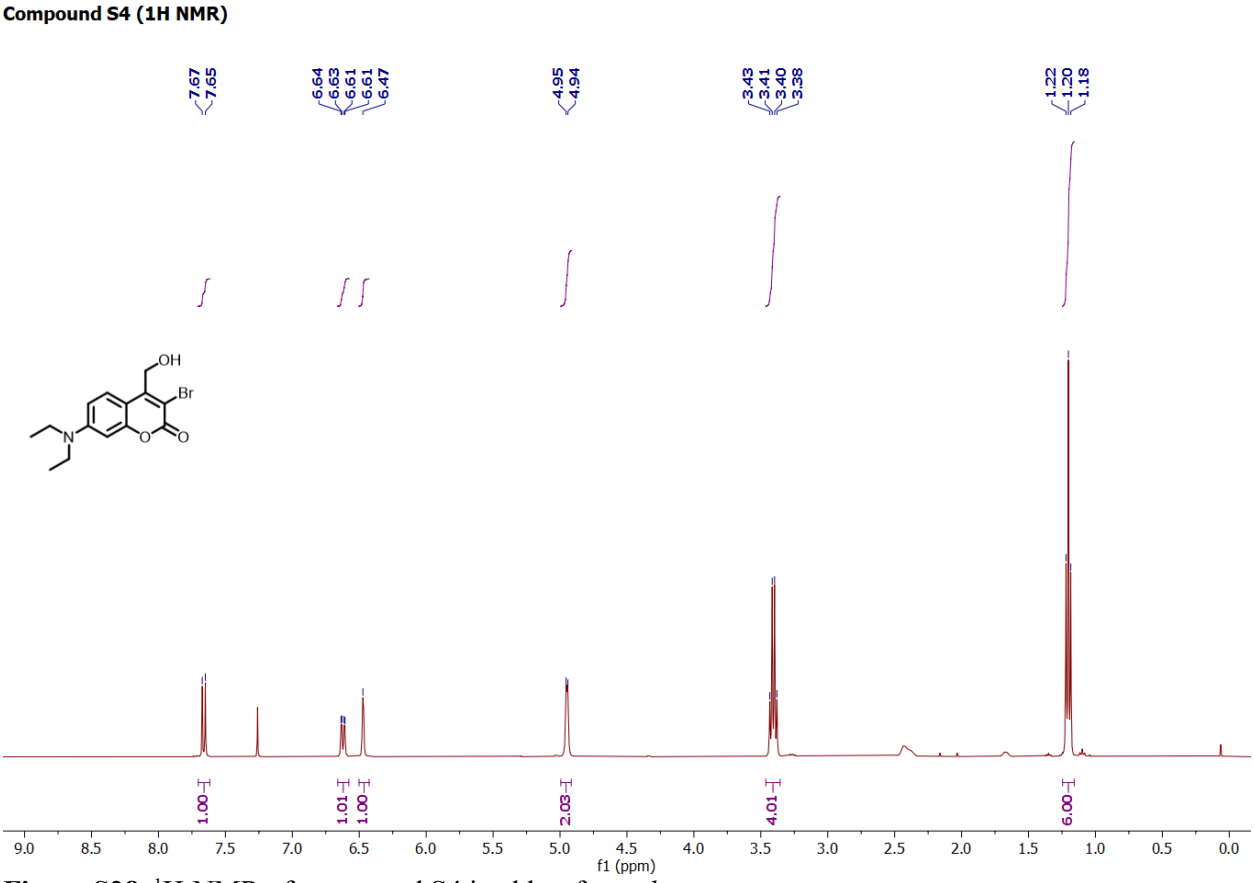

Figure S28. ^{1}H-NMR of compound **S4** in chloroform-*d*.

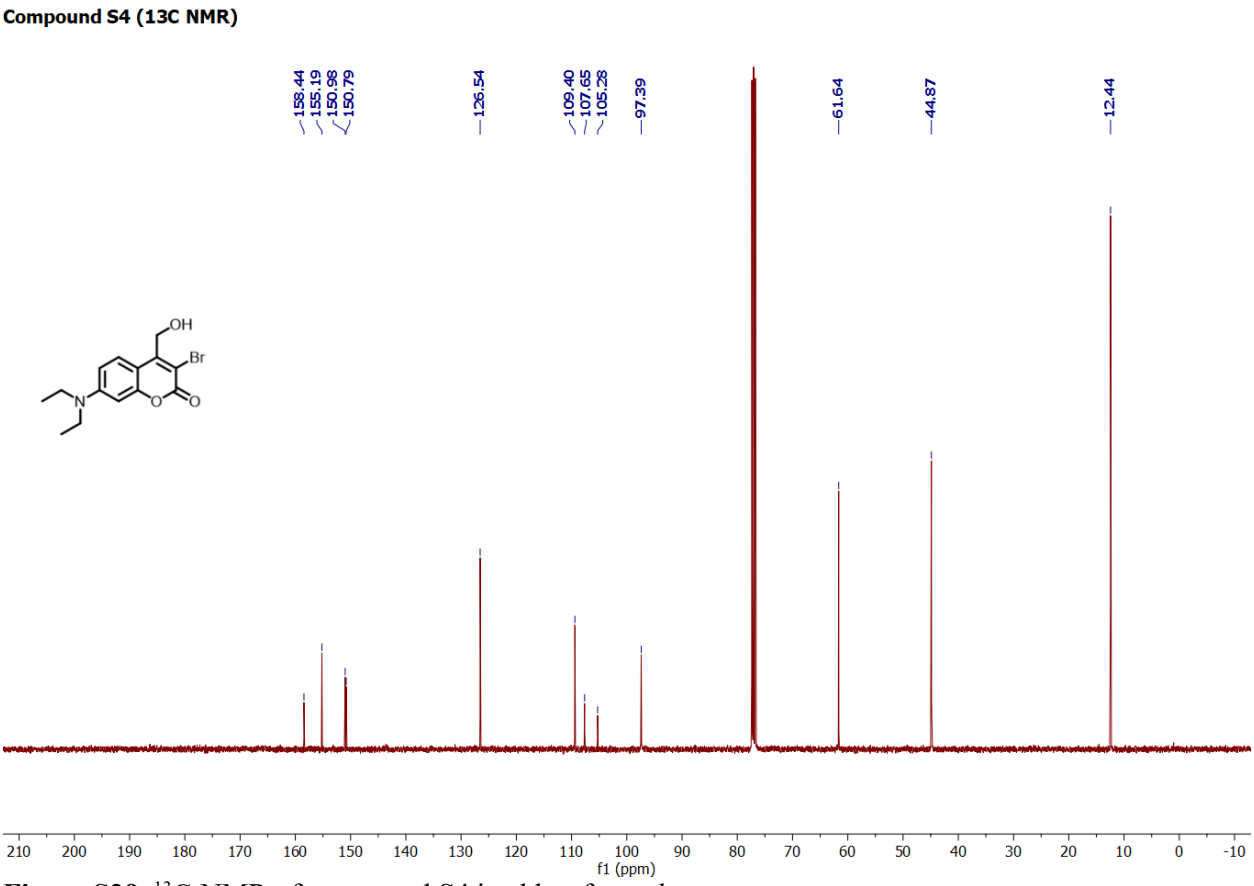

Figure S29. ^{13}C-NMR of compound **S4** in chloroform-*d*.

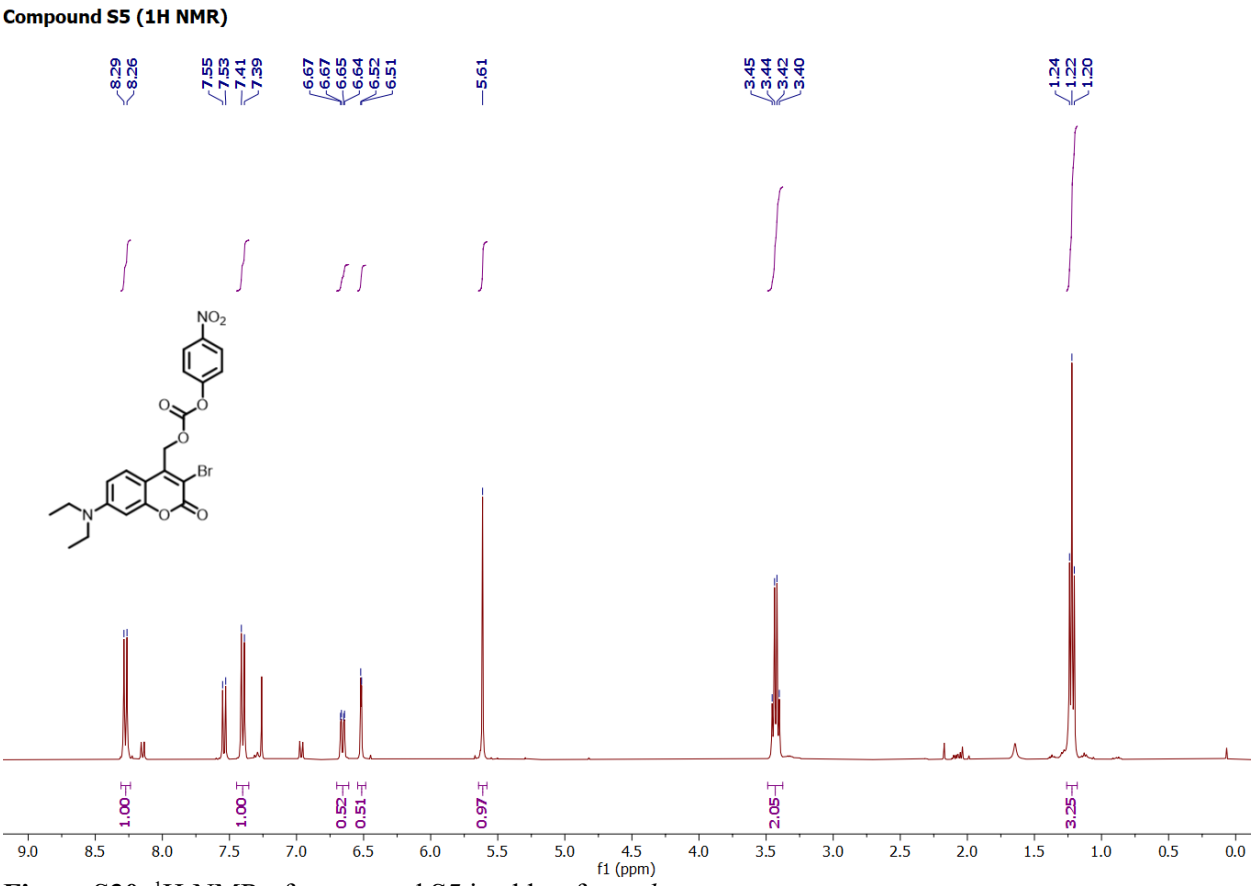

Figure S30. [1]H-NMR of compound **S5** in chloroform-*d*.

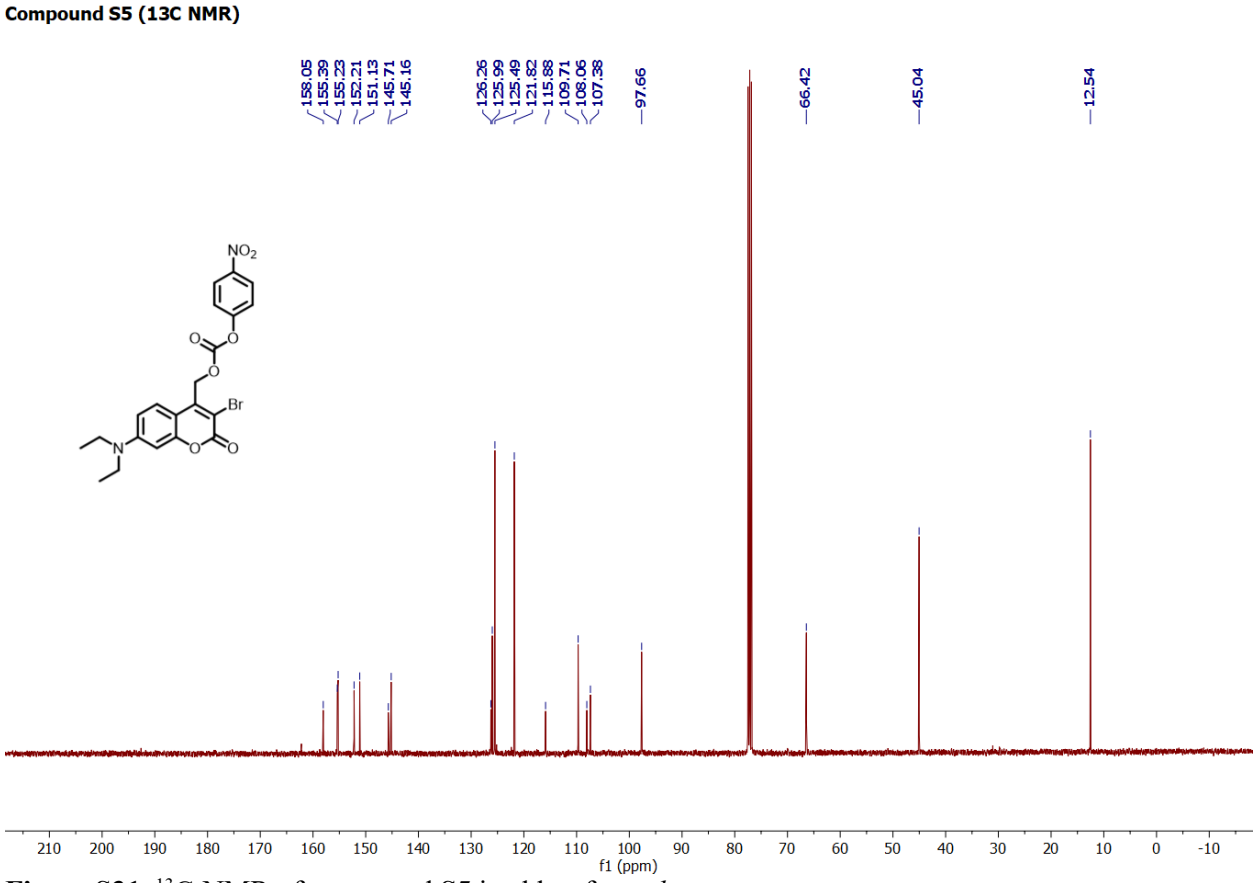

Figure S31. ^{13}C-NMR of compound **S5** in chloroform-*d*.

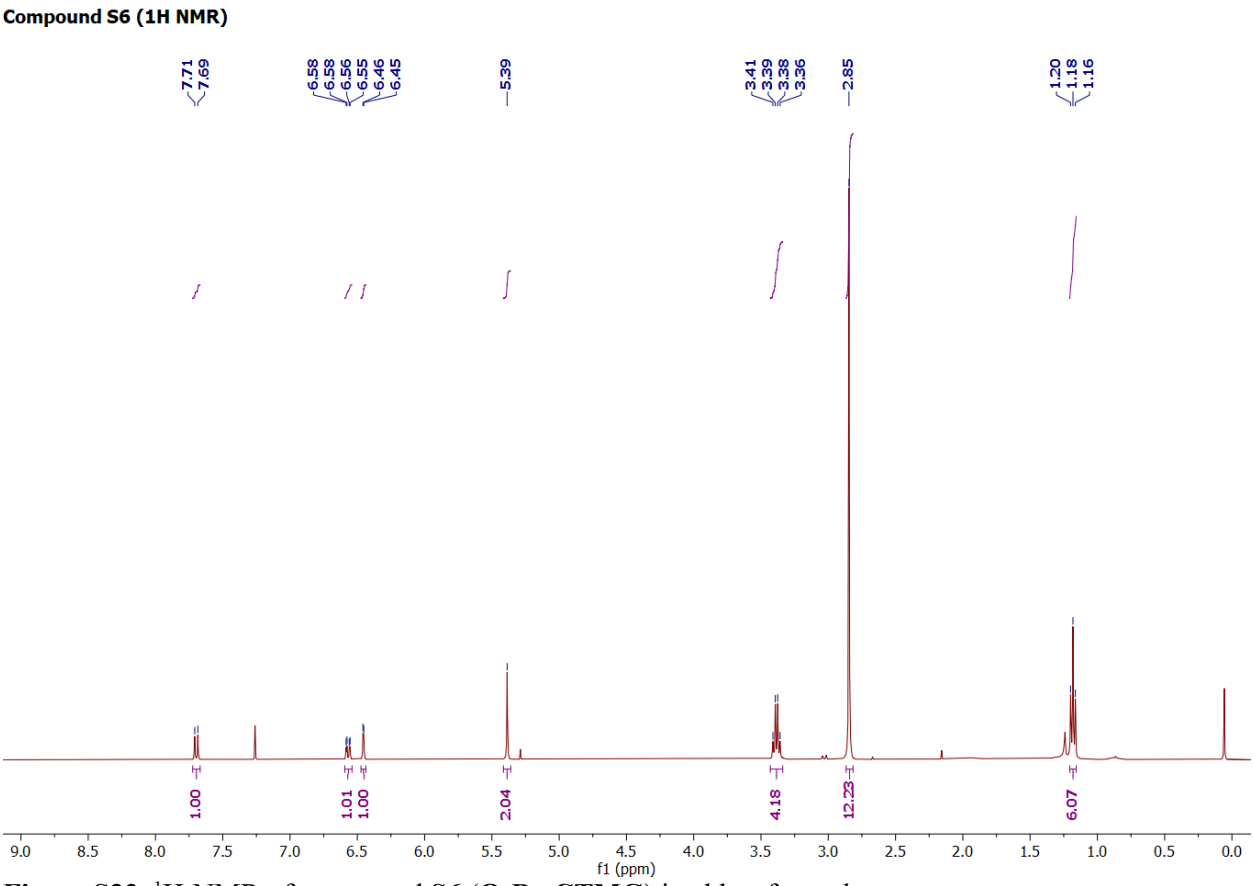

Figure S32. ^{1}H-NMR of compound **S6** (**O-Br-CTMG**) in chloroform-*d*.

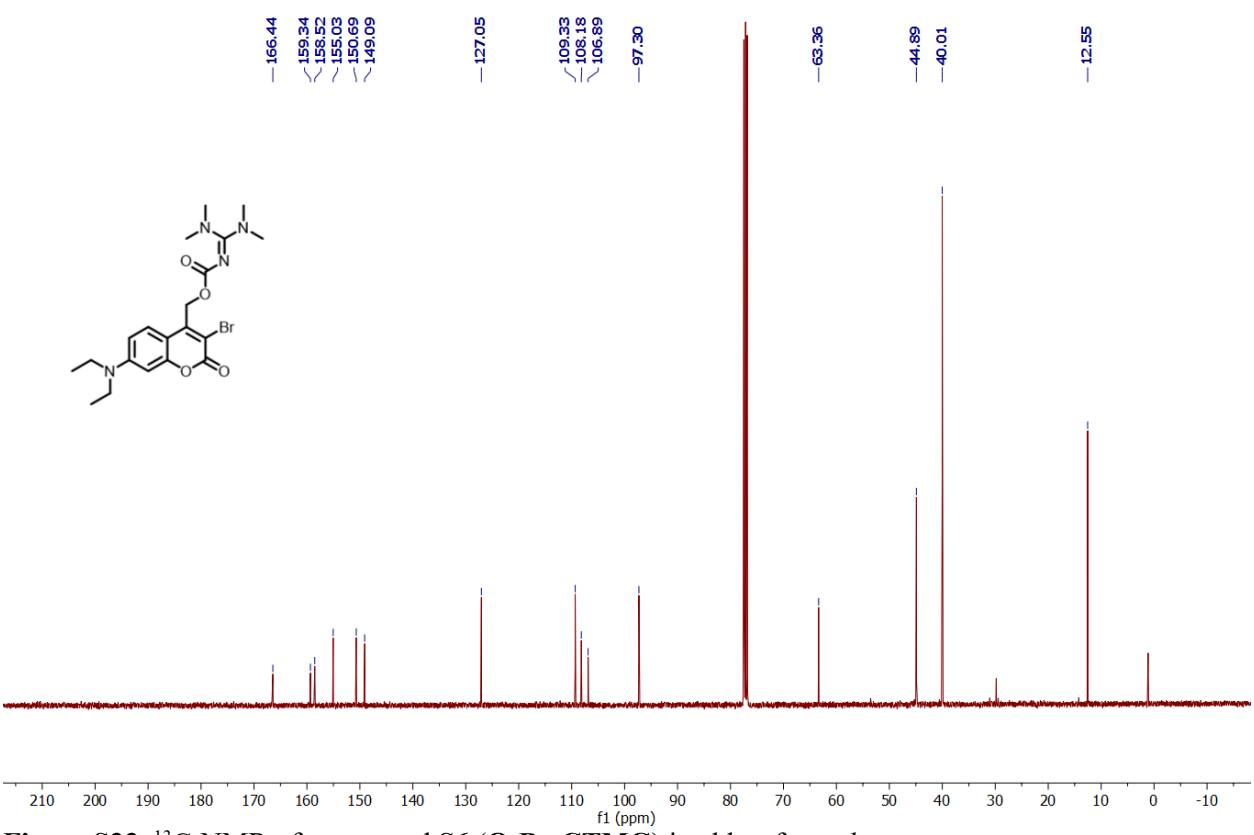

Figure S33. ^{13}C-NMR of compound **S6** (**O-Br-CTMG**) in chloroform-*d*.

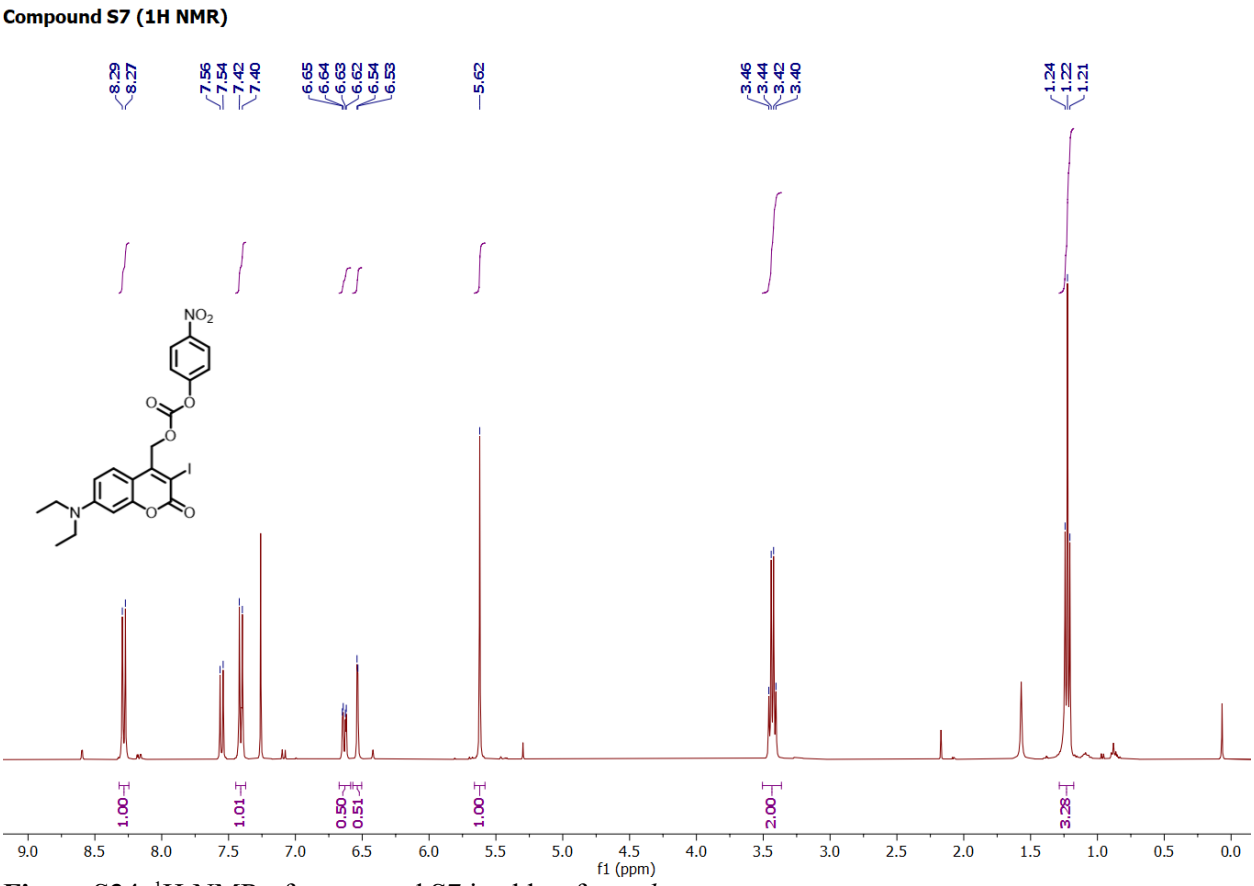

Figure S34. ^{1}H-NMR of compound **S7** in chloroform-*d*.

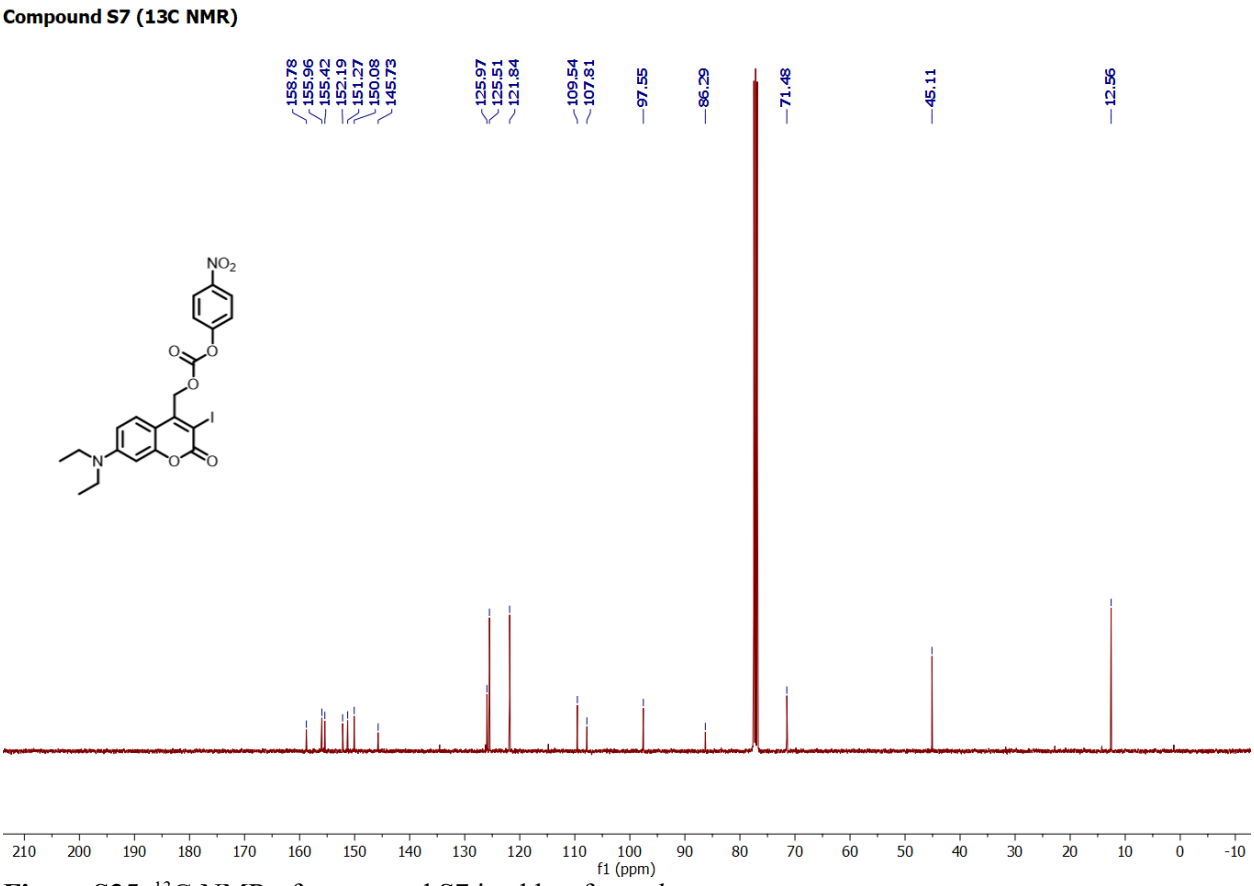

Figure S35. ^{13}C-NMR of compound **S7** in chloroform-*d*.

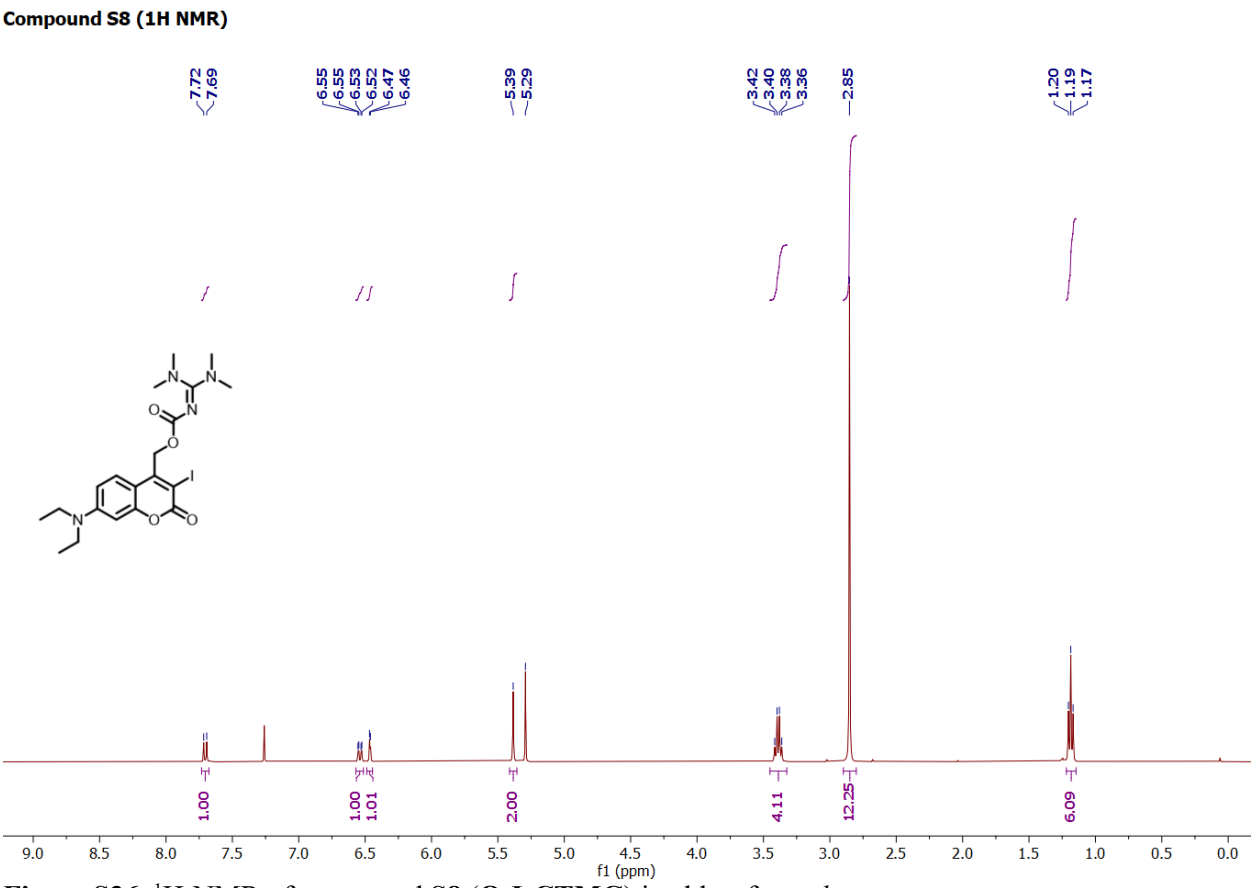

Figure S36. ^{1}H-NMR of compound **S8** (**O-I-CTMG**) in chloroform-*d*.

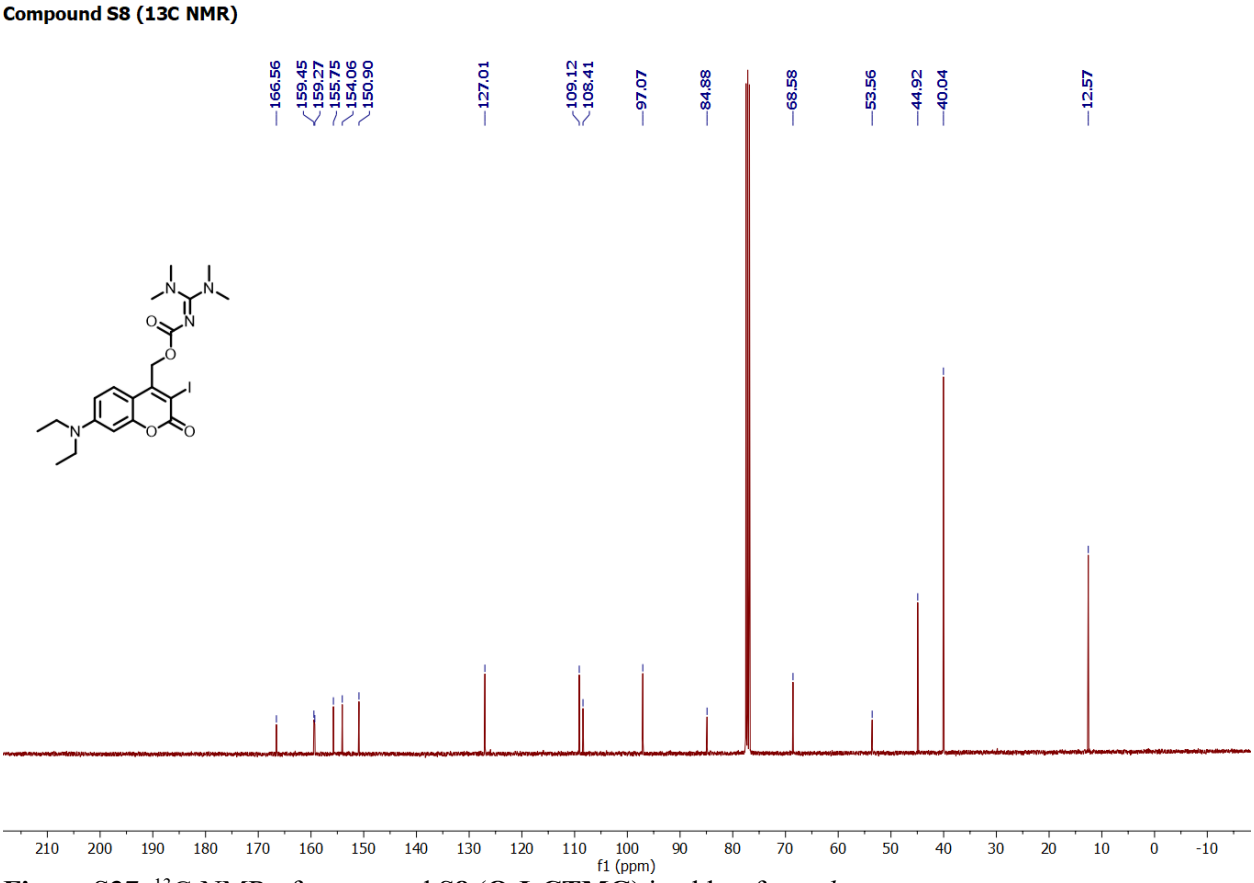

Figure S37. ^{13}C-NMR of compound **S8** (**O-I-CTMG**) in chloroform-*d*.

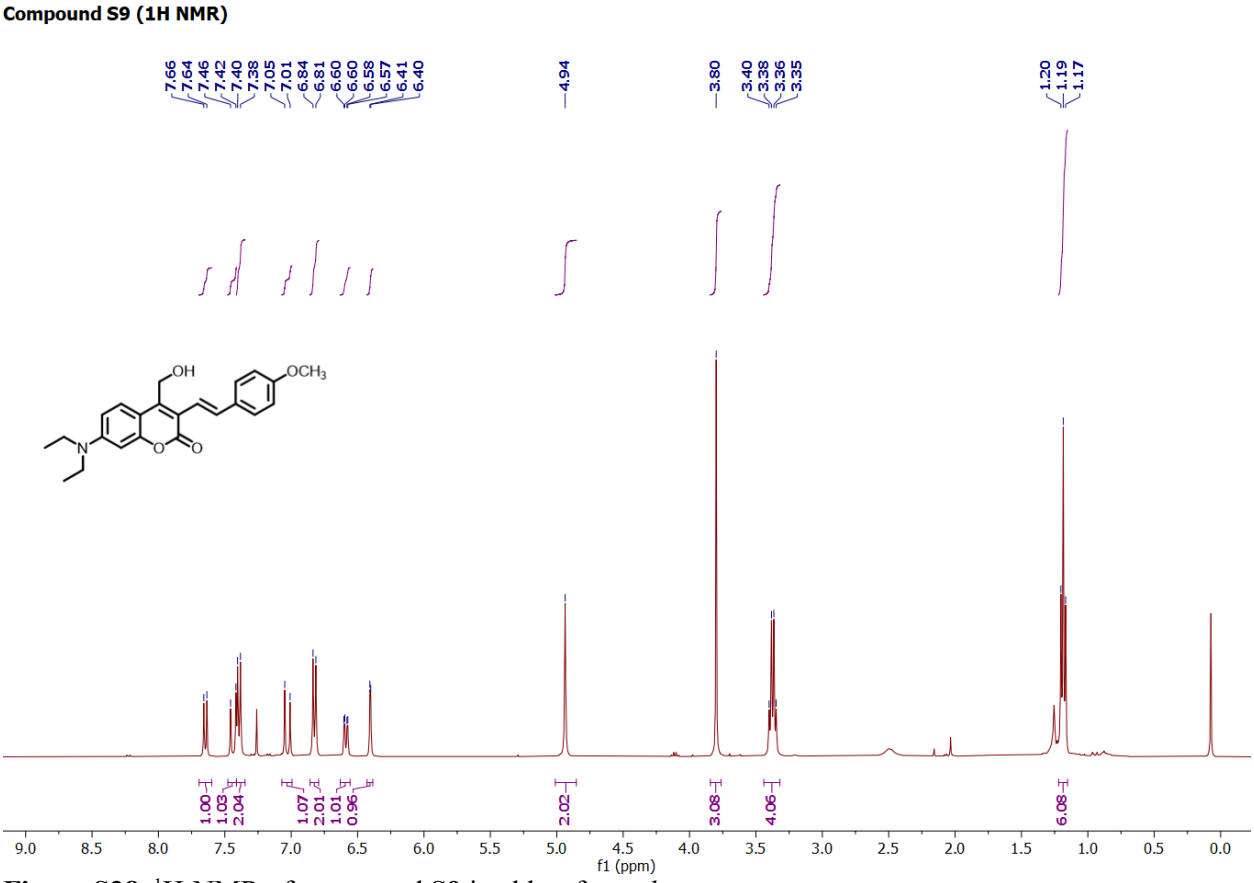

Figure S38. [1]H-NMR of compound **S9** in chloroform-*d*.

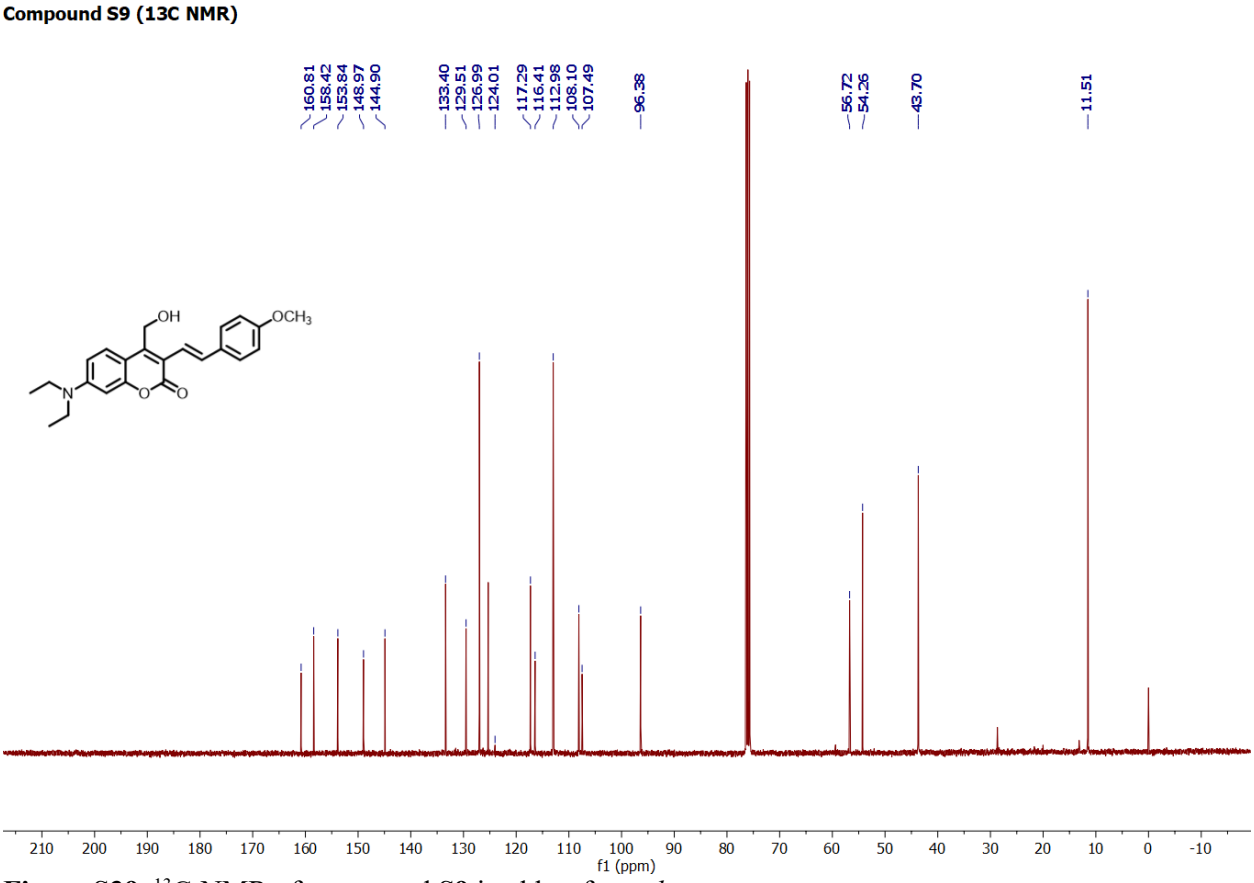

Figure S39. ^{13}C-NMR of compound **S9** in chloroform-*d*.

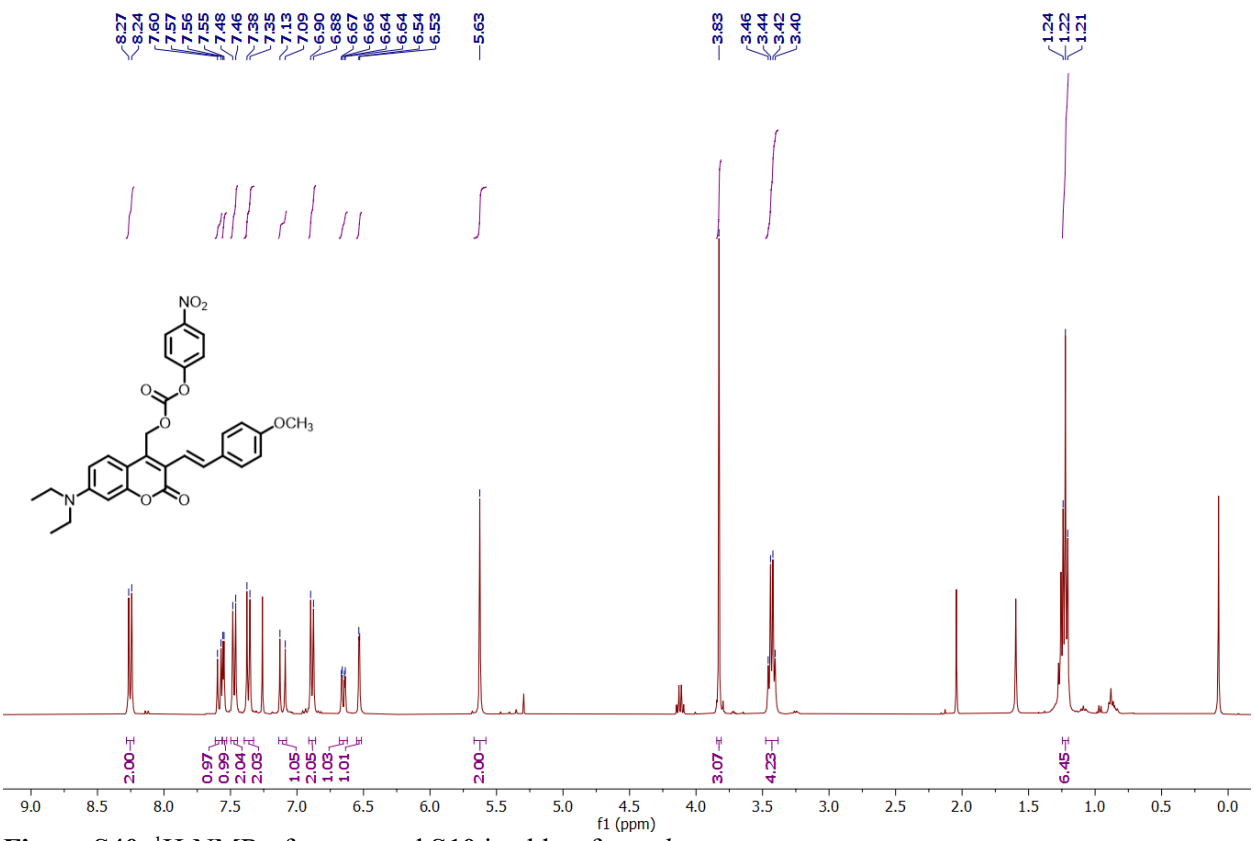

Figure S40. [1]H-NMR of compound **S10** in chloroform-*d*.

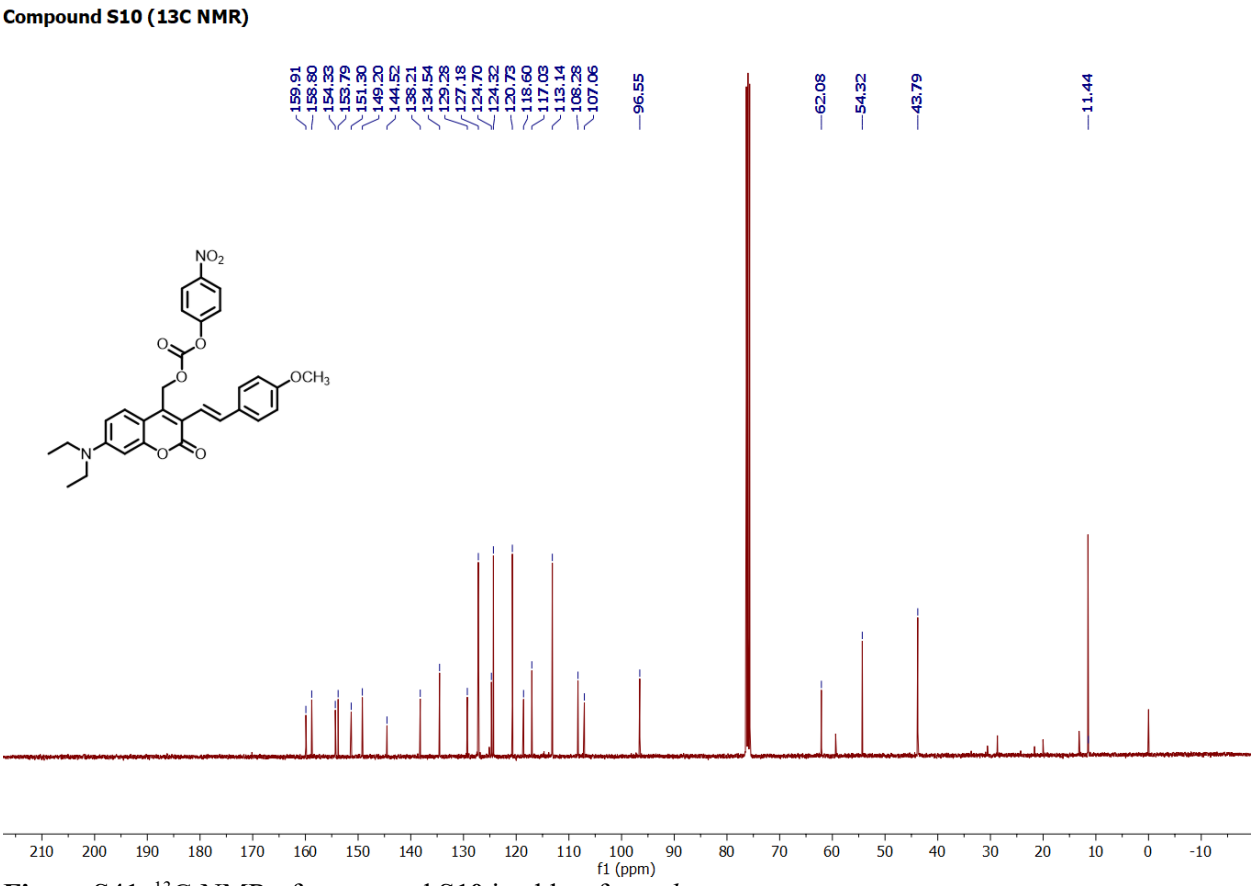

Figure S41. ^{13}C-NMR of compound **S10** in chloroform-*d*.

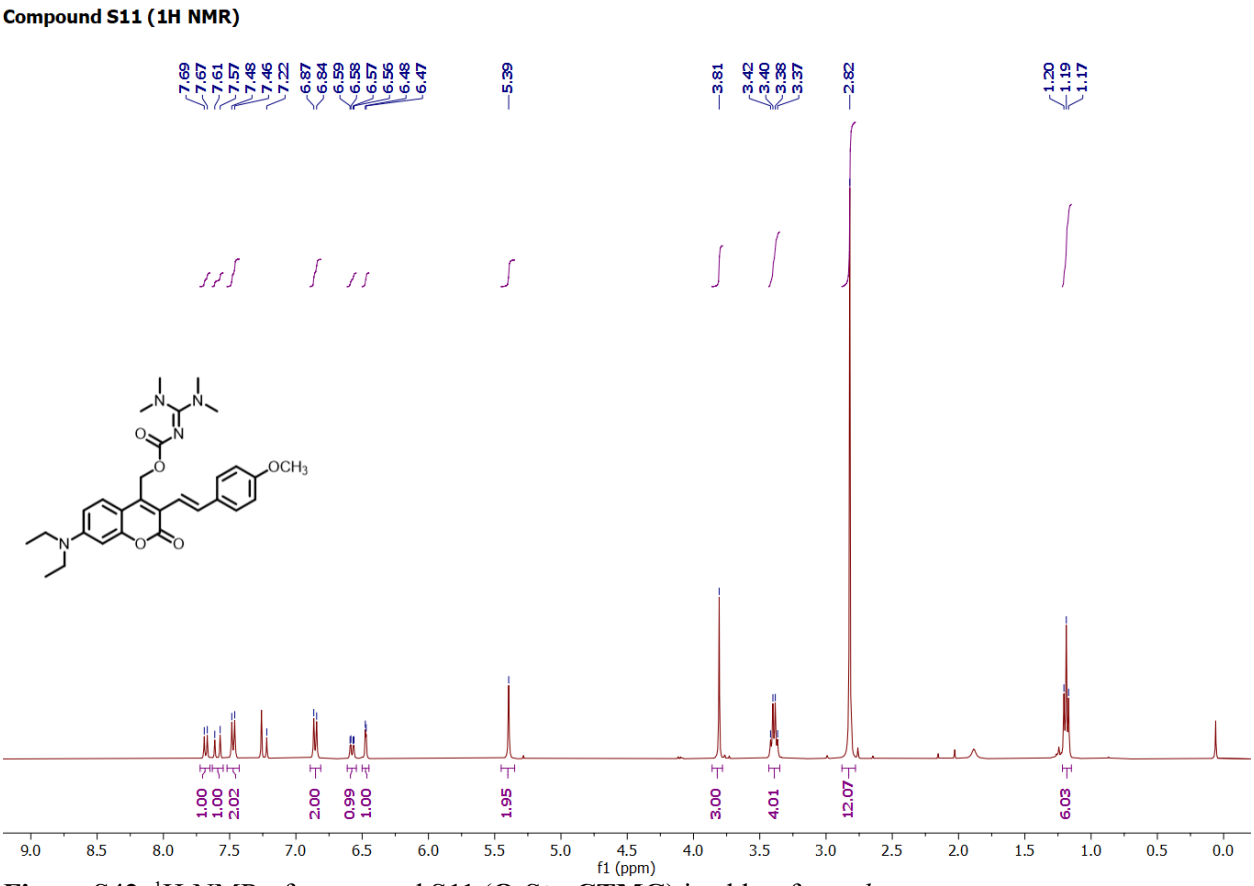

Figure S42. ^{1}H-NMR of compound **S11** (**O-Sty-CTMG**) in chloroform-*d*.

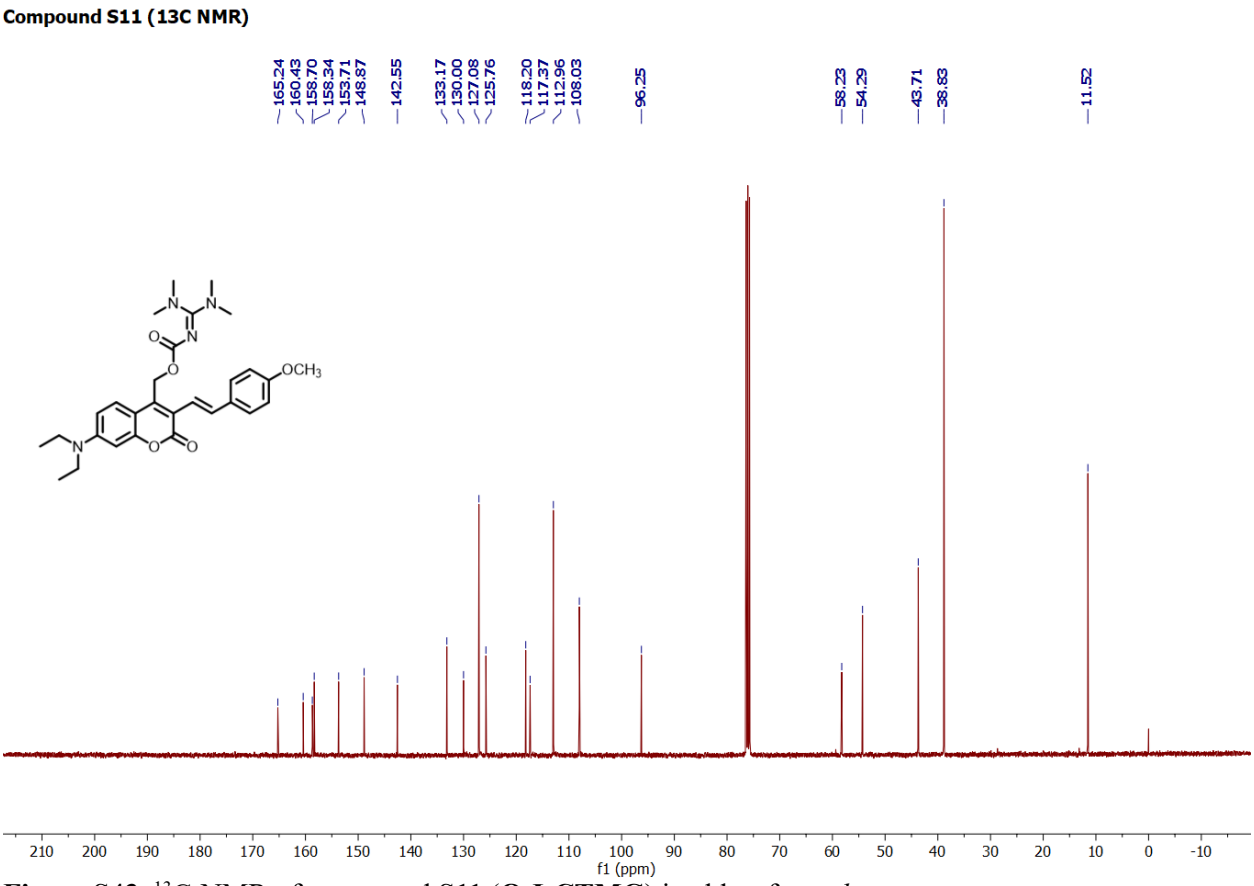

Figure S43. ^{13}C-NMR of compound **S11** (**O-I-CTMG**) in chloroform-*d*.

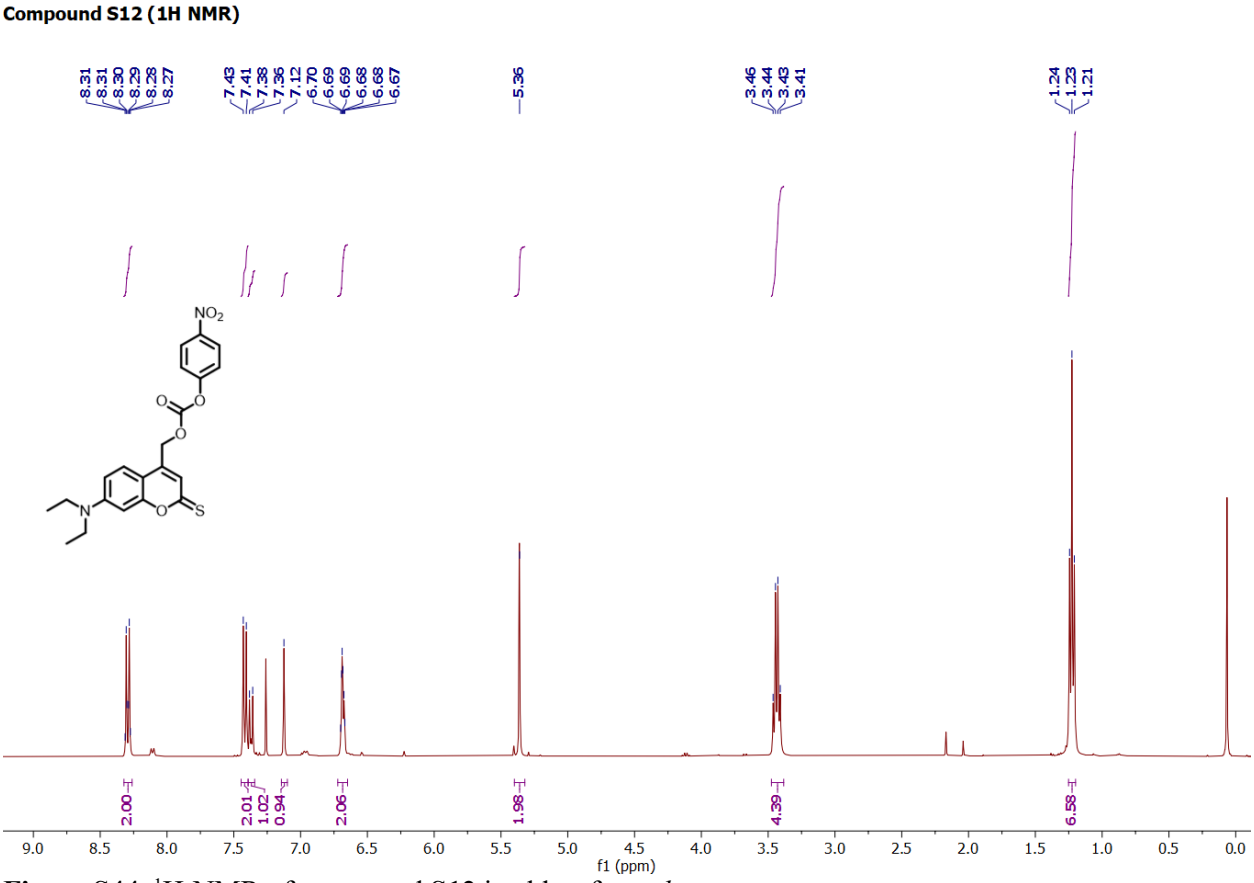

Figure S44. ^{1}H-NMR of compound **S12** in chloroform-*d*.

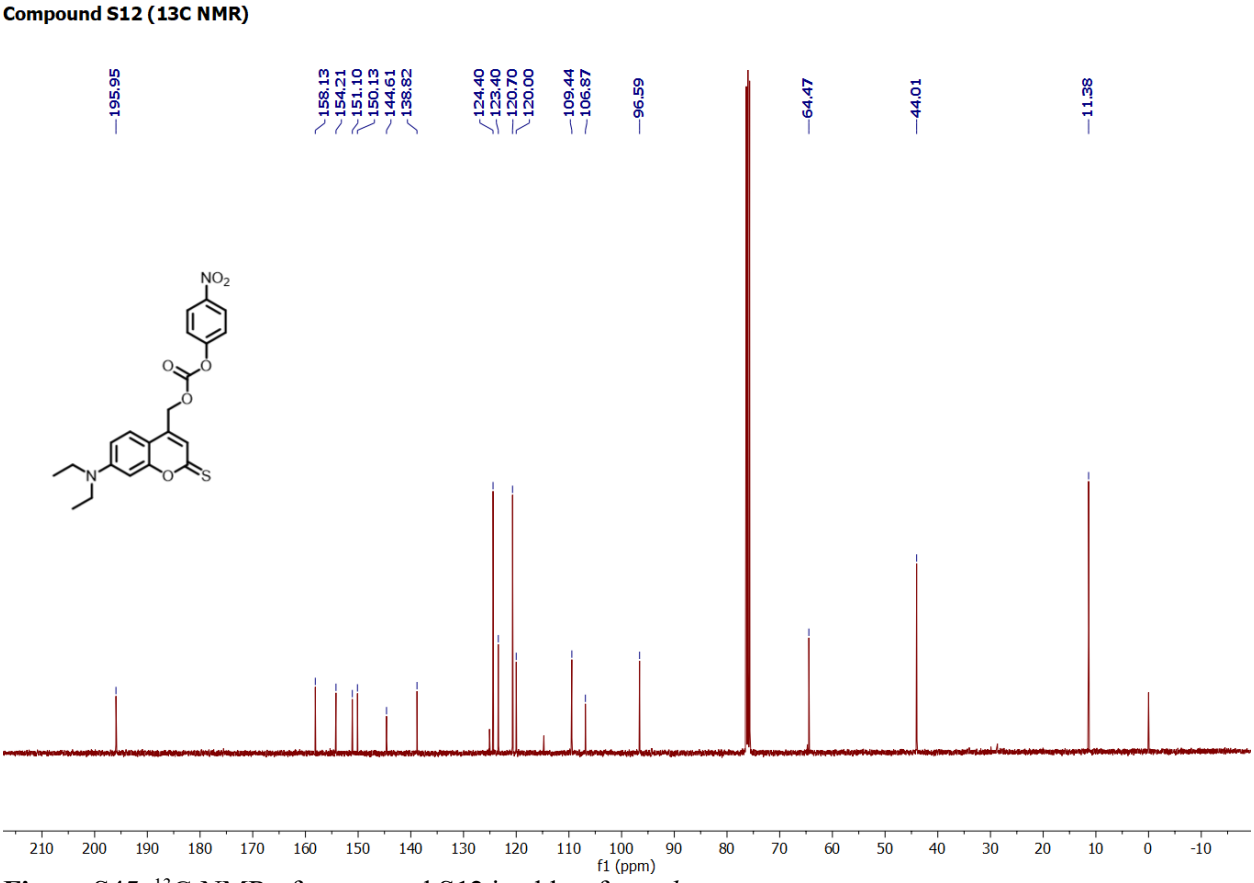

Figure S45. ^{13}C-NMR of compound **S12** in chloroform-*d*.

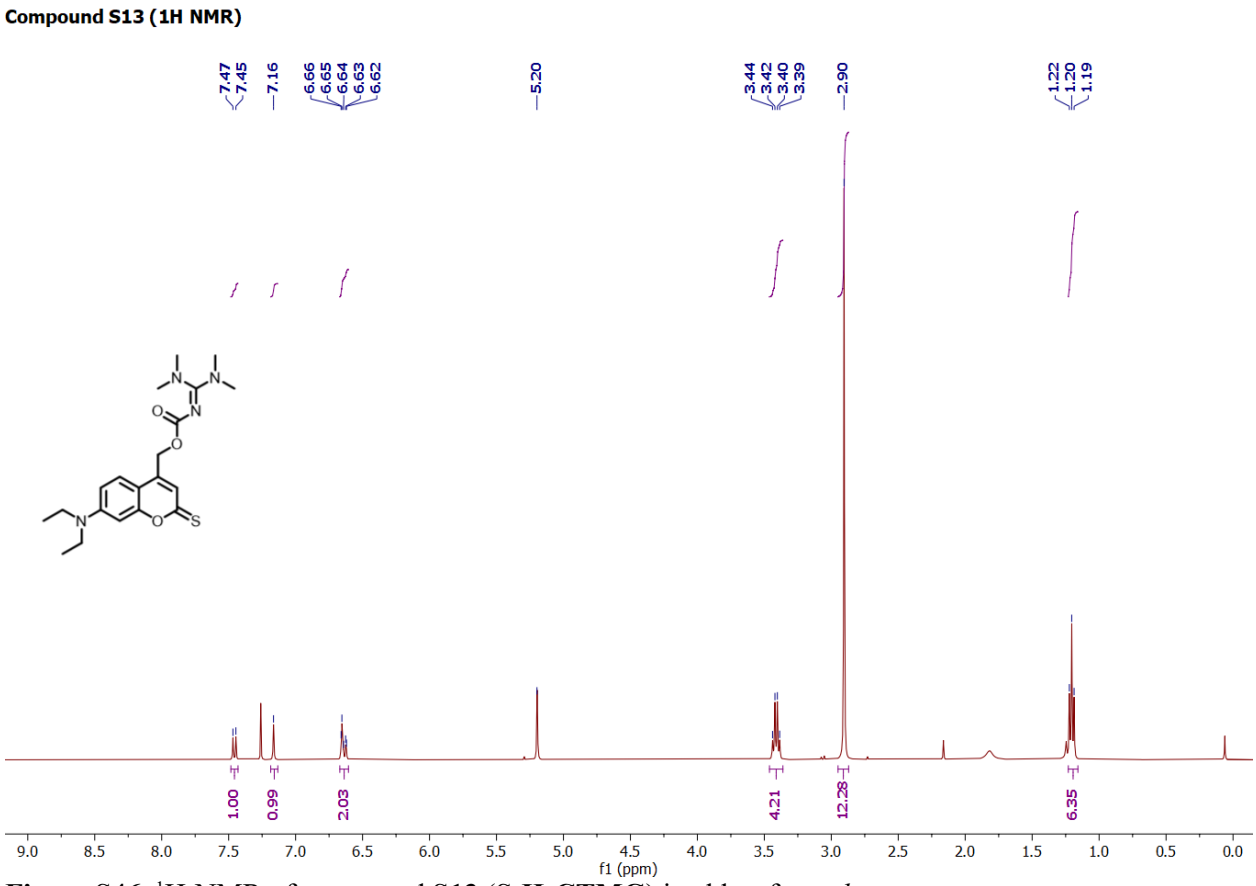

Figure S46. ^{1}H-NMR of compound **S13** (**S-H-CTMG**) in chloroform-*d*.

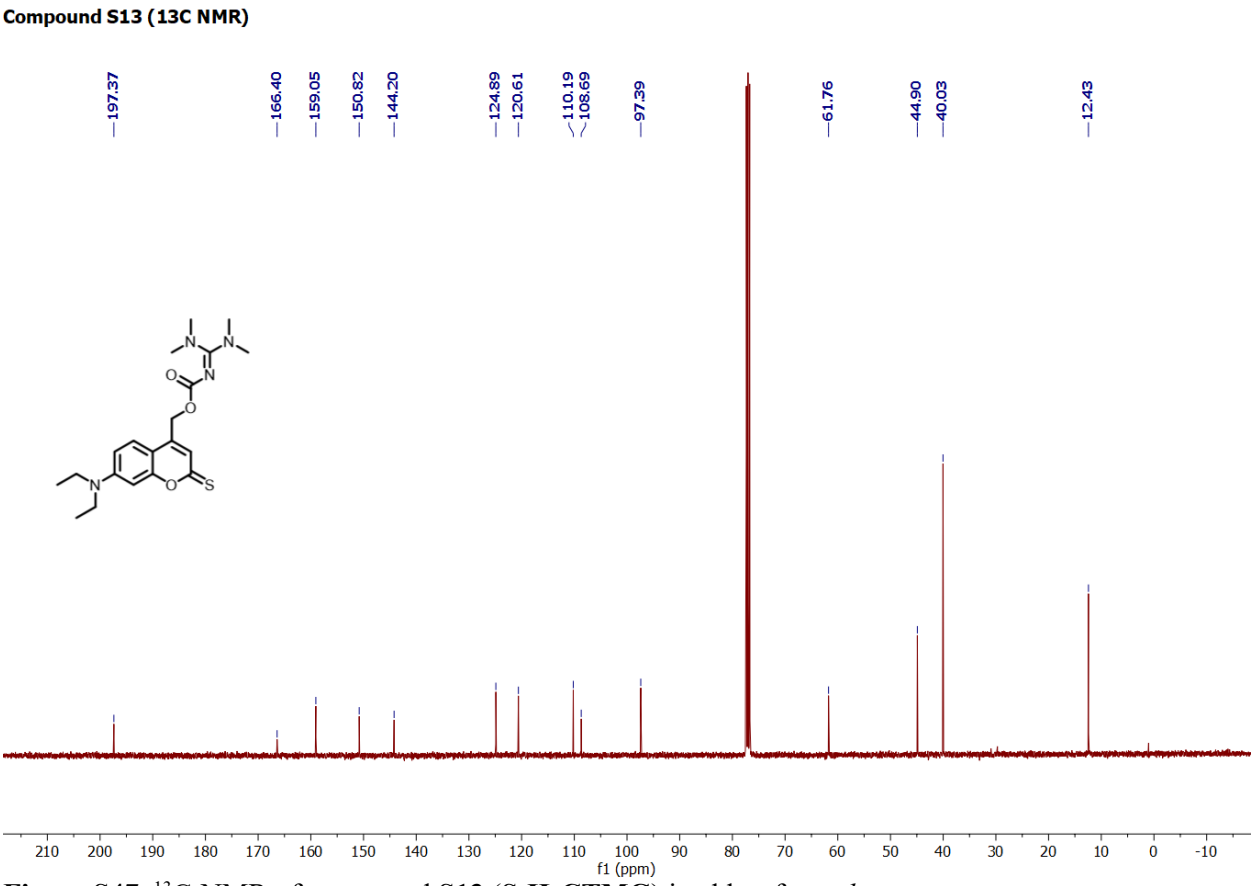

Figure S47. ^{13}C-NMR of compound **S13** (**S-H-CTMG**) in chloroform-*d*.

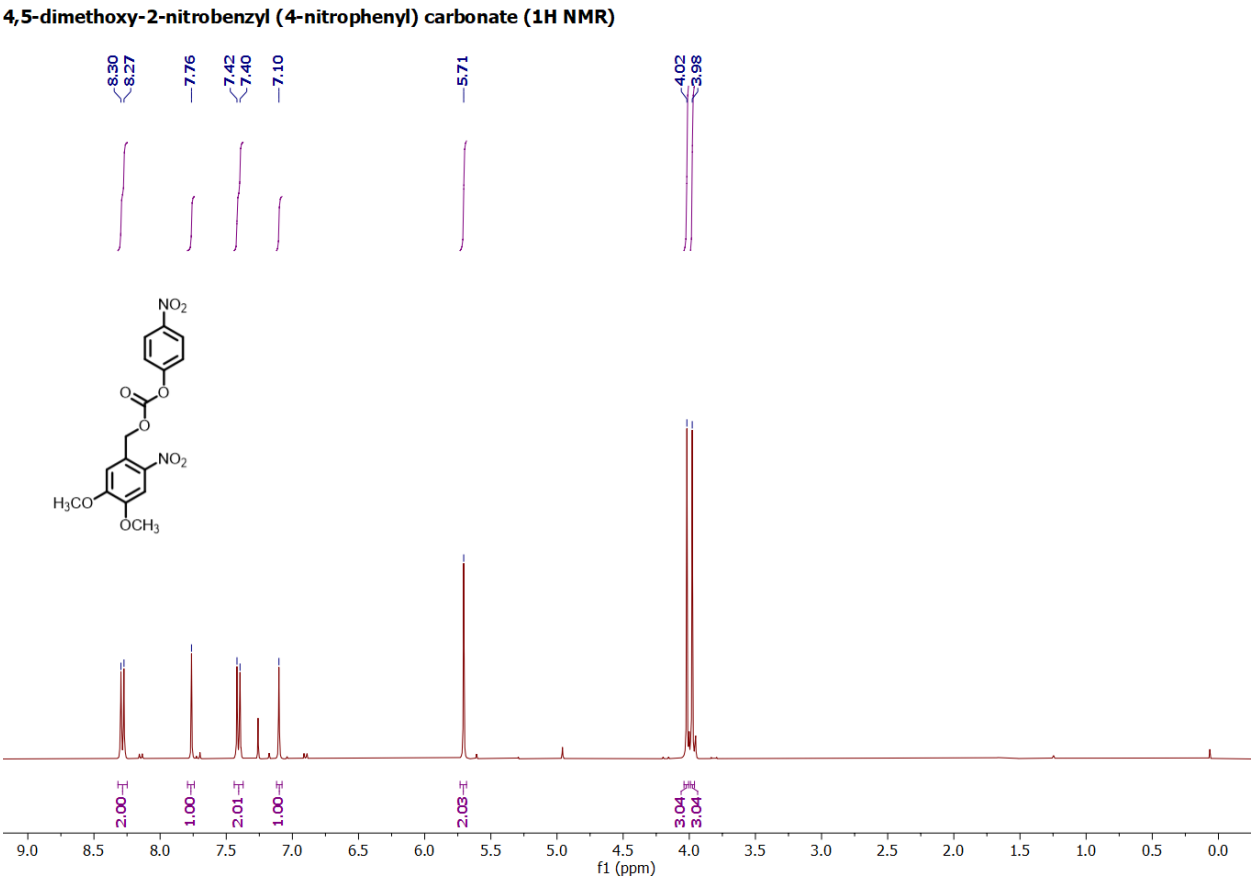

Figure S48. ^{1}H-NMR of compound **S15** in chloroform-*d*.

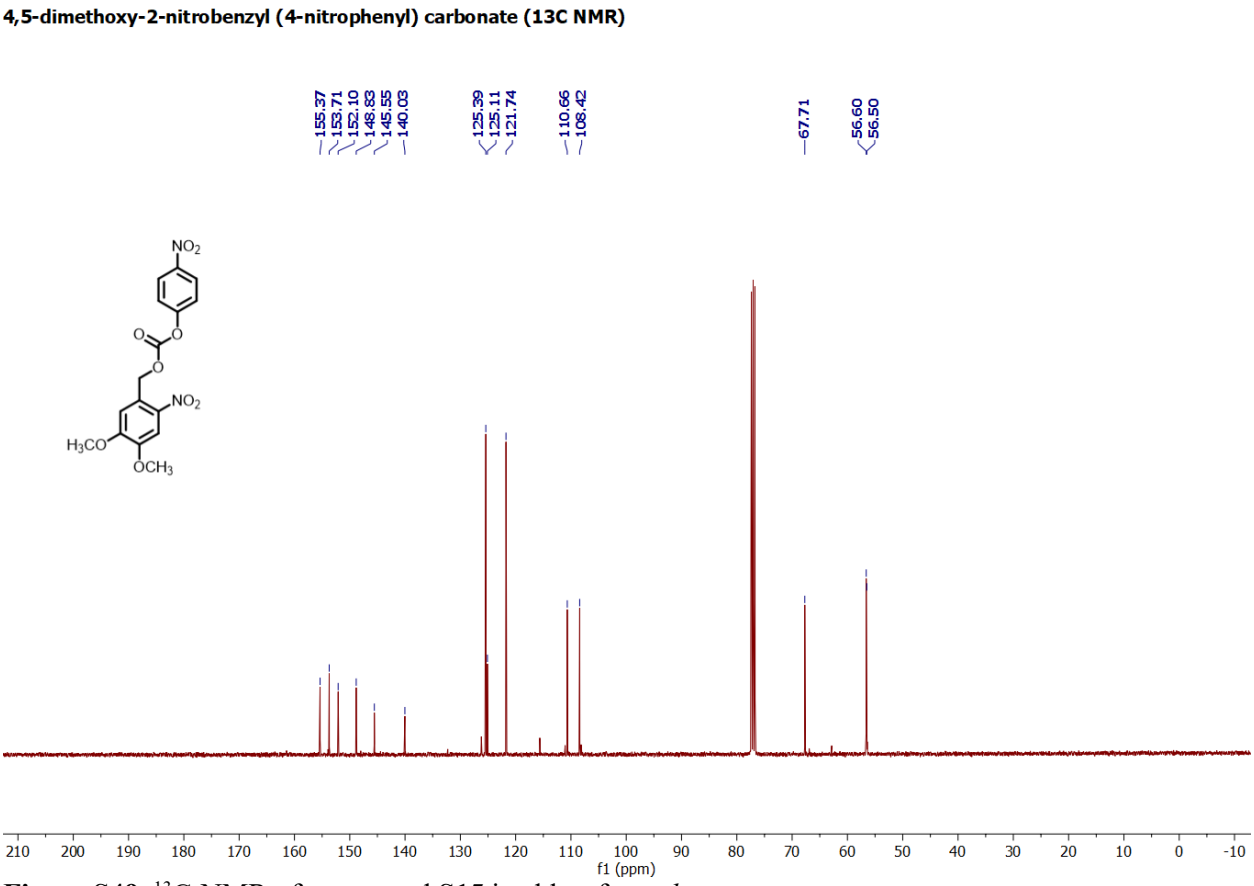

Figure S49. ^{13}C-NMR of compound **S15** in chloroform-*d*.

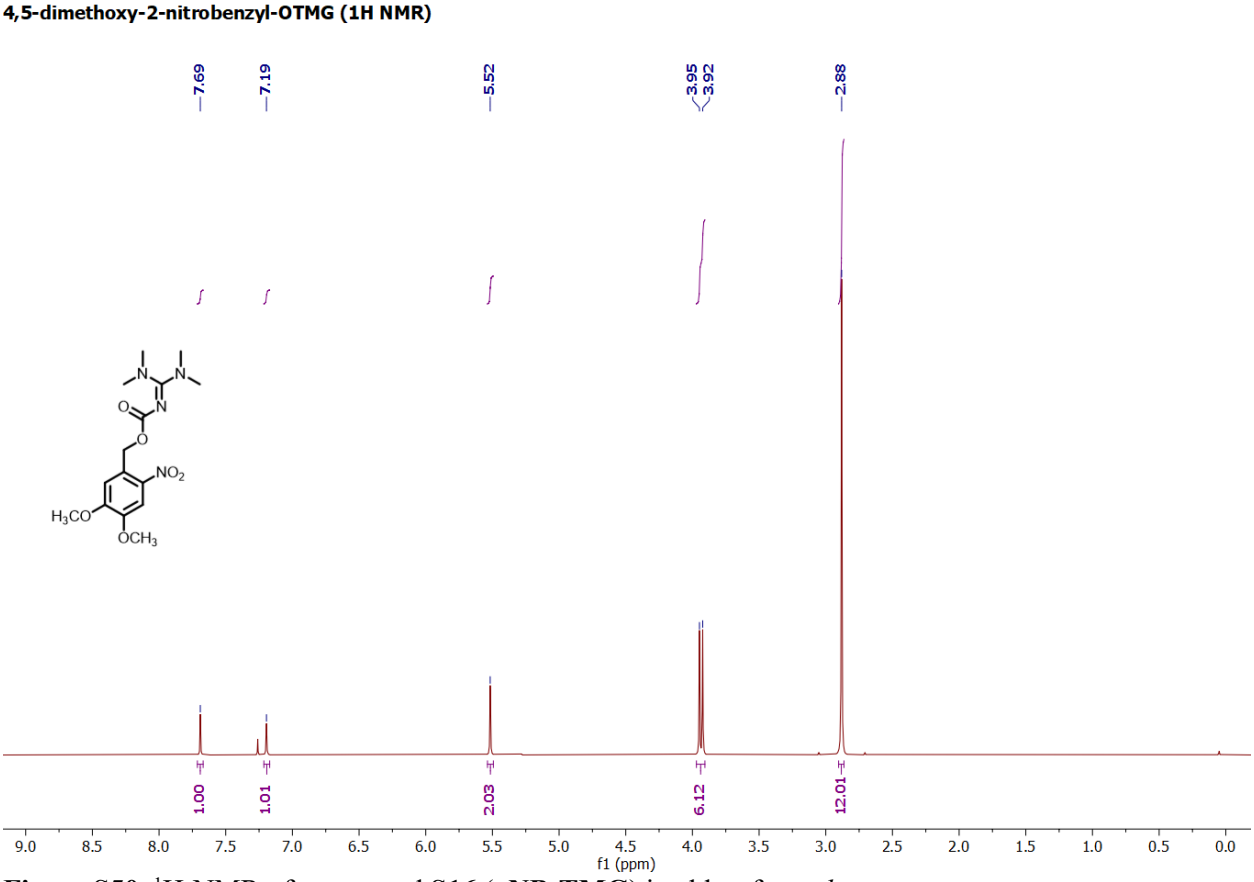

Figure S50. ^{1}H-NMR of compound **S16** (***o*NB-TMG**) in chloroform-*d*.

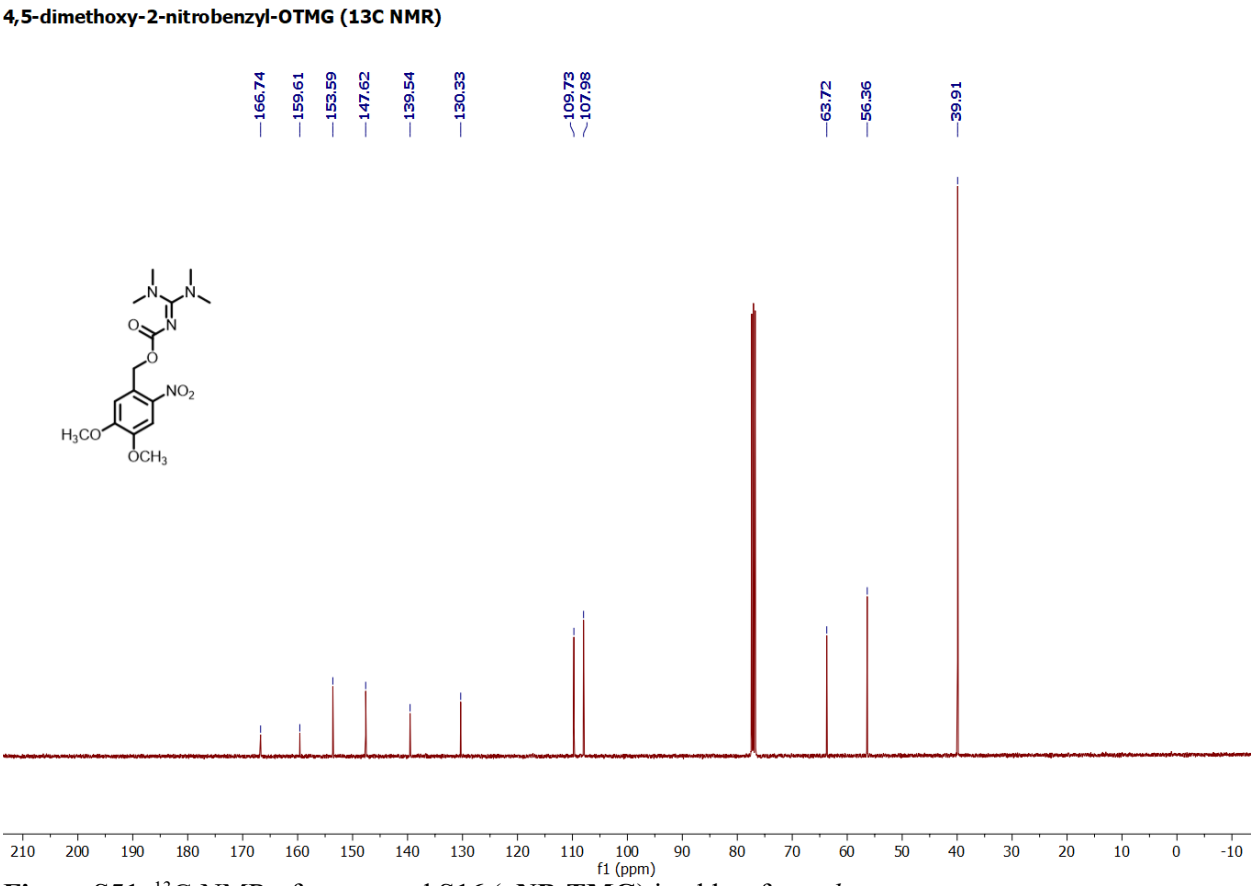

Figure S51. ^{13}C-NMR of compound **S16** (***o*NB-TMG**) in chloroform-*d*.

4. References

S1 W. Xi, H. Peng, A. Aguirre-Soto, C. J. Kloxin, J. W. Stansbury and C. N. Bowman, *Macromolecules*, 2014, **47**, 6159–6165.

S2 H. Y. Park, C. J. Kloxin, M. F. Fordney and C. N. Bowman, *Dental Materials*, 2012, **28**, 888–893.

S3 E. Pretsch, P. Bühlmann and M. Badertscher, *Structure determination of organic compounds: Tables of spectral data*, Springer Berlin Heidelberg, 2009.

S4 C. Würth, M. Grabolle, J. Pauli, M. Spieles and U. Resch-Genger, *Nat Protoc*, 2013, **8**, 1535–1550.